PB 161597

NBS

Technical Note No. 96

Boulder Laboratories

ON THE CLIMATOLOGY OF GROUND-BASED RADIO DUCTS AND ASSOCIATED FADING REGIONS

BY

E.J. DUTTON

U. S. DEPARTMENT OF COMMERCE
NATIONAL BUREAU OF STANDARDS

THE NATIONAL BUREAU OF STANDARDS

Functions and Activities

The functions of the National Bureau of Standards are set forth in the Act of Congress, March 3, 1901, as amended by Congress in Public Law 619, 1950. These include the development and maintenance of the national standards of measurement and the provision of means and methods for making measurements consistent with those standards; the determination of physical constants and properties of materials; the development of methods and instruments for testing materials, devices, and structures; advisory services to government agencies on scientific and technical problems; invention and development of devices to serve special needs of the Government; and the development of standard practices, codes, and specifications. The work includes basic and applied research, development, engineering, instrumentation, testing, evaluation, calibration services, and various consultation and information services. Research projects are also performed for other government agencies when the work relates to and supplements the basic program of the Bureau or when the Bureau's unique competence is required. The scope of activities is suggested by the listing of divisions and sections on the inside of the back cover.

Publications

The results of the Bureau's work take the form of either actual equipment and devices or published papers. These papers appear either in the Bureau's own series of publications or in the journals of professional and scientific societies. The Bureau itself publishes three periodicals available from the Government Printing Office: The Journal of Research, published in four separate sections, presents complete scientific and technical papers; the Technical News Bulletin presents abstracts and preliminary reports on work in progress; and Basic Radio Propagation Predictions provides data for determining the best frequencies to use for radio communications throughout the world. There are also five series of nonperiodical publications: Monographs, Applied Mathematics Series, Handbooks, Miscellaneous Publications, and Technical Notes.

Information on the Bureau's publications can be found in NBS Circular 460, Publications of the National Bureau of Standards ($1.25) and its Supplement ($1.50), available from the Superintendent of Documents, Government Printing Office, Washington 25, D.C.

NATIONAL BUREAU OF STANDARDS

Technical Note

96

June 16, 1961

ON THE CLIMATOLOGY OF GROUND-BASED RADIO DUCTS AND ASSOCIATED FADING REGIONS

by

E. J. Dutton

NBS Technical Notes are designed to supplement the Bureau's regular publications program. They provide a means for making available scientific data that are of transient or limited interest. Technical Notes may be listed or referred to in the open literature. They are for sale by the Office of Technical Services, U. S. Department of Commerce, Washington 25, D. C.

DISTRIBUTED BY

UNITED STATES DEPARTMENT OF COMMERCE

OFFICE OF TECHNICAL SERVICES

WASHINGTON 25, D. C.

Price $1.75

The material contained in this report is drawn in part from Telecommunications Performance Standards, Tropospheric Systems, prepared under the sponsorship of the Ground Electronics Engineering and Installation Agency (Directorate of Engineering, ROZM), United States Air Force. It has been prepared in Technical Note form for use as lecture notes for the course of Radio Propagation given by the Boulder Laboratories of the National Bureau of Standards, July 31 - August 18, 1961.

ON THE CLIMATOLOGY OF GROUND-BASED RADIO DUCTS AND ASSOCIATED FADING REGIONS

by

E. J. Dutton

ABSTRACT

An atmospheric duct is defined as occurring when geometrical optics indicates that a radio ray passing upwards through the atmosphere is sufficiently refracted that it travels parallel to the earth's surface. Maximum observed incidence of ducts was determined to be 13%, 10%, and 5% by analysis of three to five years of radiosonde data for a tropical, temperate, and arctic location, respectively. Annual maxima are observed in the winter for the arctic and summer for the tropics. Arctic ducts arise from ground based temperature inversions with the ground temperature less than -25°C; temperate zone ducts arise from radiation inversions and accompanying humidity lapse; while tropical ducts occur with slight temperature and humidity lapses when the surface temperature is 30°C and greater. The mean initial elevation angle of a radio ray trapped by these ducts is found to be about 3 mr, with the maximum value about 5.8 mr. The steepest gradient of N observed is -420 N units/km. Observed ducts trap radio-waves of frequency $\geq$ 1 kMc at all locations for at least 50% of the time.

Fading regions arising from abnormal defocussing of radio-rays passing from an elevated antenna down through the duct to a ground-based receiver are analyzed. The horizontal extent of these regions is determined for the same arctic, tropic, and temperate conditions given above.

ON THE CLIMATOLOGY OF GROUND-BASED RADIO DUCTS AND ASSOCIATED FADING REGIONS

by

E. J. Dutton

Part I: Ground Based Radio Ducts

1. INTRODUCTION

The occurrence of atmospheric ducts places limitations upon ray tracing of VHF-UHF radio waves. Ducting is defined as occurring when a radio ray originating at the earth's surface is sufficiently refracted so that it either is bent back towards the earth's surface or travels in a path parallel to the earth's surface. Although the rigorous treatment of ducting involves consideration of the full wave equation solution [Booker and Walkinshaw, 1946] rather than a simple ray treatment, the present study will be based upon a geometrical optics definition of the limiting case in which ray tracing techniques may be used. This simple criterion is then applied to several years of radiosonde observations from stations typical of arctic, temperate, and tropical climates to derive estimates of the variation of the occurrence of radio ducts with climatic conditions.

2. METEOROLOGICAL CONDITIONS ASSOCIATED WITH RADIO REFRACTIVE INDEX PROFILES

The path followed by a radio ray in the atmosphere is dependent upon the gradient of the refractive index along that path. Of the vertical and horizontal gradient components that compose the path gradient, the horizontal gradient is normally negligibly small. Thus, the atmosphere is considered horizontally homogeneous and only the vertical gradient of the refractive index is utilized. The numerical value of the vertical gradient of the index of refraction depends on the vertical distribution of atmospheric temperature, humidity, and pressure.

Normally, temperature and humidity decrease with height in the atmosphere, since turbulence prevents any great changes in structure. However, there are periods of time in which the air becomes fairly calm, whereupon temperature inversions and humidity lapses can be built up and maintained. Temperature inversions have a two-fold importance in that (a) they can be widespread in area and persist over a relatively long period of time, and (b) they exercise a stabilizing influence on air motion such that turbulence is suppressed and strong humidity gradients may develop. Layers in which there is intense superrefraction to the point of duct formation may be formed as a result of these gradients and trapping of radio waves may follow. The inversions may start at ground level or at some greater height. The thickness of the layer can show great variability. Three processes that form temperature inversions are:

Advection: Advection is the horizontal transport of air having certain properties. Such a process is of importance in microwave propagation since it may lead to a different rate of exchange of heat and moisture between the air and the underlying ground or ocean surface, thus affecting the physical structure of the lowest layers of the atmosphere. This process results in air with different refractive index characteristics being brought into the area. The most common and important case of advection is that of dry air above a warm land surface flowing out over a cold sea. This type of advection frequently appears in the English Channel during the summer when the weather has been fine for several days.

Advective duct formation depends on two quantities: (a) the excess of the unmodified air temperature above that of water, and (b) the humidity deficit (the difference between the water vapor pressures of the modified and unmodified air). If these quantities are large, especially the humidity deficit, an intensive duct may form.

Important advective processes can also occur over land, but the conditions required for duct formation occur less frequently. However, a duct may be formed when dry, warm air flows over cold, wet ground with resultant temperature and humidity structure previously discussed.

Radiation: Differences in daytime and night-time radiation are the causes of diurnal variation in refractive conditions. A subrefractive layer may be present during the day, especially at the time of maximum surface heating. Clear skies and light surface winds at night result in considerable cooling of the earth, thus causing the formation of temperature inversions. The surface heat loss produced by nocturnal radiation is a prime factor in the formation of temperature inversions. Atmospheric stratification formed by such a combination of meteorological parameters may cause trapping. A temperature inversion is seldom strong enough to produce a duct in the middle and low latitudes, but it is of major importance in the formation of ducts in the northern latitudes. Low stratus clouds or extreme amounts of moisture (as in the tropics) tend to prevent loss by radiation which lessens the possibility of duct formation.

If the ground temperature in a nocturnal inversion falls below the dewpoint temperature, the water vapor in the lowest layers of the air condenses and the heat of condensation is released directly to the air. Under conditions of radiative fog formation, the humidity lapse tends to counteract any temperature inversion present and may cause substandard refraction if the humidity "inversion" is sufficiently strong. However, the temperature inversion may be strong enough to keep the layer standard or superrefractive.

Subsidence: Subsidence is the slow settling of air from a high pressure system. The air is heated by adiabatic compression as it descends and spreads out in a layer well above the earth's surface. This process

produces stable layers and inversions of temperature with an accompanying decrease in relative humidity. Since the air has come from a high level in the atmosphere, it is dry and may overlie a cooler, moist air mass. This type of inversion may cause the formation of an elevated superrefractive layer where the air temperature usually decreases immediately above the ground, rises through the inversion layer and decreases above the layer. This is a common occurrence which may be observed at any time. Subsidence has a tendency to destroy subrefractive layers and to intensify superrefractive layers. Although the effects of subsidence are generally observed at high levels, they are occasionally observed at lower levels, especially in the subtropics. Since subsidence frequently occurs in the lee of mountains and in the southeastern regions of northern hemisphere highs, elevated ducts may also be observed.

Conditions Inimical to Ducting: Conditions inimical to ducting are those which induce mixing of the lower atmosphere. Small scale atmospheric motions (turbulence) and consequent mixing and mass exchange result from differential surface heating and surface roughness effects. Both of these processes work to destroy stratification. They ultimately result in uniform vertical distribution of moisture through considerable depths of the lower atmosphere and the establishment of neutral temperature lapse rates. Accordingly, where the process of mechanical and convectively induced mixing are at work, the probability of the occurrence of ducting is vanishingly small. Thus, few, if any, ducts are observed over snow-free, low albedo land areas from mid-morning to late afternoon when the skies are clear, or in areas of moderate to great surface roughness when the surface winds are more than a few meters per second, irrespective of cloud conditions or the time of the day.

Refractive Conditions Due to Local Meteorological Phenomena

Land and Sea Breeze: Land and sea breeze may produce ducts along the coastal regions since the winds are of thermal origin, resulting from temperature differences between land and sea surfaces. During the day, when the land gets warmer than the sea, the air above the land rises and is replaced by air from the sea, thus creating a circulation from the sea to the land, called a sea breeze. During the night, the land becomes colder than the sea and a circulation, called a land breeze, is set up in the opposite direction. This type of circulation is generally shallow and does not extend higher than a few hundred meters above the land or sea surface.

A land or sea breeze may modify the refractive conditions in different ways depending upon the distribution of moisture in the lower layers. Since these breezes are of a local nature and generally extend only a few miles, only coastal locations are usually affected. The very nature of sea and land breezes results in a marked refractive index pattern. With a sea breeze a duct may be formed over the water due to subsidence. The land breeze is accompanied by subsiding air over the land with resultant duct formation.

Fog: The formation of fog results in a decrease of superrefractive or ducting possibilities. When fog forms by nocturnal radiation, the water content of the air remains practically the same; however, part of the water changes from the gaseous to the liquid phase thus reducing the vapor pressure. The resulting humidity lapse rate tends to counteract the temperature inversion and cause sub-standard refraction. However, the temperature inversion may be strong enough to keep the layer standard or superrefractive. This process may also occur with advection fogs.

Nocturnal Ducts: The night-time temperature profile is a result of the interaction between nocturnal radiation, turbulence, and heat conduction. The associated refractive index profiles are such that a radar duct begins to form about the time of sunset, developing quickly during the early evening, more slowly after midnight, and dissipating rapidly after sunrise. This is mainly an inland effect resulting from large diurnal temperature variations observed in the interiors of large continents. However, a shallow body of water may have an appreciable diurnal temperature variation, as compared to the open ocean so that superrefraction may occur over such a location from time to time.

Limitations of Radiosonde Observations: It is generally recognized that radiosonde observations (RAOB's) do not have a sufficiently high degree of accuracy to be completely acceptable for use in observing changes in the degree of stratification of the very lowest layers of the atmosphere; however, until more accurate methods such as meteorological towers and refractometer measurements are more commonly used, the RAOB will continue to be used as a basis for forecasting the occurrence of superrefractive conditions.

3. BACKGROUND

The property of the atmosphere basic to radio ray tracing is the radio refractive index of the atmosphere, n, which, for VHF-UHF frequencies at standard conditions near the surface, is a number of the order of 1.0003. Although the refractive index is used in ray tracing theory, it is more convenient when evaluating refraction effects from common meteorological observations to use the refractivity [Smith and Weintraub, 1953], N, which, for the frequency range 0 - 30,000 Mc, is given by:

$$(n - 1)\, 10^6 = N = \frac{77.6}{T}\left[P + \frac{4810\, e_s\, RH}{T}\right], \qquad (1)$$

where P is the station atmospheric pressure in millibars, and RH is the percent of the saturation vapor pressure, e_s, in millibars at the absolute temperature, T, in degrees Kelvin.

When evaluating the meteorological conditions that give rise to refractive phenomena, it is frequently instructive to examine separately the behavior of the dry component, D, and wet component, W, of N. These components are given by:

$$D = \frac{77.6}{T}\, P, \qquad (2)$$

and

$$W = \frac{3.73 \times 10^5\, e_s\, RH}{T^2} \cdot \qquad (3)$$

The gradient of the refractivity, ΔN, with respect to height may then be expressed:

$$\Delta N = \Delta D + \Delta W \qquad (4)$$

Average values of ΔN, ΔD and ΔW are given for two increments between the earth's surface and one kilometer above sea level for Fairbanks, Alaska; Washington, D. C.; and Swan Island, W. I.; in Table I.

Table I

Gradient of N, D and W in (N units per kilometer)

Station	Height Increment	February			August		
		$-\Delta N$	$-\Delta D$	$-\Delta W$	$-\Delta N$	$-\Delta D$	$-\Delta W$
Fairbanks, Alaska	surface - 0.5 Km	37	41	-4	31	27	4
	0.5 Km - 1.0 Km	35	35	0	36	24	12
Washington, D. C.	surface - 0.5 Km	41	34	7	60	28	32
	0.5 Km - 1.0 Km	30	26	4	46	24	22
Swan Island, W. I.	surface - 0.5 Km	39	24	15	47	26	21
	0.5 Km - 1.0 Km	58	24	34	66	24	42

Several general observations may be made of the data of Table I: The gradient of the dry term is relatively less variable than that of the wet term when considered as a function of season or height; the increase of ΔN from winter to summer at a particular location or from arctic to tropical climate at a given time is most strongly reflected in ΔW rather than in ΔD. The marked increase of gradient with height for Swan Island reflects the drop of refractivity across the interface of the trade wind inversion where dry subsiding air overlies the moist oceanic surface layer.

A fundamental equation used in radio ray tracing is Snell's law which, for polar coordinates, is given by:

$$n r \cos \theta = n_o r_o \cos \theta_o, \qquad (5)$$

where n is the radio refractive index of the atmosphere, r is the radial distance from the center of the earth to the point under consideration,

θ is the elevation angle made by the ray at the point under consideration with the tangent to the circle of radius r passing through that point. The radius to any point, r, is usually given as (a + h) where a is the radius of the earth and h is the height of the point above sea level. The zero subscript refers to the value of n, r, or θ at the earth's surface.

For the present study, geometrical optics techniques, similar to those considered by Bremmer [1949], are used to indicate when refraction is sufficiently great to direct a ray either back to earth or in a circular path at a constant height above the earth, i.e.:

$$\frac{n_o r_o \cos \theta_o}{n r} \geq 1. \tag{6}$$

This condition then allows one to obtain the value of θ_o which divides the rays into two groups; those that penetrate the duct and those that are trapped within the duct. This particular value of θ_o, called the angle of penetration and designated θ_p, is obtained by noting those instances where

$$\frac{n_o r_o}{n r} \geq 1 \tag{7}$$

and solving for the value of θ_o such that (6) is equal to unity.

It is instructive to consider the order of magnitude of refractive index gradient needed for trapping for several commonly observed refractive index profiles. If we rewrite Snell's law,

$$n_t r_t \cos \theta_t = n_A r_A \cos \theta_d, \tag{8}$$

where the subscripts t and A refer to the values of the variables at the transmitter height and the top of the trapping layer, then trapping occurs when

$$\frac{n_t\, r_t}{n_A\, r_A} \geq 1, \tag{9}$$

and the angle of penetration at the transmitter, θ_p, is given by setting

$$\frac{n_t\, r_t}{n_A\, r_A} \cos \theta_p = 1 . \tag{10}$$

The maximum permissible n gradient for a given value of θ_p is then given by:

$$\frac{\Delta n}{\Delta r} = - \frac{n_t - n_A}{r_A - r_t} , \tag{11}$$

where n_d must satisfy (10), i.e.:

$$n_A = \frac{n_t\, r_t}{r_A} \cos \theta_p . \tag{12}$$

By designating $r_A = r_t + h_A$, (11) becomes

$$\frac{\Delta n}{\Delta r} = - \frac{n_t}{h_A} \left[1 - \frac{r_t\, n_t}{r_t + h_A} \cos \theta_p \right] . \tag{13}$$

By rewriting (13),

$$\frac{\Delta n}{\Delta r} = - \frac{n_t}{h_A} \left[1 - \frac{1}{1 + \frac{h_A}{r_t}} \cos \theta_p \right] , \tag{14}$$

and expanding $\left(1 + \frac{h_A}{r_t}\right)^{-1}$ and cos θ_p, one obtains the expression:

$$\frac{\Delta n}{\Delta r} = - n_t \left[\frac{1}{r_t} + \frac{\theta_p^2}{2 h_A} \right] \qquad (15)$$

by neglecting terms of the order $\frac{\theta_p^4}{4}$ and $\left(\frac{1}{r_t}\right)^2$.

For the case of $\theta_p = 0$ (15) reduces to:

$$-\frac{\Delta n}{\Delta r} = \frac{n}{a} \sim \frac{1}{a} \sim 157 \quad \text{N units/kilometer} . \qquad (16)$$

It is seen from (15) that the n gradient necessary to trap a radio ray at a given value of θ_p is practically independent of transmitting antenna height above the earth. For example, a $\theta_p = 0$ ray will be trapped by an n gradient of -157.0 N units/kilometer at sea level, where $n_t \cong 1.0003$, while the necessary n gradient at 3 kilometers above sea level will be -156.9 N units/kilometers for an $n_t \cong 1.0002$. This indicates for all practical applications, that the necessary n gradient for trapping is independent of altitude. Further, by considering the temperature and humidity gradients encountered in the troposphere, one is led to the conclusion that ducting gradients would not be expected to occur at altitudes greater than 3 kilometers. In fact, Cowan's [1953] investigation indicates that trapping gradients are nearly always confined to the first kilometer above the surface.

A consideration of (15) indicates that the magnitude of the negative gradient necessary for ducting is 1/a for $\theta_p = 0$ but increases in proportion to $\theta_p^2/2h$ as θ_p increases. The gradients necessary for

atmospheric ducts as a function of θ_o are given for several different profiles in figure 1. An analysis of radiosonde data indicates that gradients in excess of 0.5 N units per meter are seldom exceeded within atmospheric layers. It is interesting to note how rapidly the necessary gradients increase to the approximate upper limit of radiosonde-observed gradients: a ground-based layer 100 meters thick attains this gradient at 8.3 milliradians while the maximum observed gradient is intercepted by the 30-meter layer curve at θ_o = 4.5 milliradians. A third example was calculated for an elevated layer 0.5 km above the ground and 100 meters thick by assuming normal refraction between the ground and the base of the layer and solving for the necessary ducting gradient within the layer. The large values of n gradient necessary for this case explains why elevated ducts were not observed. Although the preceding examples were calculated for a ground transmitter, the combinations of θ_p, $\Delta n/\Delta r$, and Δr are very nearly the same as would be obtained for any other transmitter height within the first 3 kilometers above the surface.

4. DESCRIPTION OF OBSERVED GROUND-BASED ATMOSPHERIC DUCTS

Approximately three years of radiosonde data typical of an arctic climate (Fairbanks, Alaska), a temperate climate (Washington, D. C.), and a tropical maritime climate (Swan Island, W. I.) were examined by means of a digital computer for the occurrence of ducts during the months of February, May, August, and November. The percentage occurrence of ducts is shown on figure 2. The maximum occurrences of 13.8% for August at Swan Island and 9.2% for Fairbanks in February are significantly greater than the values observed at other times of the year.

REFRACTIVITY GRADIENTS NEEDED FOR RADIO DUCTS

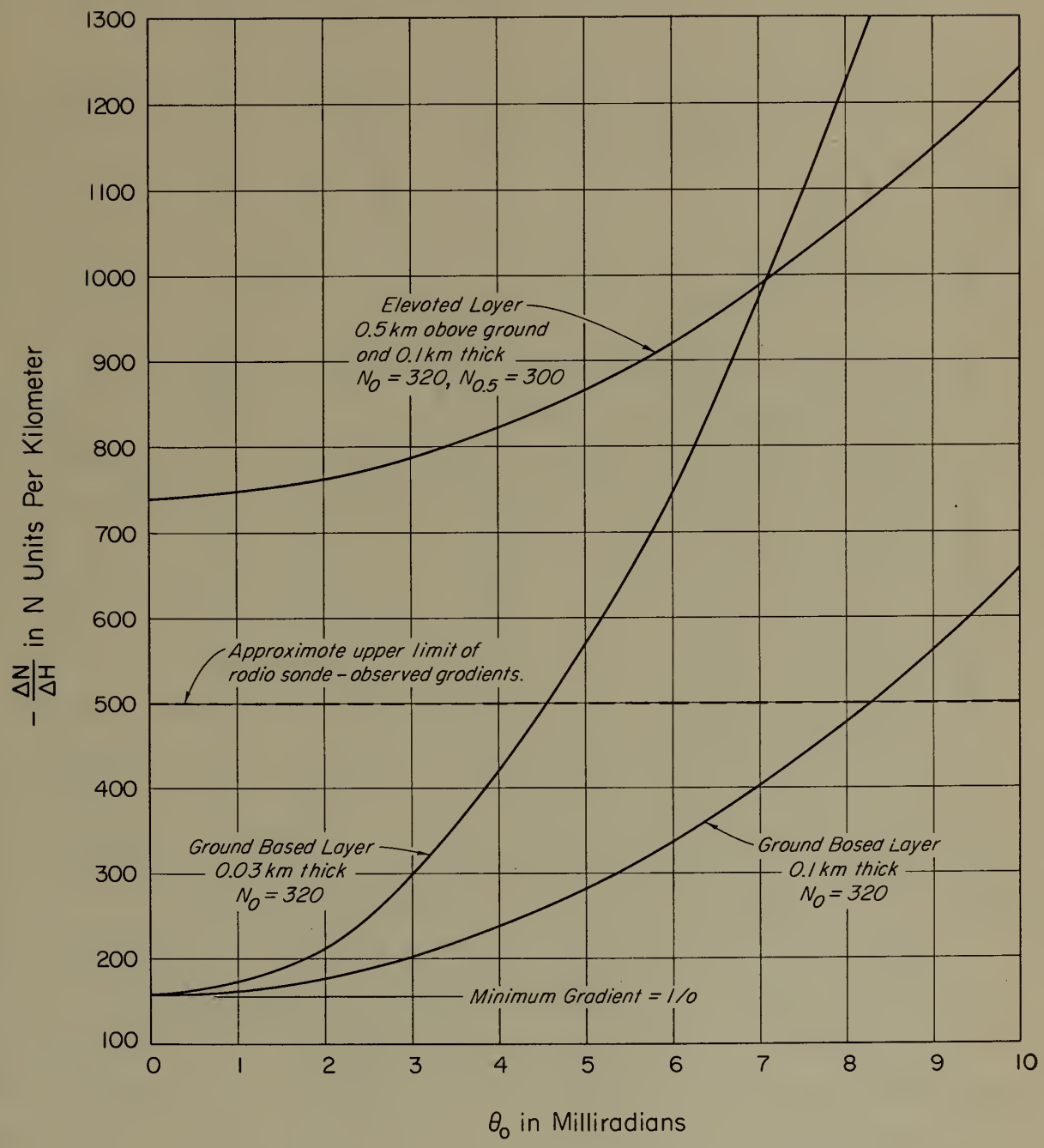

Figure 1

FREQUENCY OF OCCURRENCE OF GROUND BASED DUCTS

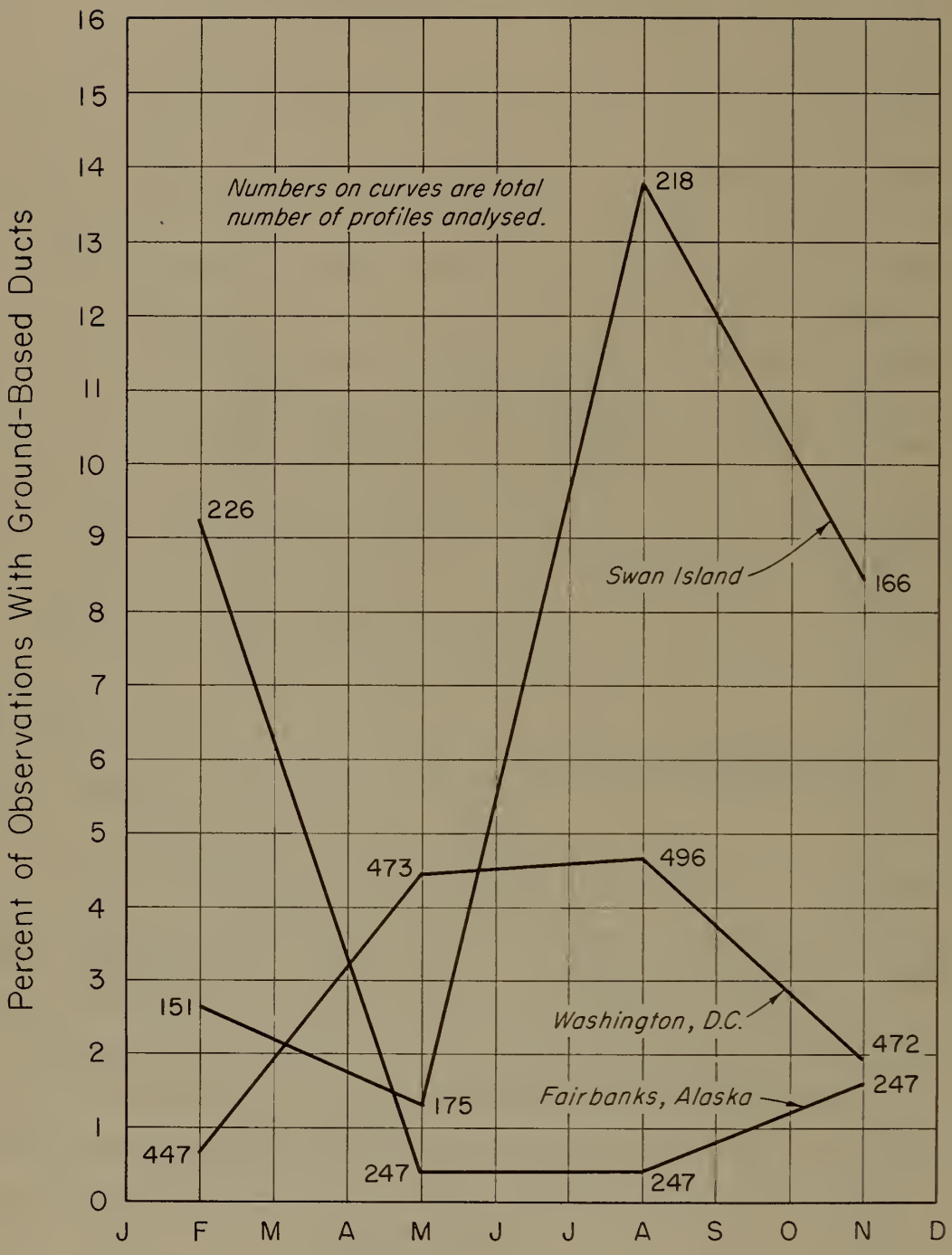

Figure 2

The Washington data display a summertime maximum of 4.6%. These data indicate that the temperate zone maximum incidence is about one-half the wintertime maximum incidence in the arctic, and about one-third of the summertime tropical maximum.

The range of observed values of θ_p is shown in figure 3. The mean value calculated for each month as well as the maximum and minimum values of θ_p observed for the limiting cases are given for each month and location. The mean value of the angle of penetration under these conditions is between 2 and 3 milliradians and appears to be independent of climate. The maximum value of θ_p observed during ducting is 5.8 milliradians.

The refractivity gradients observed during ducting are given on figure 4. The maximum gradient of 420 N units per kilometer was observed during February at Fairbanks, Alaska. The mean values of N gradient appear to follow a slight climatic trend from a high value of 230 N units per kilometer at Fairbanks to a value of 190 N units per kilometer at Swan Island.

Another property of radio ducts is their thickness which is given in figure 5. Again there is observed a slight climatic trend as the median thickness increases from 66 meters at Fairbanks to 106 meters at Swan Island. These values of thickness correspond to the gradients given in figure 4. One can then obtain, by linear extrapolation the thickness at which the gradient is equal to $-1/a$; i.e., the height corresponding to the gradient just sufficient to trap the ray at $\theta_o = 0$. These values, shown on figure 6, display an increase in the median thickness of about 25% for Swan Island, 100% for Washington, and 200% for Fairbanks, which results in a reversal of the climatic trend of the observed thickness between Fairbanks and Swan Island. This increase in height emphasized the preceding conclusion. Fairbanks is characterized by shallow layers with relative intense gradients.

ANGLE OF PENETRATION OF GROUND-BASED DUCTS

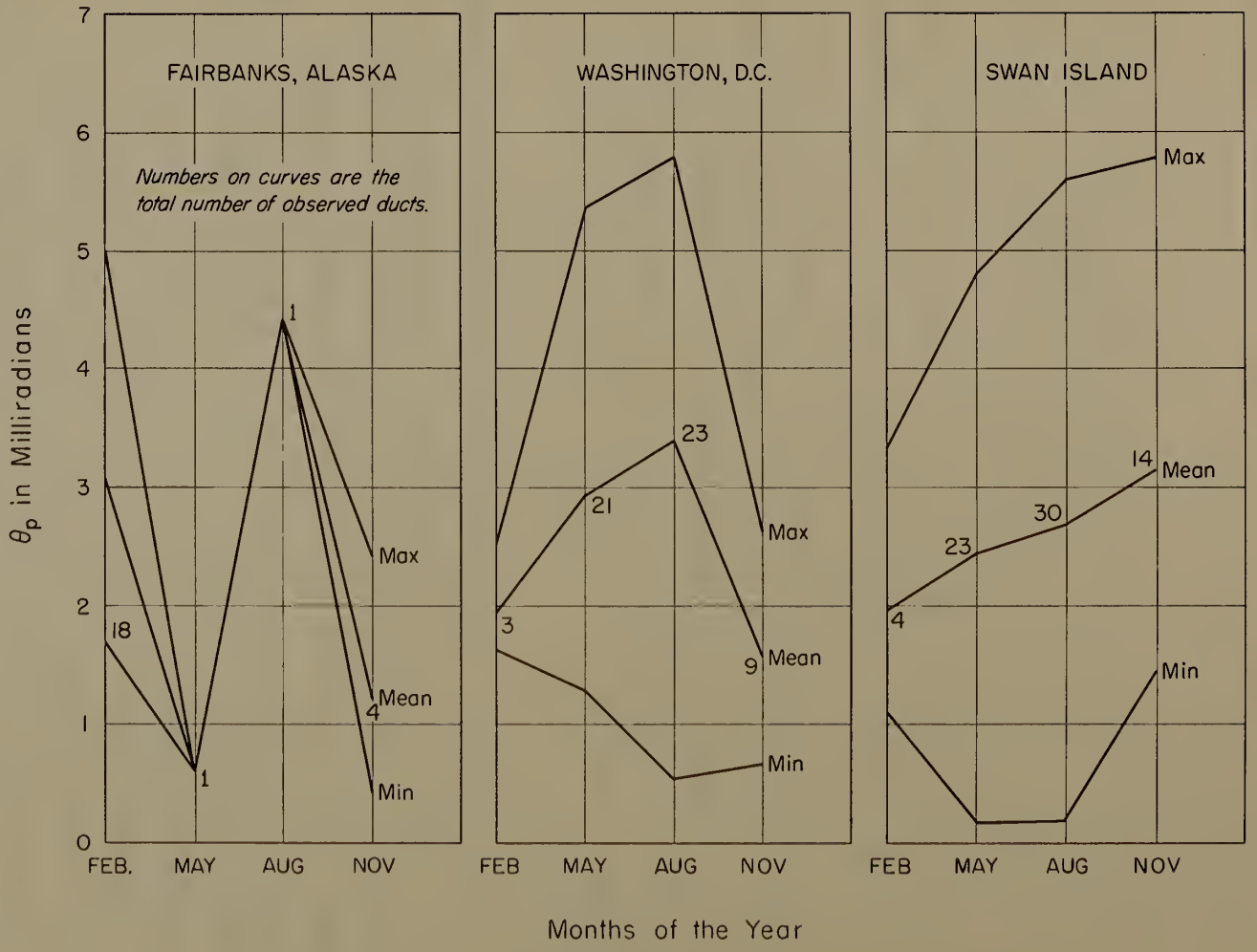

Figure 3

REFRACTIVITY GRADIENTS OF GROUND-BASED DUCTS

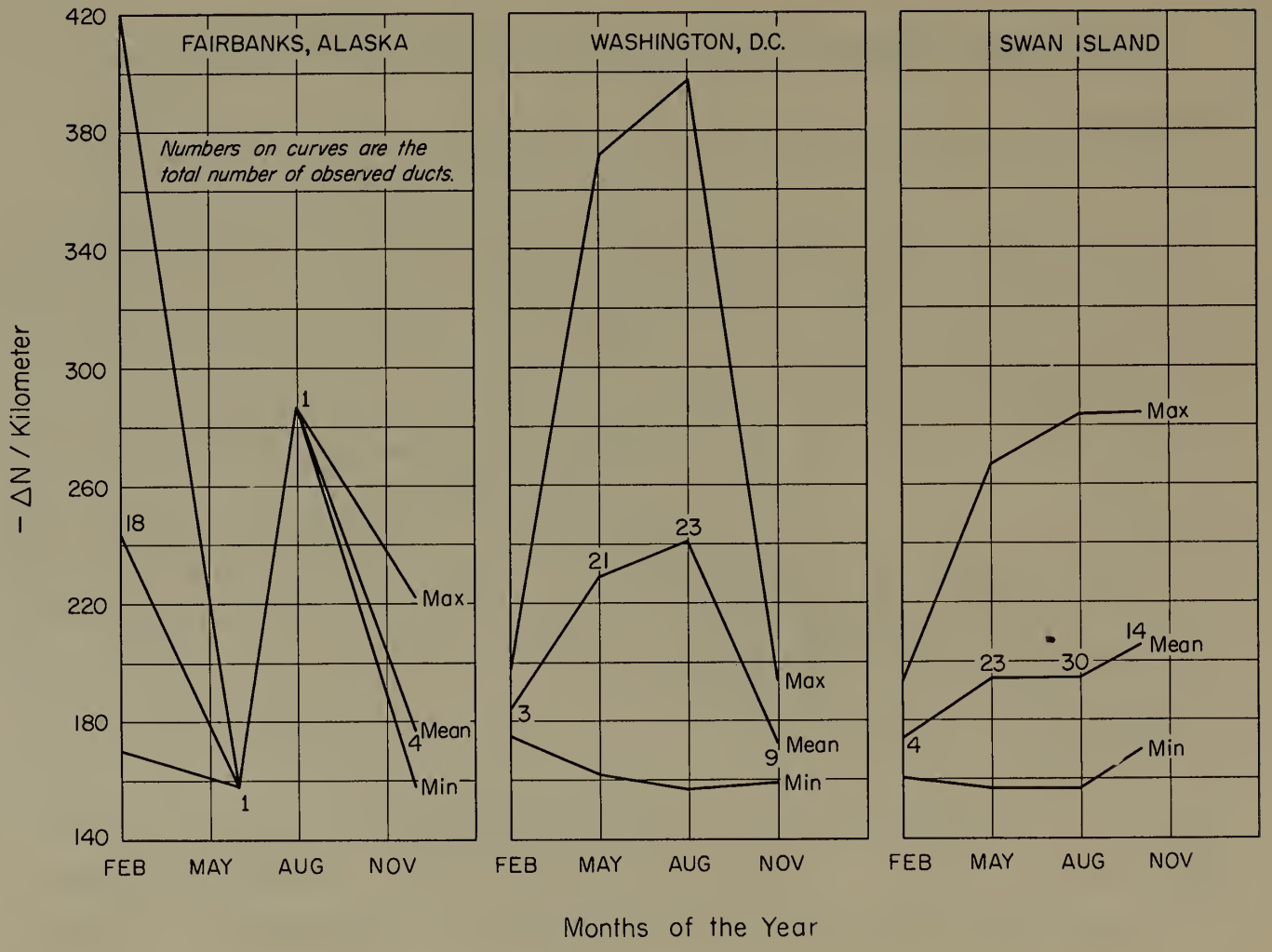

Figure 4

OBSERVED GROUND-BASED DUCT THICKNESS

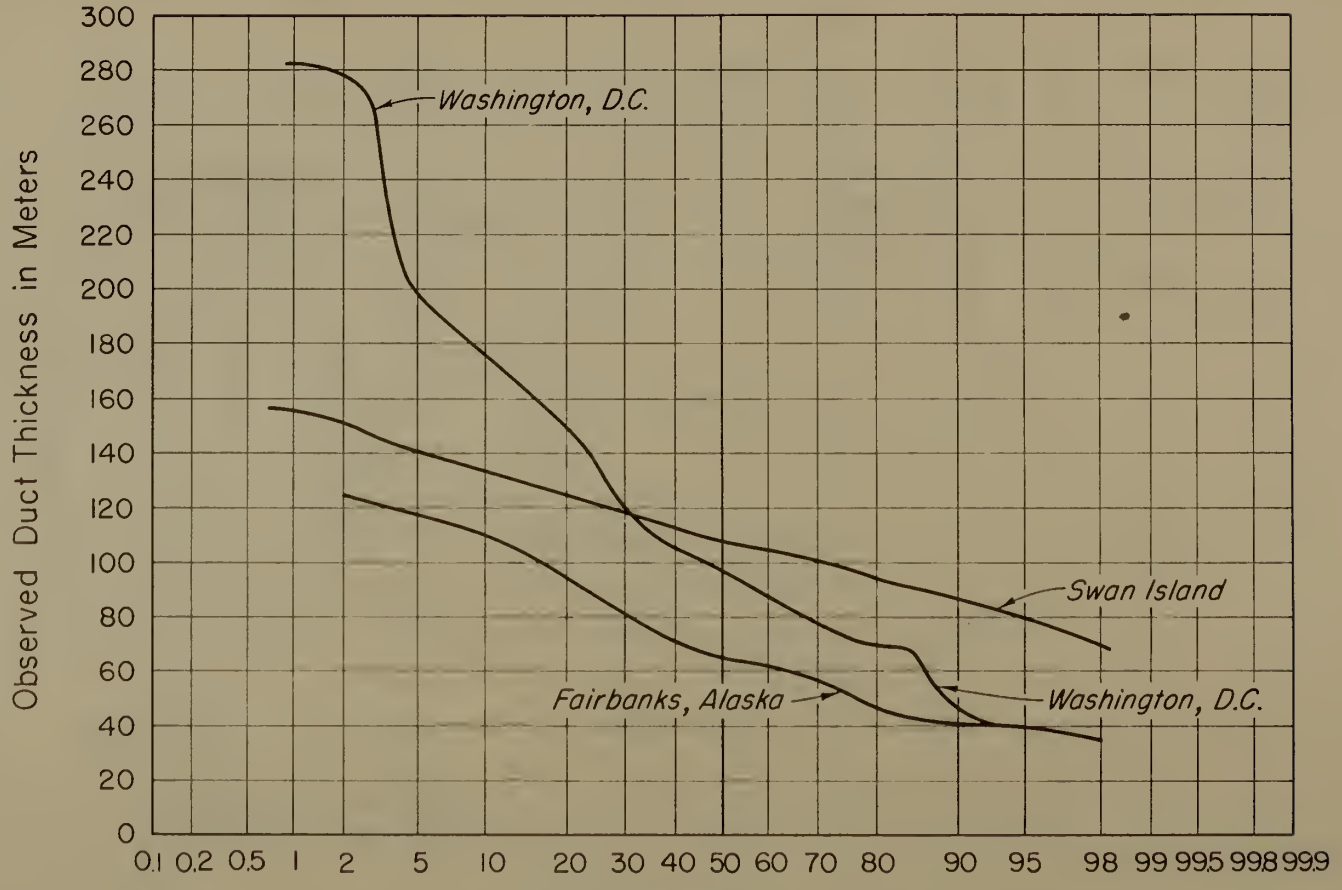

Figure 5

MAXIMUM GROUND-BASED DUCT THICKNESS

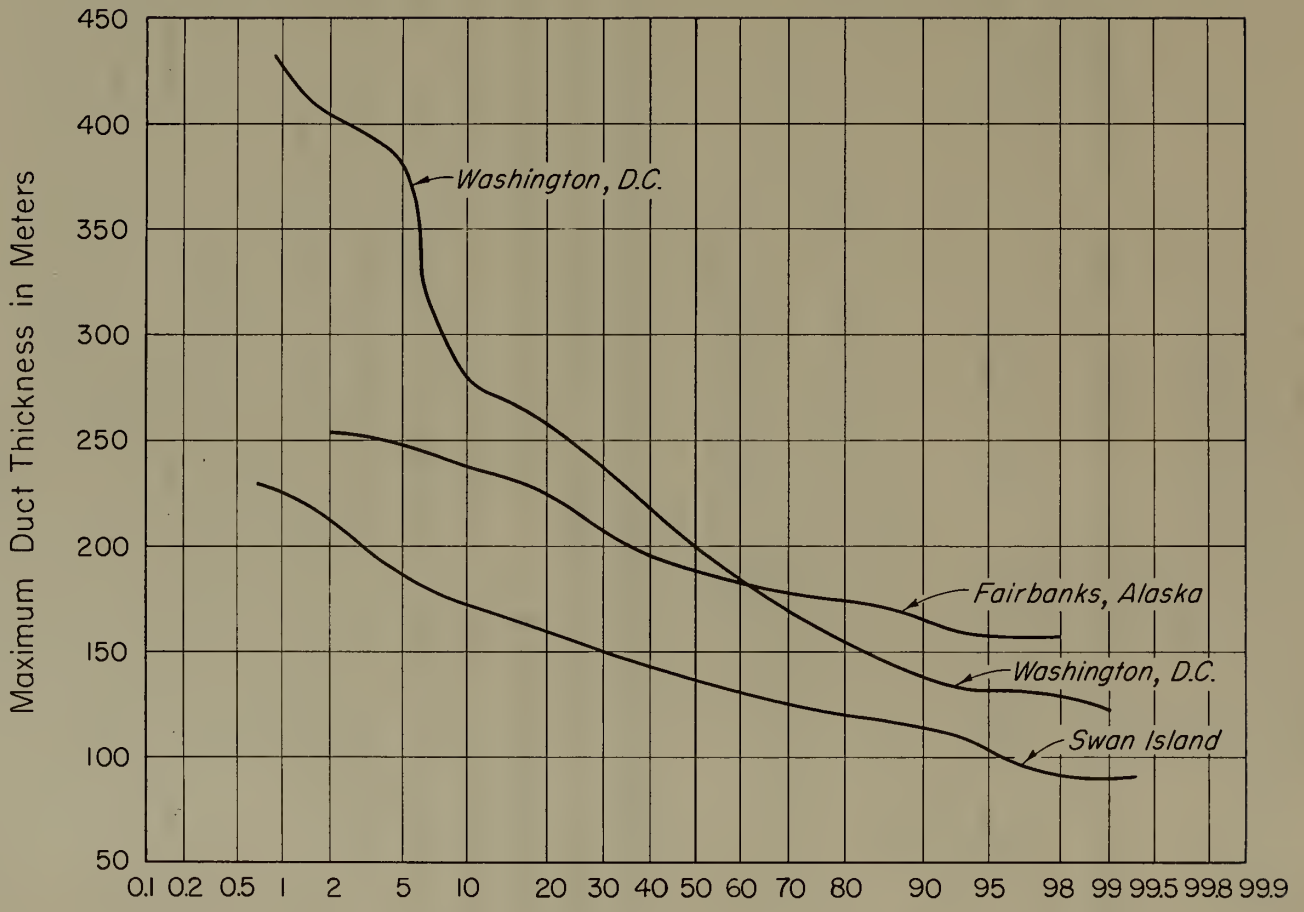

Figure 6

These maximum duct widths may be used to estimate the maximum radio wavelengths trapped. Kerr [1951] gives the maximum wavelength, λ, trapped by given thickness, d:

$$\lambda_{max} = c\gamma^{1/2} d^{3/2}, \tag{17}$$

by assuming a linear decrease of n within the duct. The coefficient c is a constant and γ is a function of the n gradient excess over the minimum value of $\Delta N/\Delta H = 1/a$. Expressing λ_{max} in centimeters, and d in meters, then

$$\gamma = \left(\frac{N_t - N_d}{d} - .157 \right) .10^{-6}, \tag{18}$$

and

$$c = 2.514 \times 10^{2}.$$

The maximum wavelengths trapped during ducting conditions were estimated by (17) for the maximum duct thicknesses of figure 6. These values, given in Table II, were determined for the month with the maximum occurrence of ducts, thus allowing an estimate of the radio frequencies likely to be effected by ducting conditions. Note, for example, that the data of Table II indicate that 1000 Mc rays (λ = 30 cm) will be trapped by 50% of the ducts regardless of location.

The reader is cautioned that an atmospheric duct does not have the sharp boundaries of a metallic waveguide. Thus the maximum wavelengths obtained by (17) do not represent cut-off frequencies but, as Kerr is so careful to emphasize, merely suggest lower limits under the assumptions of this rudimentary theory.

Table II

Estimated Maximum Wavelength Trapped at $\theta_o = 0$

Station	Percentage of ducts that trap wavelengths in centimeters equal to or shorter than tabulated value						
	95%	90%	75%	50%	25%	10%	5%
Fairbanks, Alaska (February)	20.5	22.6	25.5	34.0	43.5	61.5	69.0
Washington, D. C. (August)	7	10	27	50	112	164	200
Swan Island (August)	12	23	41.5	60	82.3	92	132

5. TEMPERATURE AND HUMIDITY DISTRIBUTIONS ASSOCIATED WITH DUCTS

An example of the temperature and humidity distribution typical of each station is given on figure 7. The Fairbanks duct is accompanied by a surface temperature of -25°C with a strong temperature inversion and a slight humidity lapse, indicating temperature inversions associated with wintertime cooling of the air next to the ground. The Washington example appears to be typical of the temperate zone temperature inversion. The Swan Island profile shows a moderate lapse of both temperature and humidity. This apparent contradiction is explained by the strong lapse in vapor pressure associated with the moderate lapse in temperature when the initial temperature is near 30°C. The strong vapor pressure lapse presumably arises from evaporation from the sea surface. This effect was further examined by studying the percentage of the total N gradient of each duct that was contributed by the gradient of the dry and wet terms. The median contribution of the dry term gradient, summarized in Table III, displays strong seasonal and geographic differences.

Table III

Median Contribution of $\Delta D/\Delta H$ to $\Delta N/\Delta H$ for Ducting Conditions

	Fairbanks	Washington, D. C.	Swan Island
February	103%	73.0%	9.5%
May	40.5%	33.5%	2.0%
August	37.0%	26.5%	4.5%
November	62.0%	55.0%	6.0%

The dry term contribution decreases from summer to winter and from arctic to tropical climates. The Swan Island ducting gradients are at least 90% due to humidity lapse, while the Fairbanks winter time maximum is due to the strong temperature inversion associated with very low surface temperatures. In fact, under these conditions, vapor pressure increases with height with the result that the dry term contributes more than 100% of the ducting gradient.

TEMPERATURE AND HUMIDITY PROFILES FOR TYPICAL GROUND-BASED DUCTS

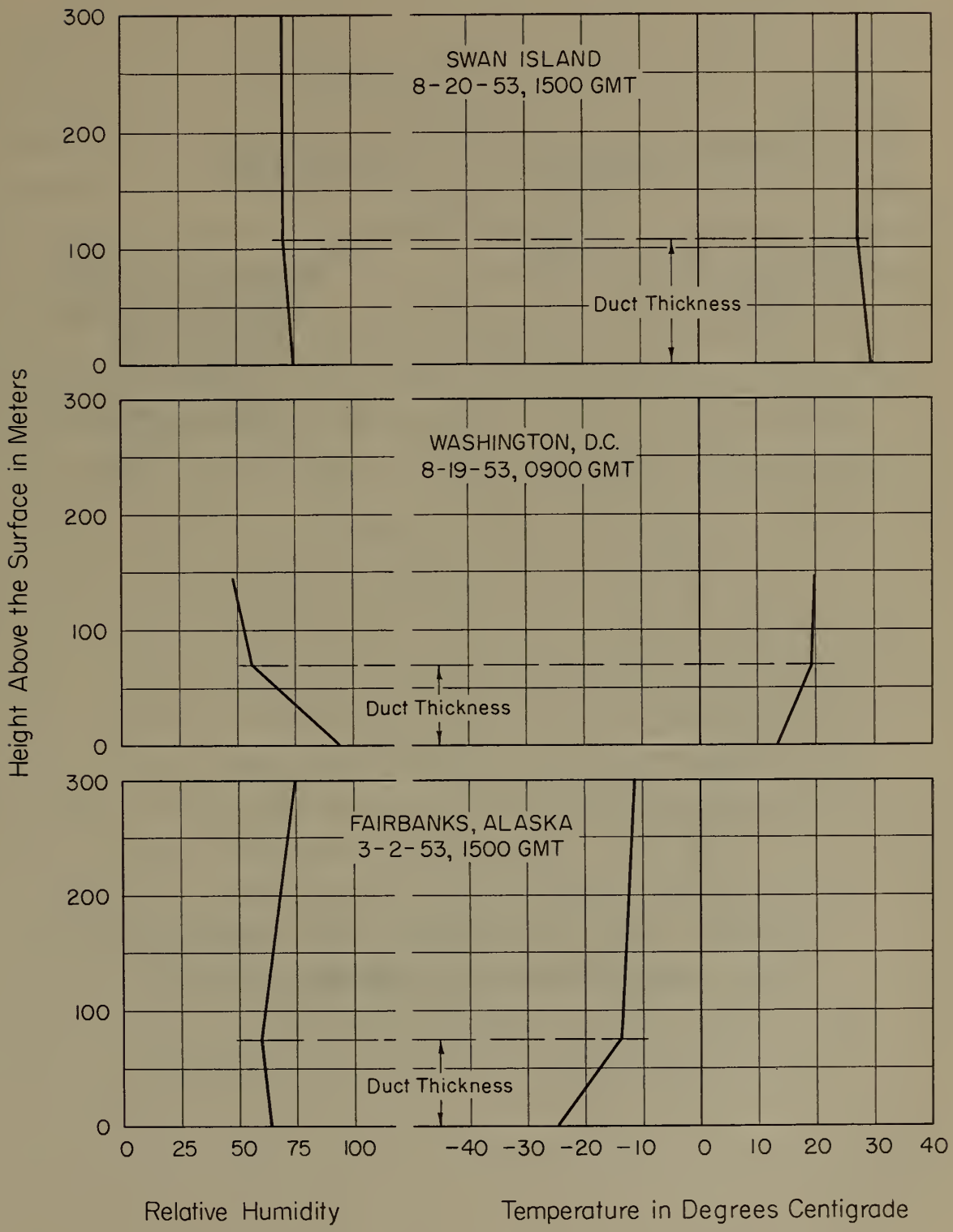

Figure 7

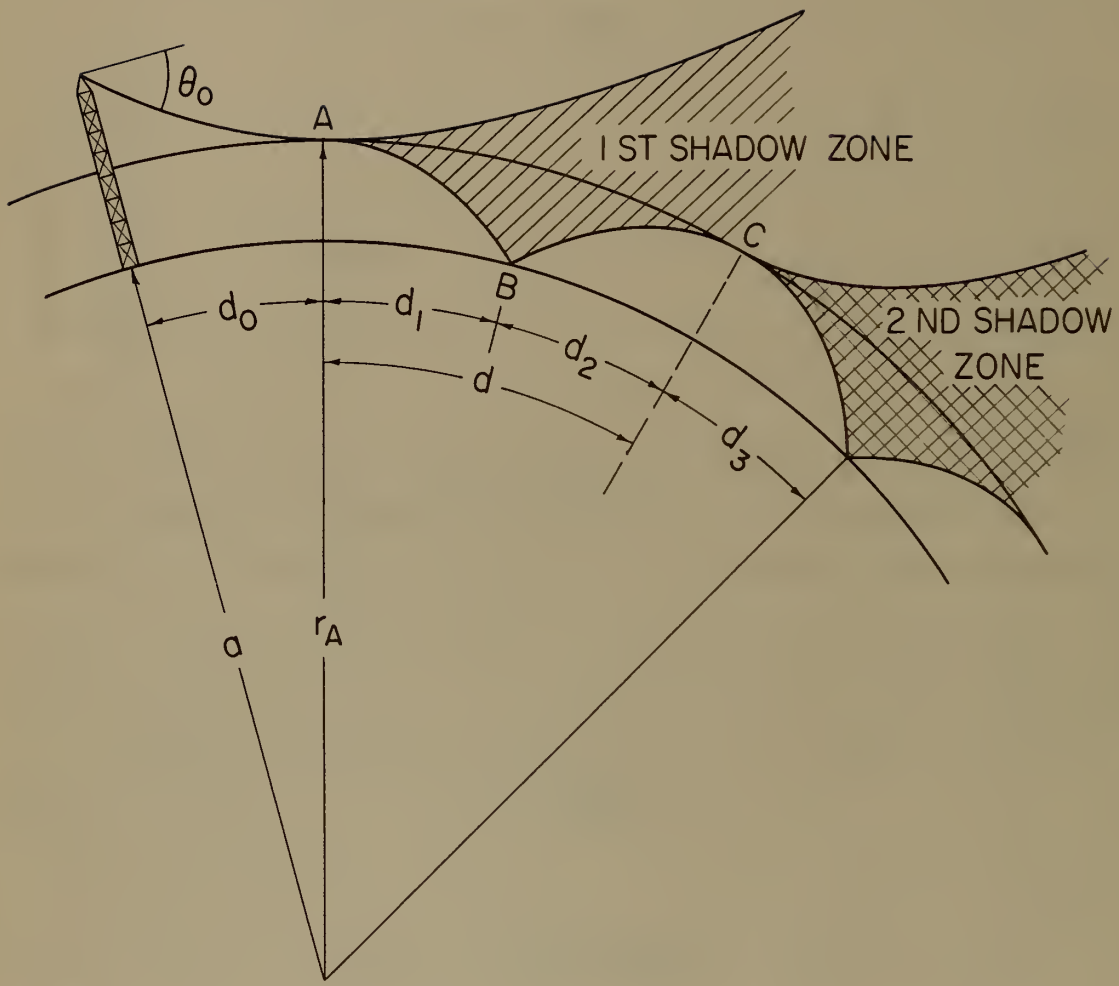

SHADOW ZONE OCCURRENCE ON A CURVED EARTH
WITH THE TRANSMITTER ABOVE THE DUCT

Figure 8

6. CONCLUSIONS: Part I

The results given above were derived from a consideration of radiosonde data. Although the radiosonde is not an extremely sensitive instrument, it is readily available and is the only source of climatic information involving the temperature and humidity structure of the atmosphere. It is believed that the radiosonde data will at least yield the climatic trend of radio ducts as well as their probable temperature and humidity distributions. Further, it is evident that the choice of stations will definitely affect the percentage of ducts observed. For example, it is almost certain that a greater percentage of ducts would be observed over water in the sub-tropics than over Swan Island.

With these reservations in mind, the present study has shown:

(a) Ducts occur no more than 15% of the time.

(b) The annual cycle of the incidence of ducts is reversed for the arctic and tropical stations studied. The arctic station has a wintertime maximum and the tropic station a summertime maximum. The temperate station has a summertime maximum incidence of less than 5%.

(c) The maximum initial elevation angle is limited to 5.8 mr with a mean value of about 3 mr.

(d) The steepest gradient of N observed is -420 N units per kilometer.

(e) The maximum thickness of observed ducts is such as to trap radio-waves of 1000 Mc and above at all locations for at least 50% of the observed ducts.

(f) Ducts in the arctic appear to be associated with temperature inversions at ground temperatures of $-25^{\circ}C$ or less; temperate zone, with the common radiation inversion and accompanying humidity lapse; tropics, with a moderate temperature and humidity lapse for temperatures of about $30^{\circ}C$.

Part II. A Study of Fading Regions Within the Horizon Caused by A Surface Duct Below a Transmitter.

7. INTRODUCTION

Among the factors influencing the choice of an antenna site for a microwave receiver operating on a line-of-sight path is the desirability of locating in a region relatively free from space-wave fadeouts. Although line-of-sight propagation is normally characterized by steady, high, dependable signals, deep, prolonged space-wave fadeouts are observed from time to time. Since serious disruptions occur during such fadeouts, a systematic discussion of fading phenomena is of considerable interest to the radio circuit engineer.

This section describes the conditions under which fading occurs, fading variations, and locations that favor the occurrence of fading within the radio horizon.

Fading, or fadeout, of a radio wave may be defined as a drop in power or field strength below a specified level of intensity. For a given site, criteria may be set up by the communications engineer to establish the magnitude of drop that defines the onset of fading conditions. This magnitude usually ranges from about 5 to 30 db below the specified level of intensity. The specified level is derived from some ideal propagation condition.

Fading is also a time-dependent occurrence. It may be classified as (a) prolonged fading, which is fading of sufficient interval to cause continued communication disruptions, and (b) short-term or "roller" fading, which is only instanteously observed by a receiver. The differentiation between prolonged and short-term fading is left to the discretion of the communications engineer.

One of the main causes of deep fading of field strength within the horizon as compared with the free space field strength value is the structure of the atmosphere. When one refers to the "structure" of the atmosphere, one generally means the refractive index structure. An easier way of representing the structure of the atmosphere is by means of the radio refractivity, N. Theoretically, the atmosphere might be considered horizontally homogeneous and in spherical stratifications concentric with the earth, and N can be considered to decrease exponentially with increasing height above the earth's surface. However, in reality, this picture of the atmosphere is rarely, if ever, realized, because of the synoptic meteorological conditions that are perpetually present. Stratifications caused by the synoptic meteorological pattern give rise to field strength fading within the horizon by defocusing the lobe pattern of the transmitter along a given path. Whenever the rate of change of refractivity from the surface value with height (called the gradient of N with height) is less than -157 N units per kilometer, a "ducting" condition is said to exist at the surface, and, as shown in figure 1, certain rays will tend to be "trapped" or guided within the surface duct. It is this atmospheric condition of surface ducting which will be further explored herein with respect to fading within the radio horizon.

8. REGIONS AND EXTENT OF FADING WITHIN THE HORIZON IN THE PRESENCE OF SUPERREFRACTION

Serious disruptions in reception from a transmitter above a duct to a receiver within a duct can occur at particular points within the horizon. It is these disruptions, and these locations, which are of interest to the communications engineer establishing a given transmitting-receiving path. Whenever these disruptions occur between a transmitter and receiver within the horizon, a corresponding increase in the field strength characterized by steady high, dependable signals, is usually expected beyond the horizon. The high signal strength is in keeping with the properties of a surface duct. Nevertheless, deep, prolonged fadeouts can occur in regions beyond the horizon as well as within the horizon.

Price [1948] has theoretically determined regions of deep radio fading associated with surface ducts, which he has termed "shadow zones". In the case of a transmitter above a surface duct, a representation of what occurs is shown in figure 9. It shows the location of a shadow zone above the radio horizon line in the normal interference region. In the interference region, a fadeout of signal strength due to the presence of superrefraction must be compared with the value of the field when only the interference pattern is present. Papers such as those by Norton [1941], and Kirby, Herbstreit, and Norton [1951] give methods for calculation of the normal interference field. Ikegami [1959] gives a more general method for the calculation of received power in the presence of ground-based ducts.

In the procedure that follows, a model for the determination of the location and extent of shadow zones, rather than the determinations of the actual received field strengths and powers at any particular point, will be

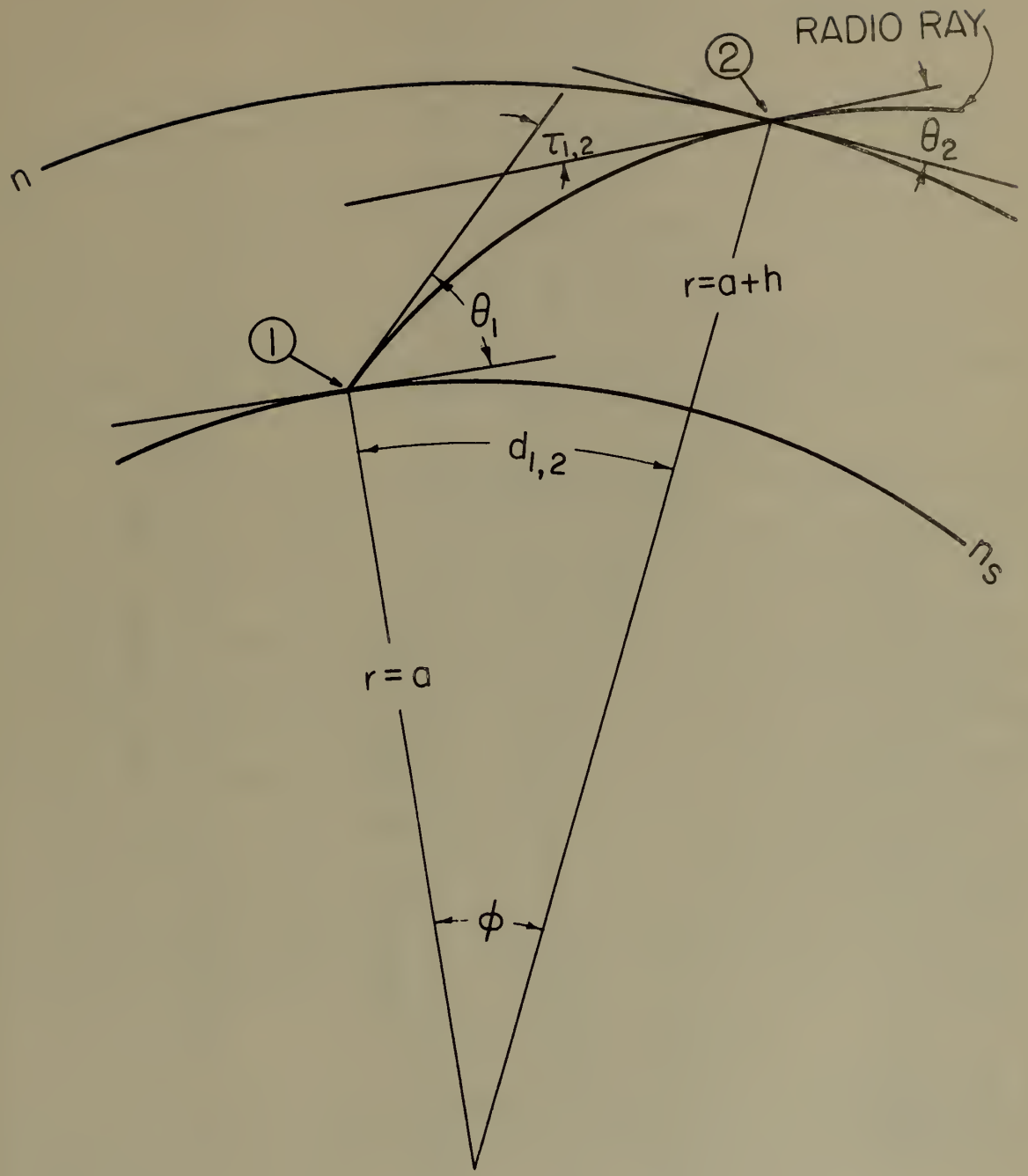

Figure 8a

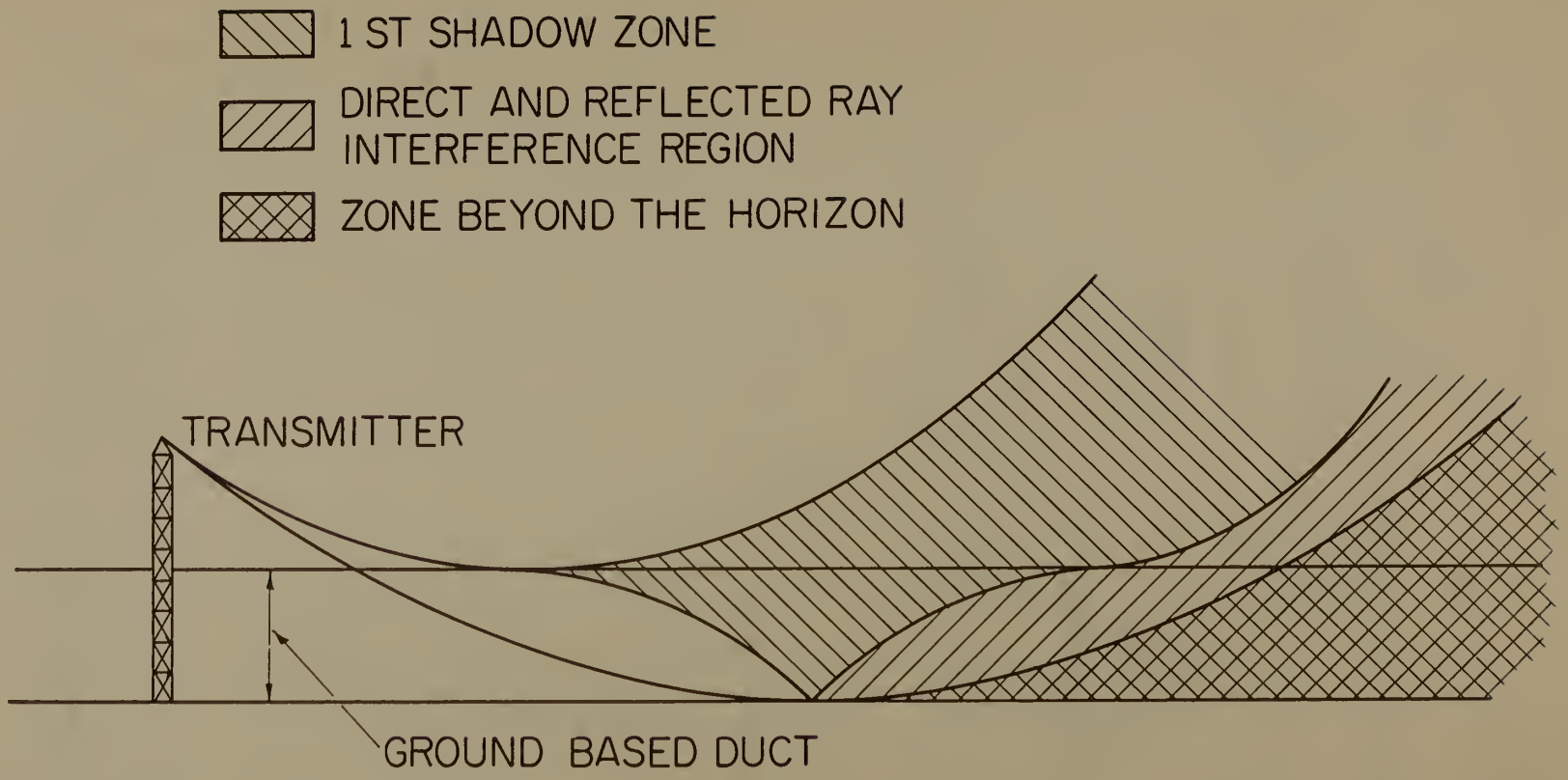

REGIONS OF FADING FROM DIFFERENT EFFECTS OF THE RADIO RAYS

Figure 9

given for conditions typical of the arctic, temperate, and tropical climates to aid the radio circuit engineer in avoiding these troublesome interference areas.

Washington, D.C., is taken to represent an average temperate zone climate, Swan Island an average tropical zone climate, and Fairbanks, Alaska, an average arctic zone climate. Considerable work has been done in determination of various ducting conditions at these three stations as well as with the average exponential refractivity above these stations. Therefore, these three stations will be used as models for all following calculations.

The gradient of N with height determines whether or not a surface duct will exist. Therefore, surface ducting atmospheres corresponding to conditions at Washington, D. C., Swan Island, and Fairbanks, consisting of a ducting gradient up to any desired height and the N_s = 313.0, 377.2, and 313.0 exponential atmospheres of Bean and Thayer [1959] above this height, have been chosen for this study. The ducting gradients chosen are maximum, mean, and minimum values for February, May, August, and November (representing the middle of winter, spring, summer, and fall, respectively) taken from figure 4 and given in Table IV. Also in these particular models the duct is assumed to be of uniform height throughout the region considered in the calculations.

9. THEORY AND RESULTS

In figure 8, although it is known that ray theory does not explain what happens to the radio ray at the point A when the ray is tangent to the top of the duct, because of the apparent ray intersection, it is sufficient to define the first shadow zone as that zone between the two possible paths of the ray tangent to the duct at a point A (this is the ray emitted from the transmitter with an initial angle of θ_o with the horizontal).

TABLE IV

Ranges of Surface Ducting Gradients

Duct Gradients at Washington D.C.	N units/km February	N units/km May	N units/km August	N units/km November
Max	-200	-372	-395	-195
Mean	-185	-230	-240	-170
Min	-175	-162	-158	-159

Duct Gradients at Swan Island	N units/km February	N units/km May	N units/km August	N units/km November
Max	-195	-268	-282	-282
Mean	-173	-193	-193	-203
Min	-160	-158	-158	-170

Ducts Gradients at Fairbanks, Alaska	N units/km February	N units/km May	N units/km August	N units/km November
Max	-420	-159	-286	-222
Mean	-242	-159	-286	-177
Min	-169	-159	-286	-159

This is possible because it can be readily seen that no radiation will be able to enter the shadow zone, and thus, a receiver located in the shadow zone will theoretically receive no signal from the transmitter. The portion of the "split" ray that enters the duct at A will be reflected at point B to point C, where it "splits" again. The distance, d, from point A to C projected along the earth's surface will be designated the "length" of the first shadow zone. If the surface duct is homogeneous throughout, the ray will be symmetrical about point B and, therefore,

$$d_1 = d_2 = d/2 = d_{h.\ell}\,, \tag{19}$$

where d_1, and d_2 are the "half-lengths", $d_{h\ell}$, of the shadow zone.

Schulkin [1952] shows that the bending, $\tau_{1,2}$, of a radio wave between any two points in the atmosphere is given by

$$\tau_{1,2} = \frac{d_{1,2}}{a} + (\theta_1 - \theta_2), \tag{20}$$

where $d_{1,2}$ is the distance between the two points 1 and 2 (See figure 8a) projected along the earth's surface, a is the radius of the earth, and θ_1 and θ_2 are the angles in radians the ray makes with the horizontal at points 1 and 2 respectively. Schulkin [1952] also gives $\tau_{1,2}$ in radians as

$$\tau_{1,2} = \frac{\Delta n_1 - \Delta n_2}{\theta_m} \quad \text{for } 0 \leq \theta_o \leq 10^o, \tag{21}$$

where $\Delta n_1 = n_1 - 1$, $\Delta n_2 = n_2 - 1$, $\theta_m = (\theta_1 + \theta_2)/2$. In terms of refractivity, equation (21) becomes

$$\tau_{1,2} = \frac{(N_1 - N_2) \times 10^{-6}}{\theta_m} = \frac{\Delta N \times 10^{-6}}{\theta_m}\,. \tag{22}$$

Considering now the case of the half-length, $d_{h\ell}$, equation (22) becomes

$$\tau_{1,2} = \frac{d_{h\ell}}{a} + \theta_p\,, \tag{23}$$

since $\theta_2 = 0$ at the top of the duct, and $\theta_1 = \theta_p$ (See figure 8). Now substituting equation (22) in equation (23):

$$\frac{2\Delta N \times 10^{-6}}{\theta_p} = \frac{d_{h\ell}}{a} + \theta_p\,, \tag{24}$$

since here $\theta_m = \theta_p / 2$. Rearranging equation (24)

$$d_{h\ell} = a \left[\frac{2\Delta N \times 10^{-6}}{\theta_p \text{ (rad)}} + \theta_p \text{ (rad)} \right] . \tag{25}$$

Since

$$\theta_{p \text{ (rad)}} = \cos^{-1} \frac{n_A r_A}{n_o a} \simeq \sqrt{2 \left[\Delta N \times 10^{-6} - \frac{(r_A - a)}{a} \right]} , \tag{26}$$

where n_A is the index of refraction at the top of the duct, r_A is the distance from the center of the earth to the top of the duct, and n_o is the index of refraction at the earth's surface, it is seen that $d_{h\ell}$ is uniquely determined from the surface gradient of N with height inside the duct, provided the height of the duct is known.

If one desires to know the distance, d_h, for a particular height, h, from the reflection point of the ray in the duct (point B in figure 8), where d_h is such that

$$0 \leq d_h \leq d_{h\ell} , \tag{27}$$

then equation (20) becomes

$$d_h = a \left[\frac{2\Delta N' \times 10^{-6}}{\theta_p + \theta_2} + (\theta_p - \theta_2) \right] , \tag{28}$$

since θ_2 is no longer just equal to zero, but is such that

$$0 < \theta_2 \leq \theta_p , \tag{29}$$

and $\Delta N'$ will no longer be the same as the ΔN for the duct width.

θ_2 may be determined from the formula:

$$\theta_2 \cong \sqrt{\theta_p^2 + \frac{2h}{a} - 2\Delta N'} \quad , \tag{30}$$

In figures 10 - 18 the shadow zone half-lengths are given as a function of duct height for the various seasons of the year. In figures 19 - 22 the Washington, D. C., values of shadow zone half-length are again given as a function of duct height, but this time the ducting gradient is used as a parameter. This was done specifically to point out the seasonal trend of the half-lengths. Washington is the only station plotted since it is the only station of the three considered that has an appreciable seasonal variation in weather along with sufficient data with which to plot the trend. As might be expected, a wider range of distance variations is to be found in the spring and summer months than in the fall and winter months because of the greater percentage of ducts at Washington, D. C., during the spring and summer seasons. As shown in figure 5, the 50% level, or median of observed ground-based duct thickness at Washington, D. C., is about 100 meters, at Swan Island about 108 meters, and at Fairbanks, Alaska, about 65 meters. The 50% levels of observed maximum ground-based duct thicknesses are about 200, 135, and 185 meters, respectively, for Washington, D. C., Swan Island, and Fairbanks, Alaska. In Table V, the values of $d_{h\ell}$ during the four seasons are shown for the 65, 100, 108, 135, 185, and 200 meter surface duct heights.

As previously mentioned, the atmospheres above the assumed duct were taken to coincide with the N_s = 313.0, 377.2, and 313.0 exponential atmospheres of Bean and Thayer [1959] because these values most nearly correspond to the annual average N_s value at Washington, D. C., Swan Island, and Fairbanks, respectively. Figures 23 - 26 show the distance measured along the earth's surface that a ray with an initial elevation angle

SHADOW ZONE HALF-LENGTHS FOR MAXIMUM DUCTING CONDITIONS AT WASHINGTON, D.C.

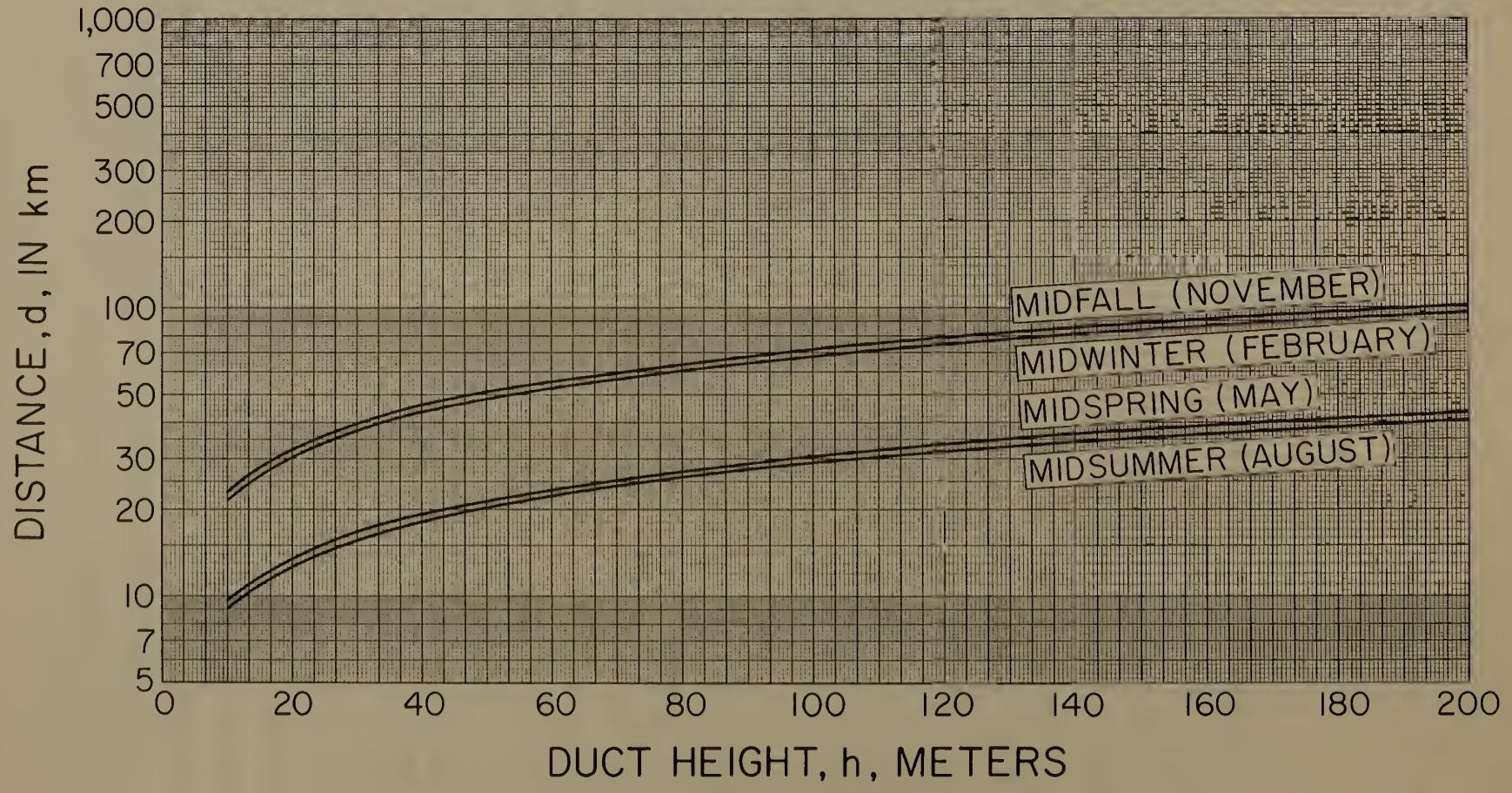

Figure 10

SHADOW ZONE HALF-LENGTHS FOR MEAN DUCTING CONDITIONS AT WASHINGTON, D.C.

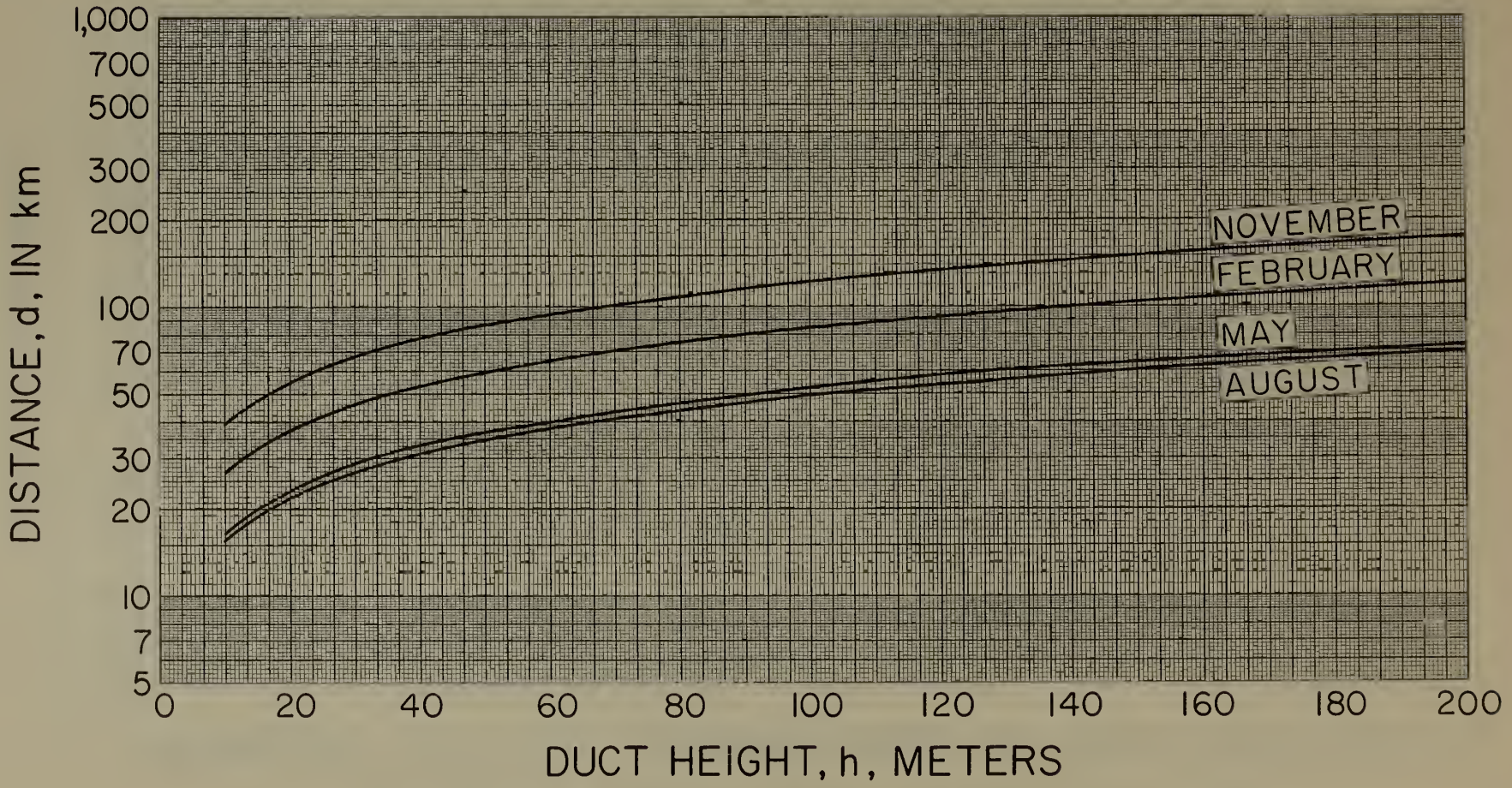

Figure 11

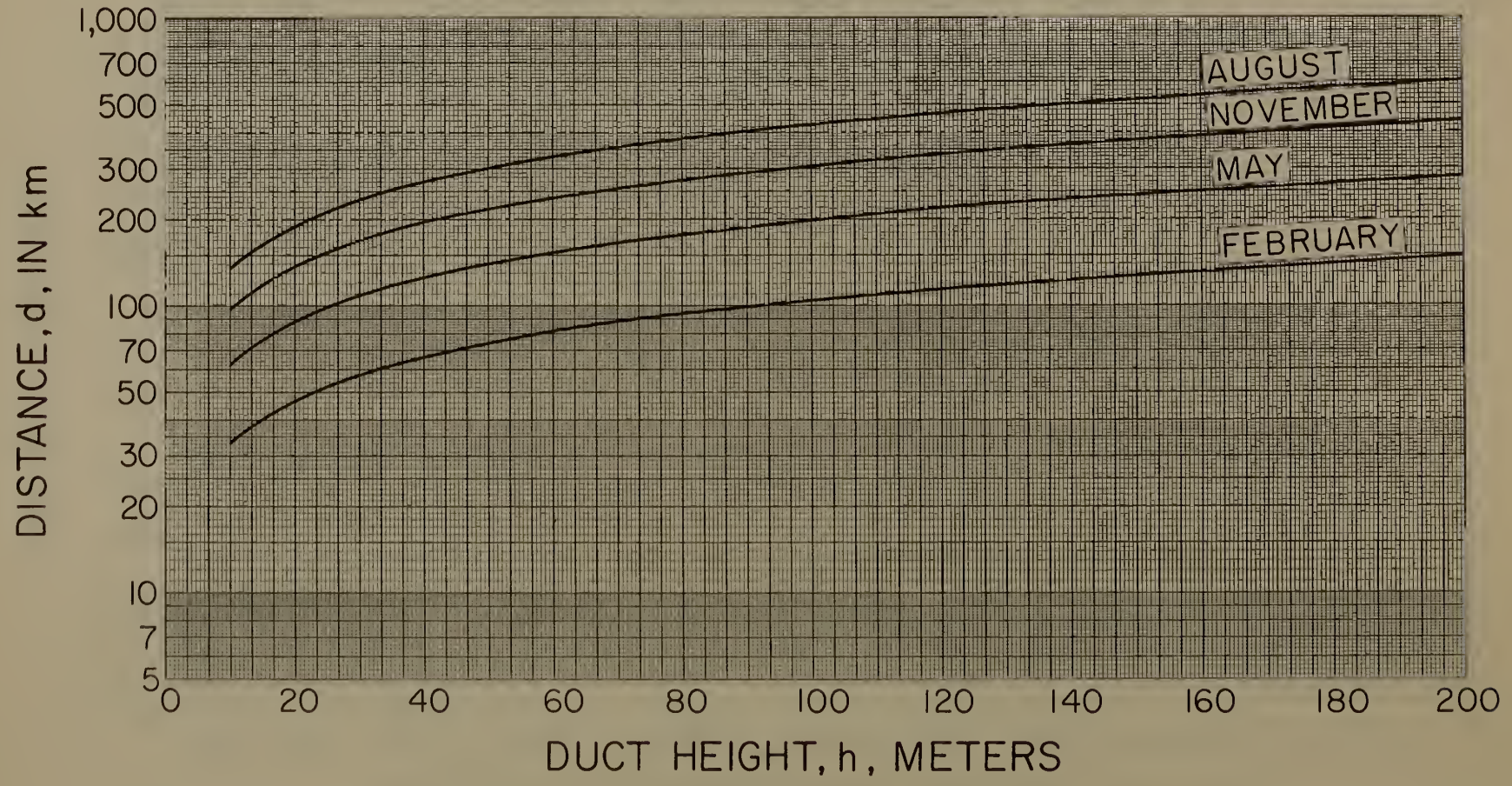
SHADOW ZONE HALF-LENGTHS FOR
MINIMUM DUCTING CONDITIONS AT WASHINGTON, D.C.
DISTANCE, d, IN km
1,000
700
500
300
200
100
70
50
30
20
10
7
5
AUGUST
NOVEMBER
MAY
FEBRUARY
0
20
40
60
80
100
120
140
160
180
200
DUCT HEIGHT, h, METERS

Figure 12

SHADOW ZONE HALF-LENGTHS FOR MAXIMUM DUCTING CONDITIONS AT SWAN ISLAND

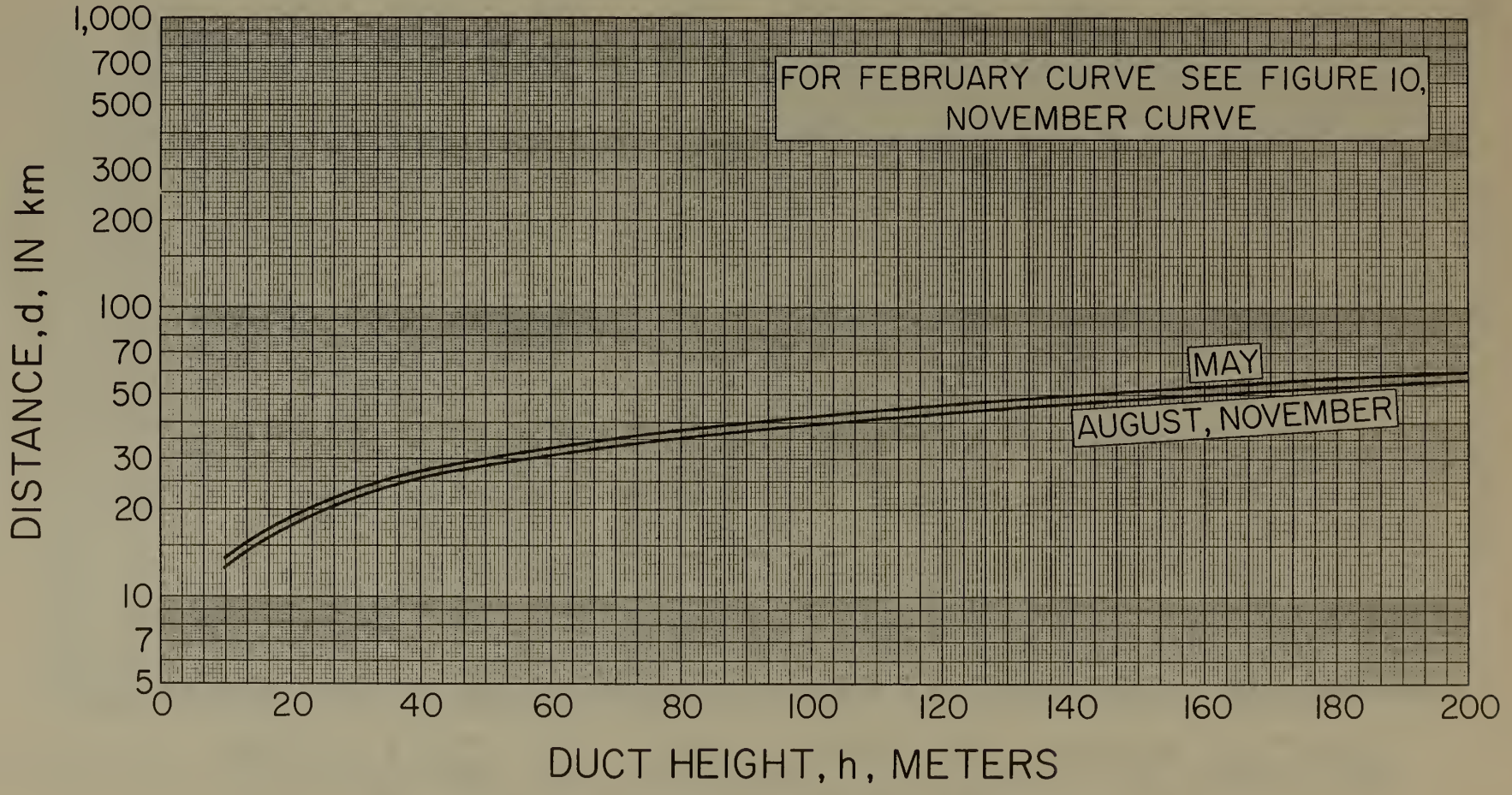

Figure 13

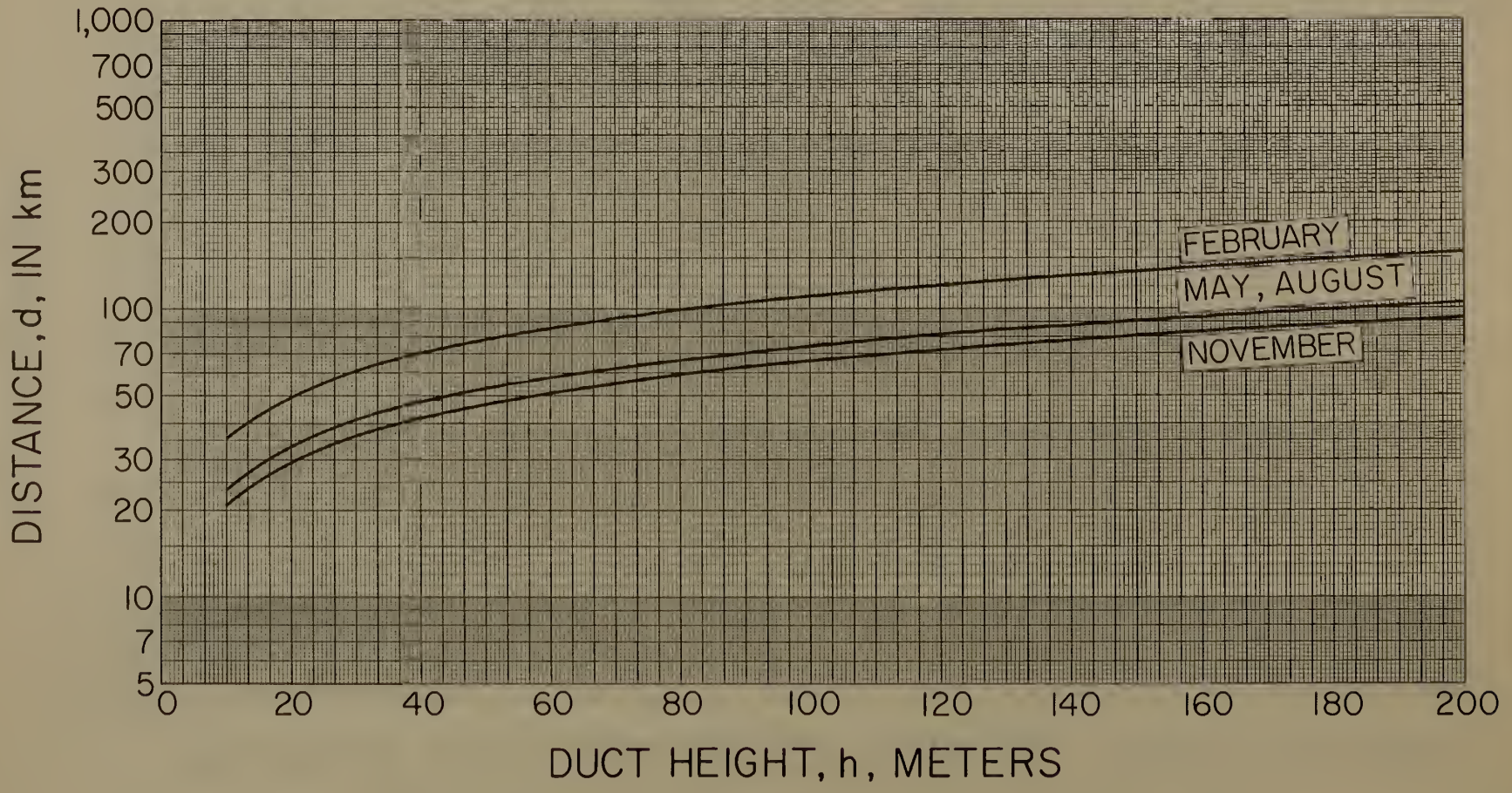
SHADOW ZONE HALF-LENGTHS FOR
MEAN DUCTING CONDITIONS AT SWAN ISLAND
DISTANCE, d, IN km
1,000
700
500
300
200
100
70
50
30
20
10
7
5
0
20
40
60
80
100
120
140
160
180
200
DUCT HEIGHT, h, METERS
FEBRUARY
MAY, AUGUST
NOVEMBER

Figure 14

SHADOW ZONE HALF-LENGTHS FOR MAXIMUM DUCTING CONDITIONS AT FAIRBANKS, ALASKA

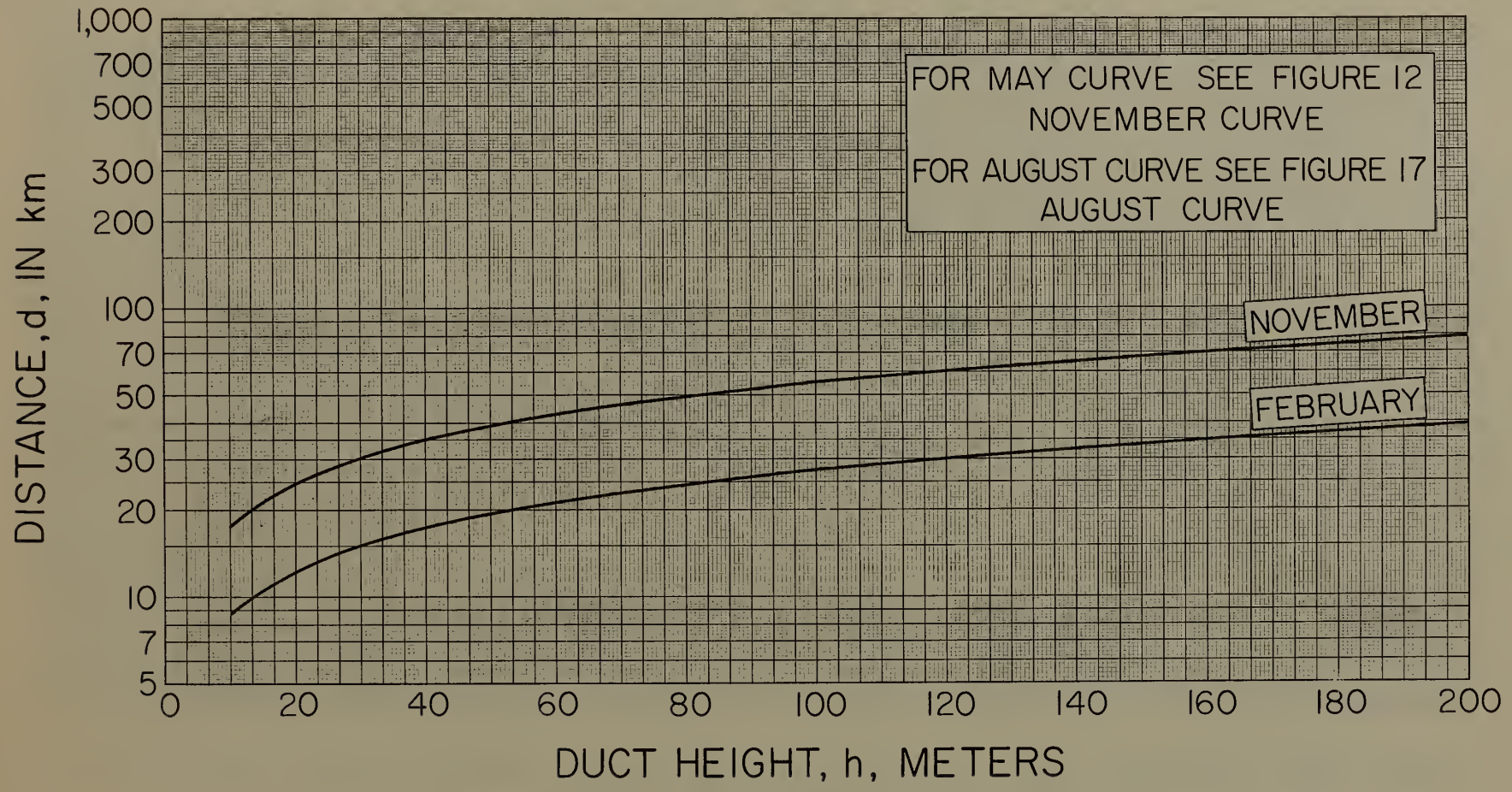

Figure 16

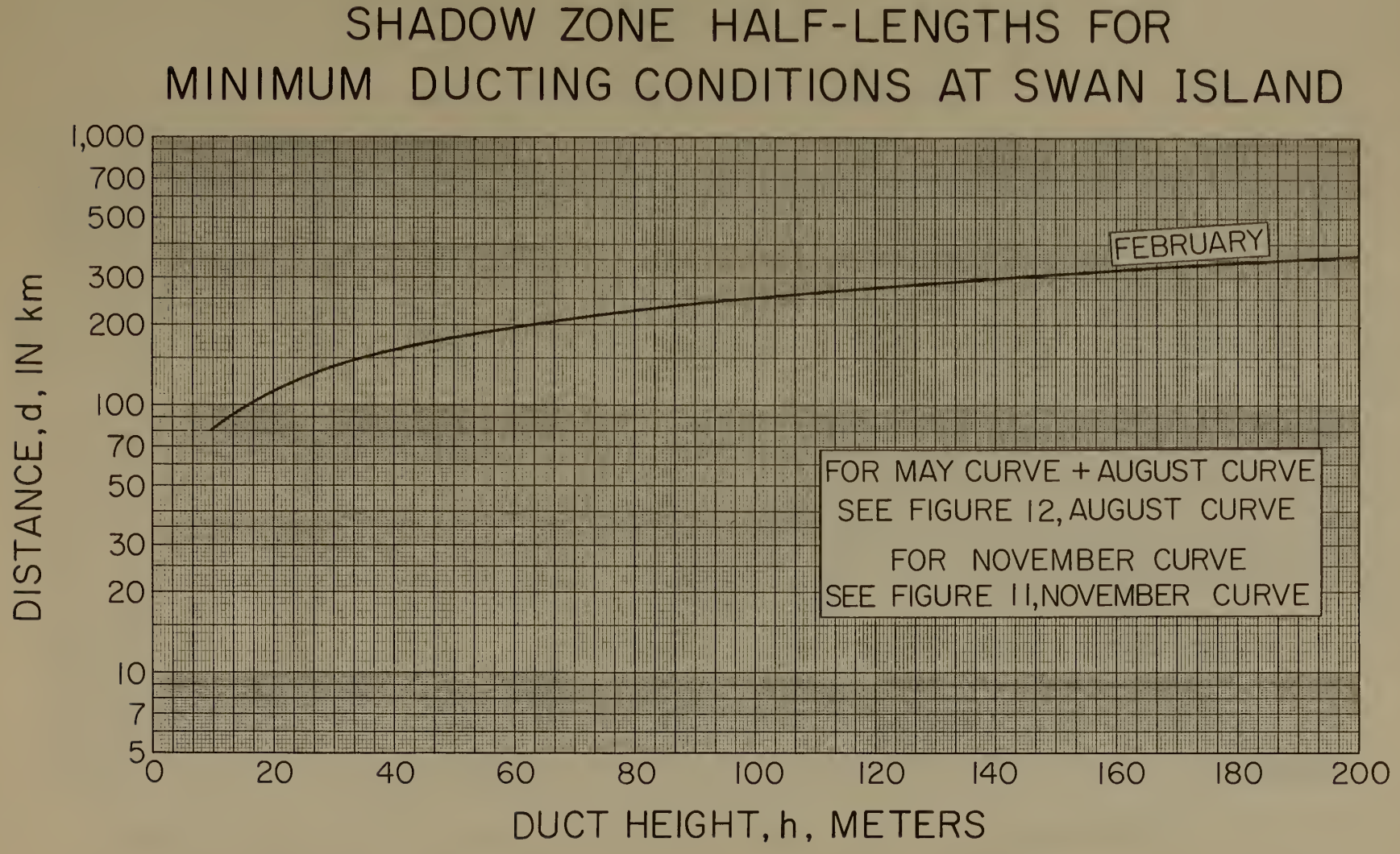
SHADOW ZONE HALF-LENGTHS FOR
MINIMUM DUCTING CONDITIONS AT SWAN ISLAND
DISTANCE, d, IN km
1,000
700
500
300
200
100
70
50
30
20
10
7
5
0
20
40
60
80
100
120
140
160
180
200
DUCT HEIGHT, h, METERS
FEBRUARY
FOR MAY CURVE + AUGUST CURVE
SEE FIGURE 12, AUGUST CURVE
FOR NOVEMBER CURVE
SEE FIGURE 11, NOVEMBER CURVE

Figure 15

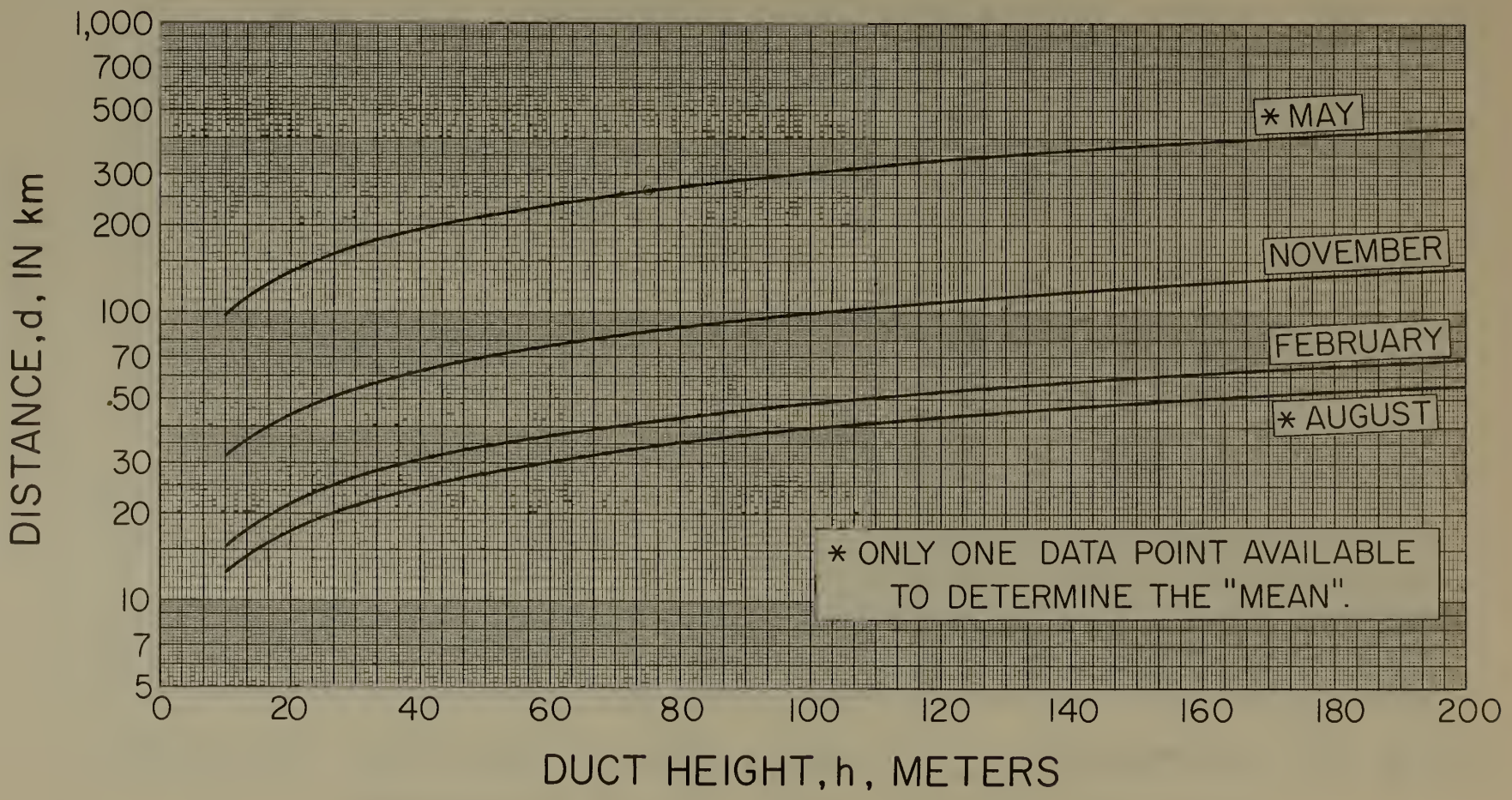
SHADOW ZONE HALF-LENGTHS FOR
MEAN DUCTING CONDITIONS AT FAIRBANKS, ALASKA
DISTANCE, d, IN km
1,000
700
500
300
200
100
70
50
30
20
10
7
5
0
20
40
60
80
100
120
140
160
180
200
DUCT HEIGHT, h, METERS
* MAY
NOVEMBER
FEBRUARY
* AUGUST
* ONLY ONE DATA POINT AVAILABLE
TO DETERMINE THE "MEAN".

Figure 17

SHADOW ZONE HALF-LENGTHS FOR MINIMUM DUCTING CONDITIONS AT FAIRBANKS, ALASKA

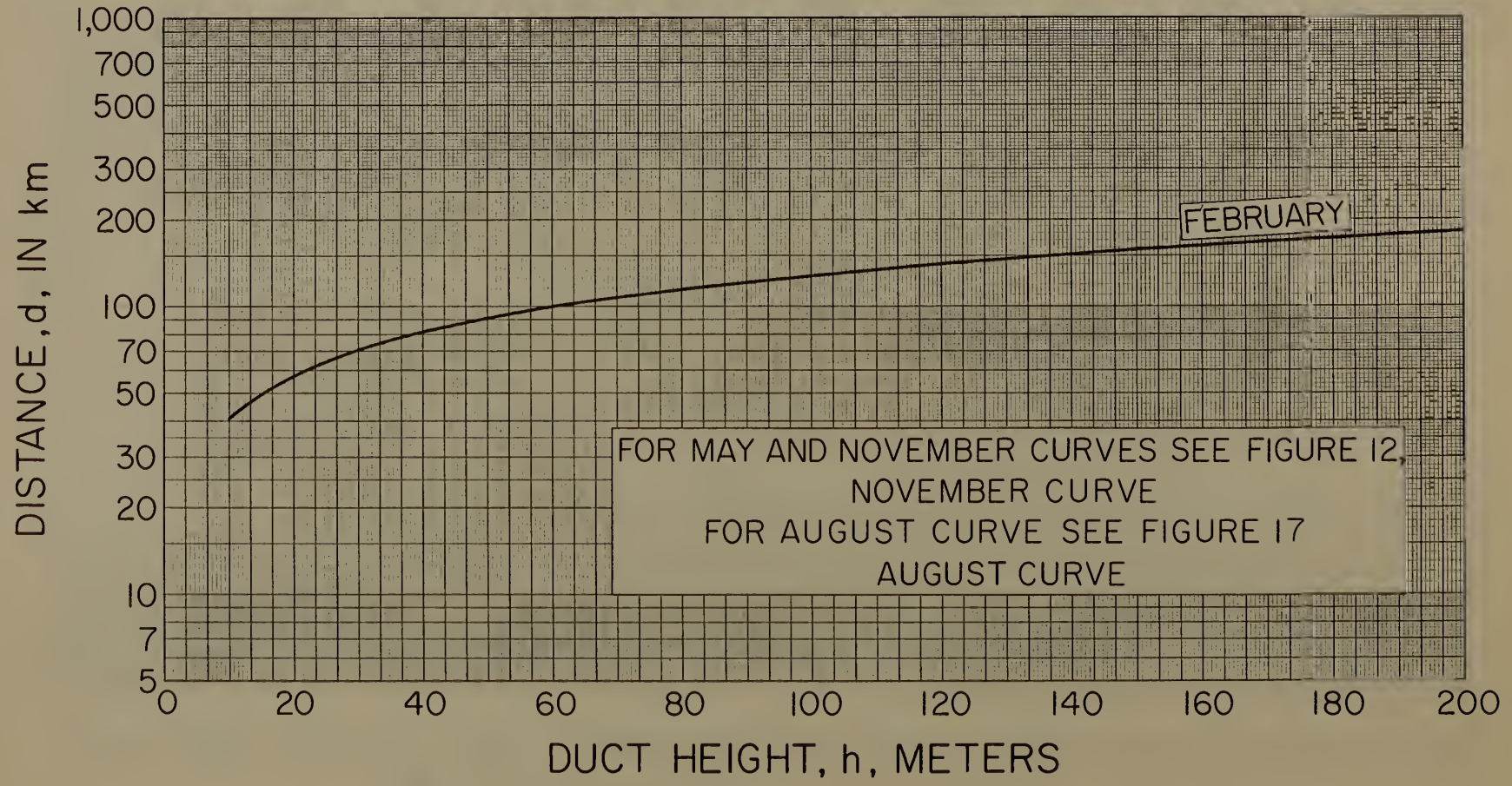

Figure 18

SHADOW ZONE HALF-LENGTHS FOR WASHINGTON, D.C. DUCTING CONDITIONS IN MIDWINTER (FEBRUARY)

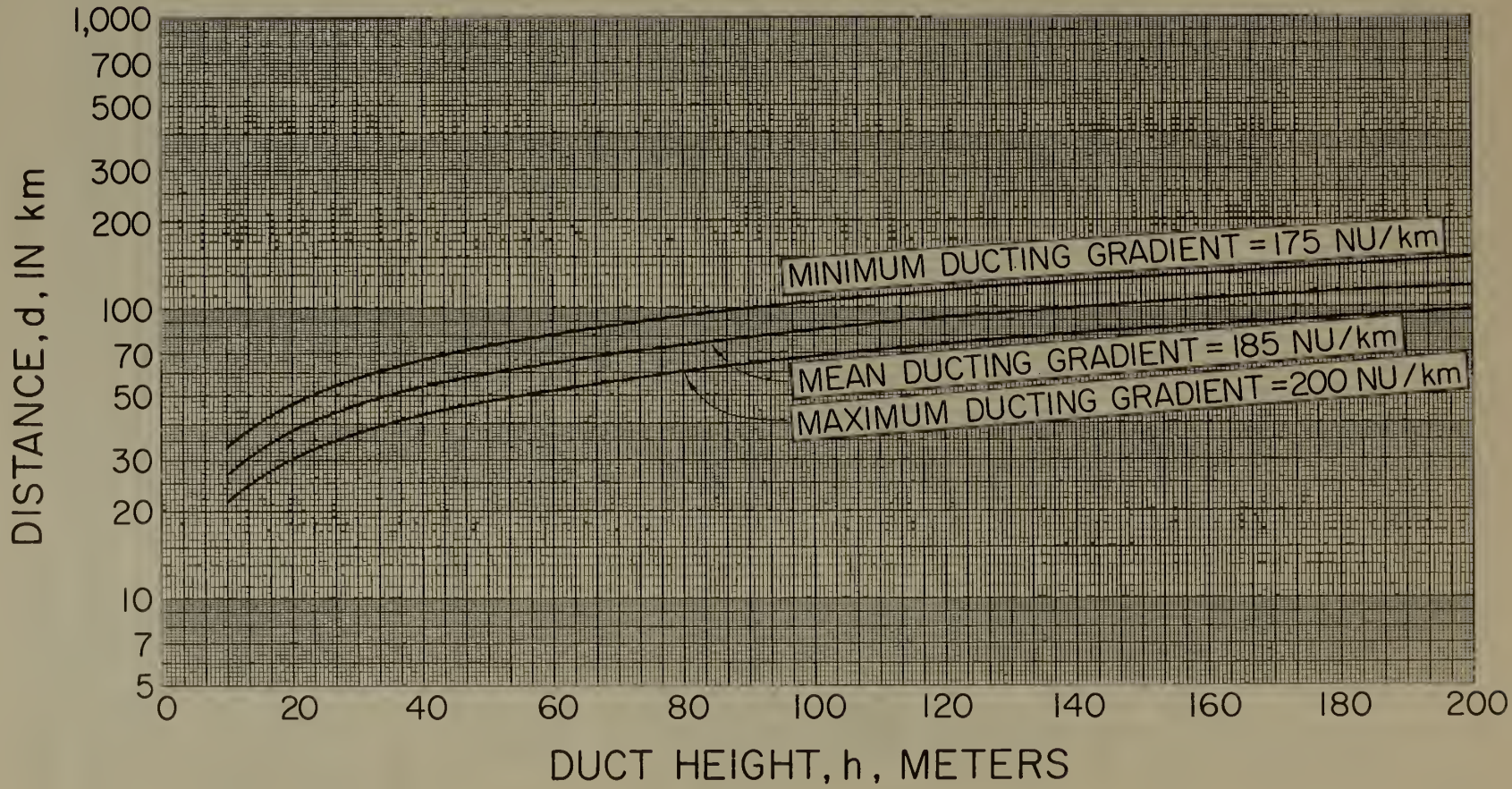

Figure 19

TABLE V

Half-lengths for Various Duct Heights and Surface Gradient Conditions

		Washington, D.C.		Fairbanks, Alaska		Swan Island	
	Cond. \ Duct ht.	100m	200m	65m	185m	100m	135m
	Max	68.21	96.46	22.08	37.25	74.00	98.96
Feb.	Mean	84.50	119.50	38.63	65.18	112.80	147.63
	Min	105.35	148.98	100.54	169.61	248.75	325.56
	Max	30.53	43.17	231.60	390.71	43.65	57.13
May	Mean	52.37	74.05	231.60	390.71	75.99	99.46
	Min	199.42	281.95	231.60	390.71	401.86	525.95
	Max	29.02	41.04	31.43	53.03	41.16	53.87
Aug.	Mean	49.12	69.46	31.43	53.03	75.99	99.46
	Min	440.73	622.53	31.43	53.03	401.86	525.95
	Max	72.56	102.60	44.10	74.40	41.16	53.87
Nov.	Mean	123.93	175.24	78.53	132.49	67.38	88.19
	Min	313.61	443.23	231.60	390.71	124.70	163.20

of zero will travel in the N_s = 313.0 and 377.2 exponential atmospheres. The value of zero for an initial elevation angle is used because the ray can be thought of as leaving the position A, tangent to the duct in figure 8 and "arriving" at the transmitter, even though the reverse process is actually what is occurring. Thus, from figures 23 - 26, knowing the height of the transmitter, h_t, and the height of the ground-based duct, h_A, the distance, d_o, that the radio ray travels from the transmitter to the top of the duct is given by

$$d_o = d_{(h_t - h_A)}, \tag{31}$$

i.e., the distance obtained by using the difference of h_t and h_A as the value of height on the abscissa in figures 23 - 26 gives the distance d_o.

The distance, d_{ho}, to the standard radio horizon from the transmitter is

$$d_{ho} = \sqrt{2h_t} \tag{32}$$

if h_t, the transmitter height, is in feet and d_{ho} is in miles. Using this fact and figures 23 - 26, Table VI, which shows the ratio of d_o to d_{ho}, is derived for various transmitter heights and various duct heights. This table is useful in determining the portion of the distance (measured from the transmitter) within the horizon where fading due to the presence of superrefraction has no effect on transmission. Table VII shows the number (sometimes a fraction) of half-lengths of shadow zones contained within the standard radio horizon for the maximum, mean, and minimum ducting gradients during the four seasons. Table VII is for the 50 per cent level, mean, and maximum surface duct thicknesses - to represent ordinary and maximum conditions of ground-based ducts described previously.

10 SAMPLE COMPUTATIONS

It can be seen from figure 51 that

$$h_1 \leq \text{loss region} \leq h_A + h_2, \tag{33}$$

where h_1 can be determined from figures 27 - 50, which depend upon the station location and the season of the year; h_A is the height of the duct; and h_2 is determined from figures 23 - 26. The following example will illustrate the determination of the shadow zone.

As an illustrative problem, assume a 500-meter transmitting antenna in the spring of the year at 40°N latitude, and that one desires to place the receiving antenna at (a) 40 km and (b) 90 km from the transmitter.

SHADOW ZONE HALF-LENGTHS FOR WASHINGTON, D.C. DUCTING CONDITIONS IN MIDSPRING (MAY)

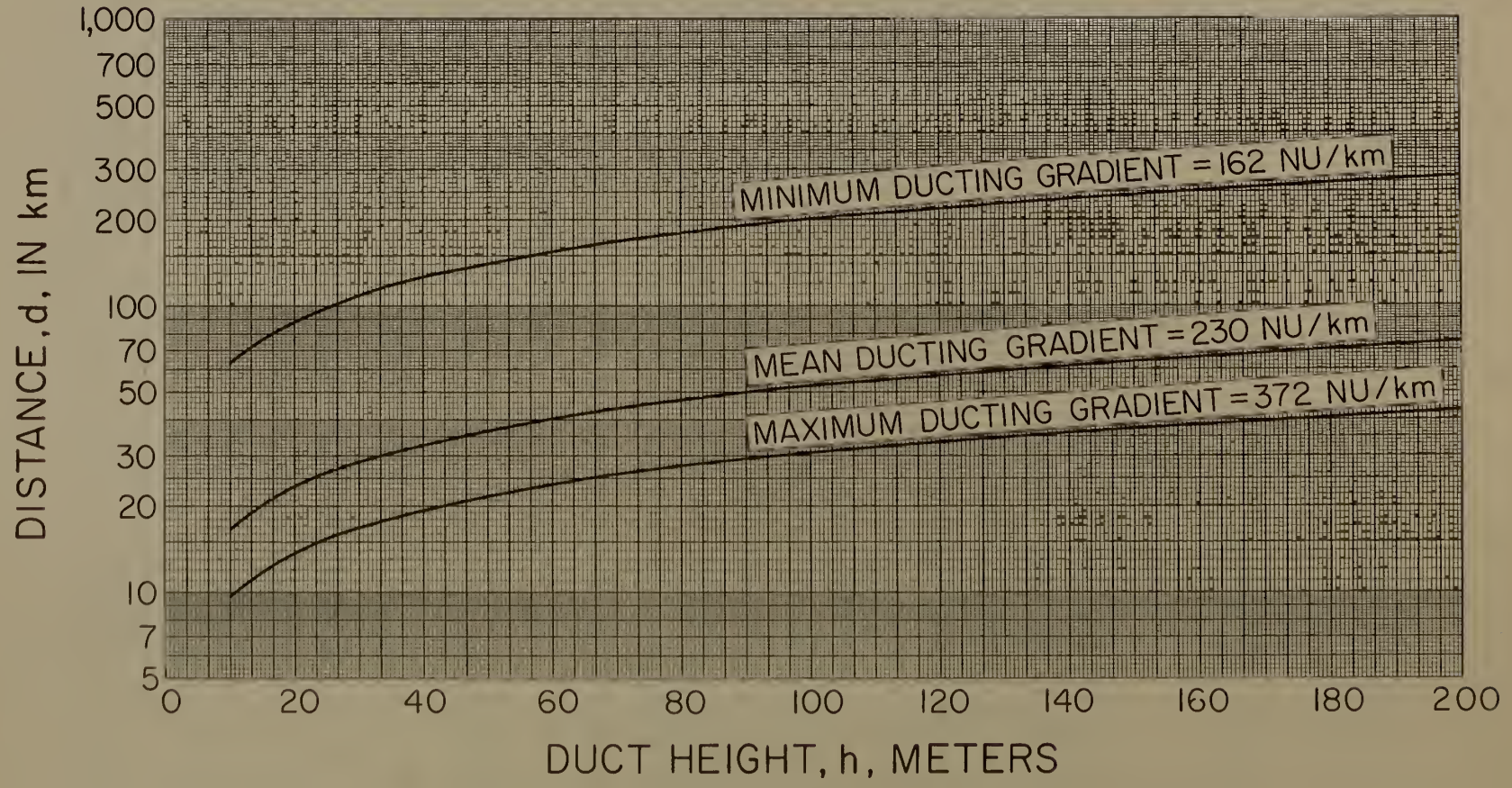

Figure 20

SHADOW ZONE HALF-LENGTHS FOR WASHINGTON, D.C. DUCTING CONDITIONS IN MIDSUMMER (AUGUST)

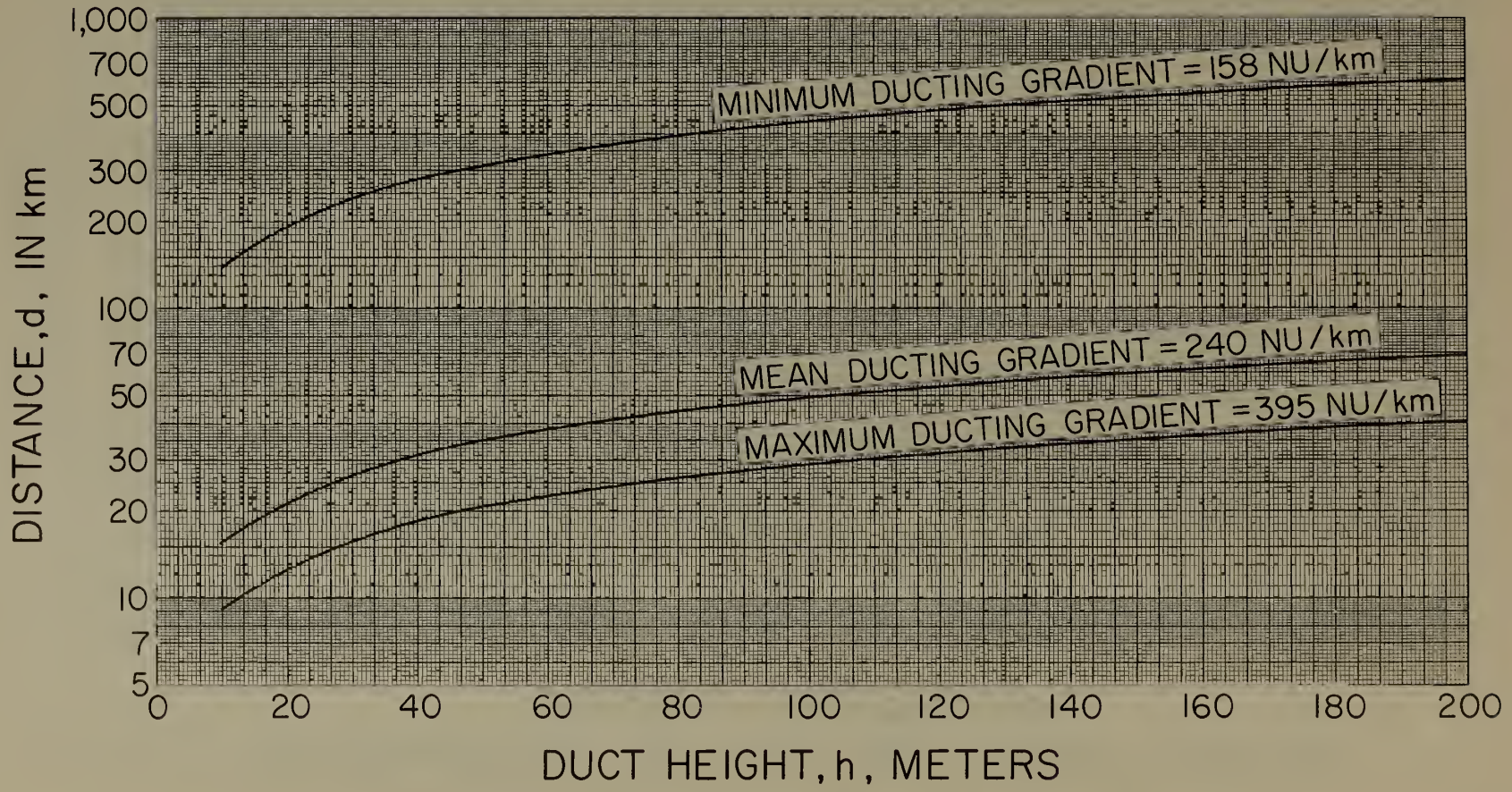

Figure 21

SHADOW ZONE HALF-LENGTHS FOR WASHINGTON, D.C. DUCTING CONDITIONS IN MIDFALL (NOVEMBER)

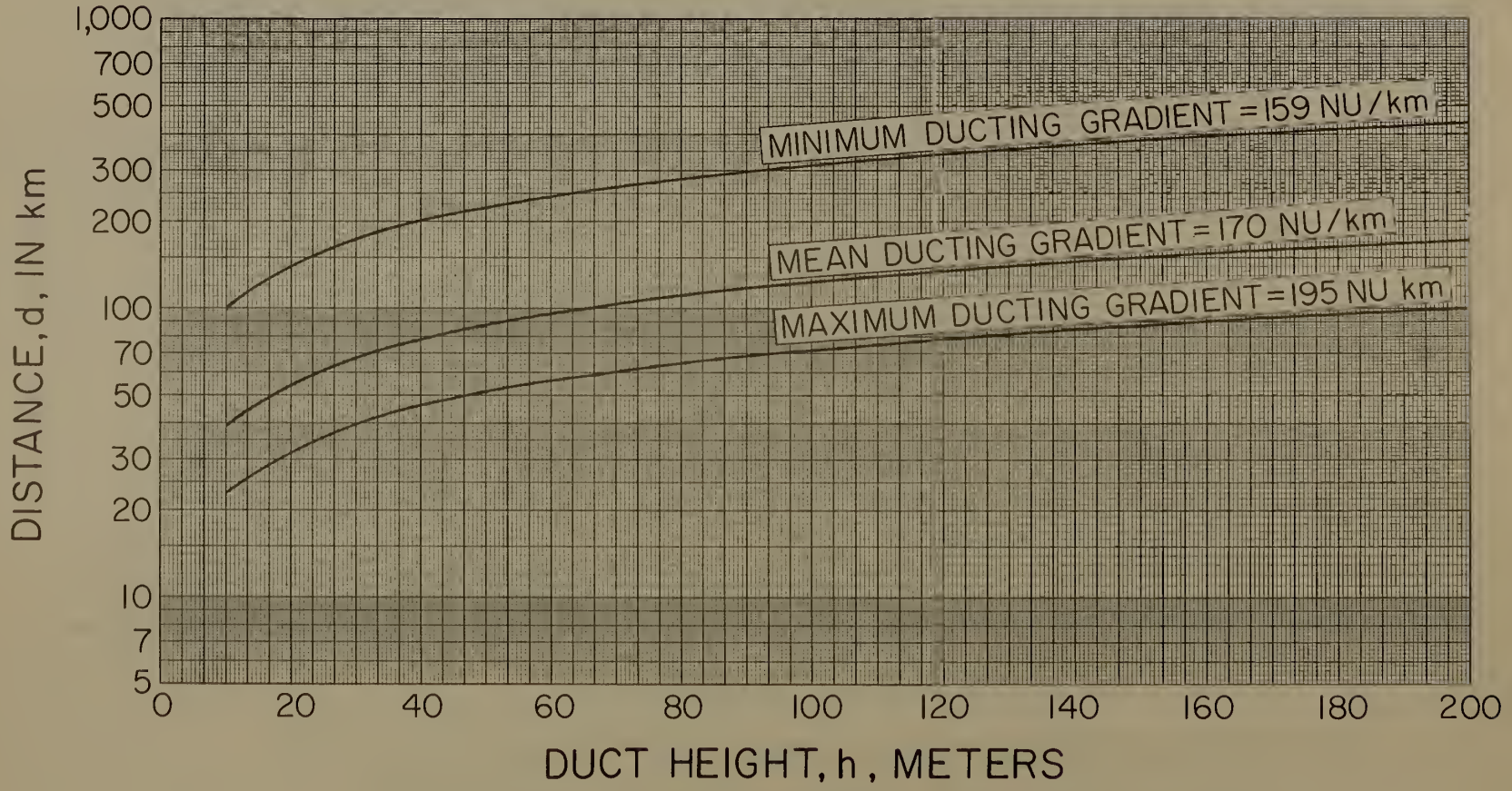

Figure 22

TABLE VI

Ratio of onset point of fading zones from transmitter to distance of radio horizon from the transmitter = S for various transmitter heights

Ht. of * Trans. \ Duct Ht. (Mtrs.)	Washington, D. C. and Fairbanks, Alaska 10	20	50	100	200	Ht. of * Trans. \ Duct Ht. (Mtrs.)	Swan Island 10	20	50	100	200
200	0.795	0.699	0.512	0.300	0	200	0.866	0.773	0.565	0.331	0
300	0.837	0.759	0.605	0.432	0.187	300	0.913	0.837	0.668	0.476	0.206
500	0.878	0.818	0.699	0.565	0.375	500	0.960	0.901	0.770	0.621	0.412
800	0.907	0.860	0.765	0.659	0.509	800	0.992	0.945	0.841	0.724	0.559
1000	0.918	0.876	0.792	0.697	0.563	1000	1.004	0.962	0.869	0.764	0.617
1500	0.935	0.900	0.831	0.754	0.644	1500	1.020	0.986	0.910	0.825	0.704
2000	0.944	0.914	0.854	0.787	0.692	2000	1.028	0.999	0.933	0.859	0.755
3000	0.953	0.928	0.880	0.825	0.747	3000	1.035	1.011	0.957	0.897	0.811
5000	0.959	0.940	0.902	0.859	0.799	5000	1.035	1.016	0.974	0.928	0.861
7000	0.959	0.943	0.911	0.875	0.825	7000	1.030	1.014	0.979	0.940	0.884

* Transmitter

DISTANCE VERSUS HEIGHT ABOVE DUCT REPRESENTING AVERAGE WASHINGTON D.C. AND FAIRBANKS, ALASKA ATMOSPHERE

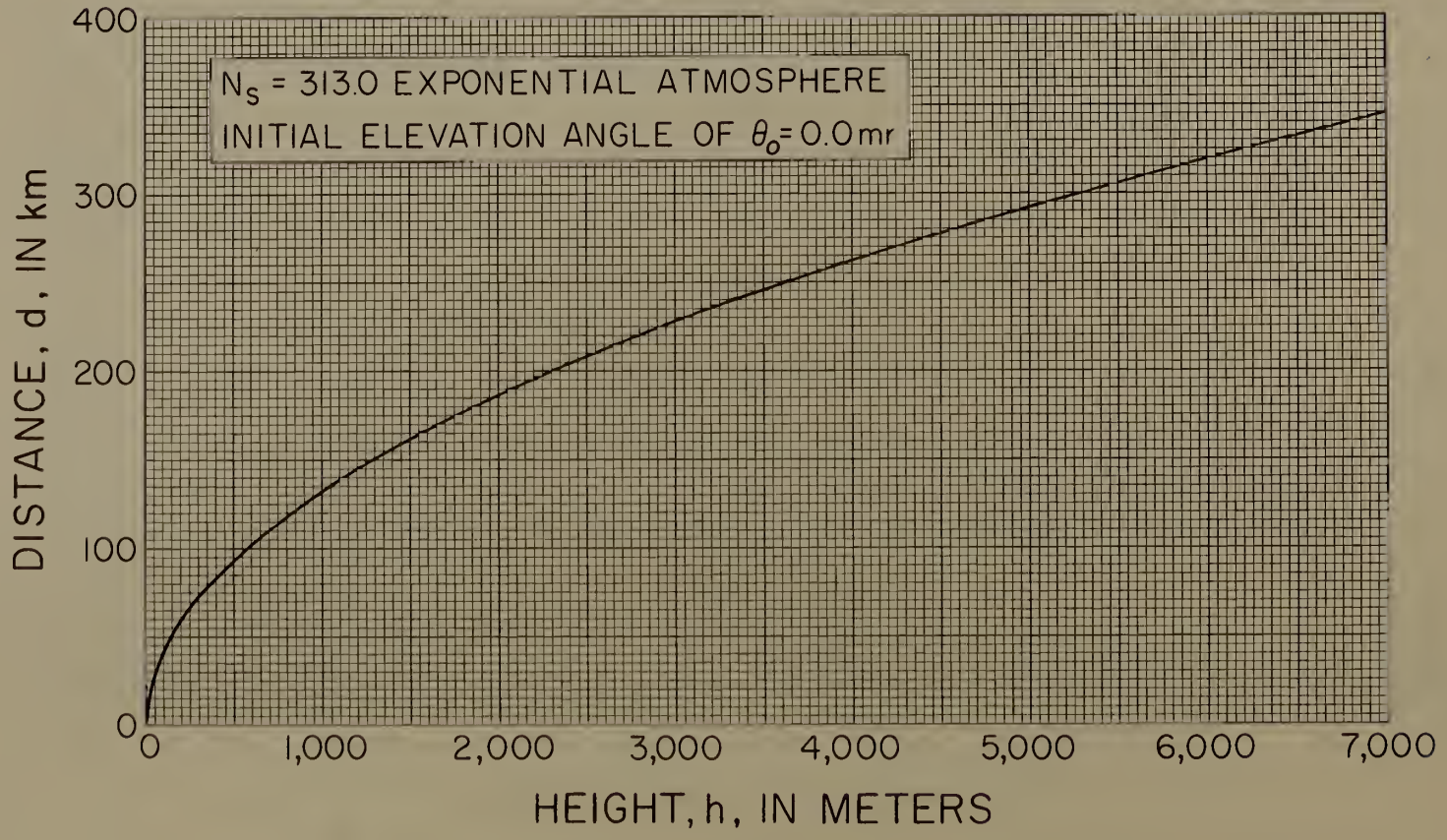

Figure 23

DISTANCE VERSUS HEIGHT ABOVE DUCT REPRESENTING AVERAGE WASHINGTON D.C. AND FAIRBANKS ALASKA ATMOSPHERE

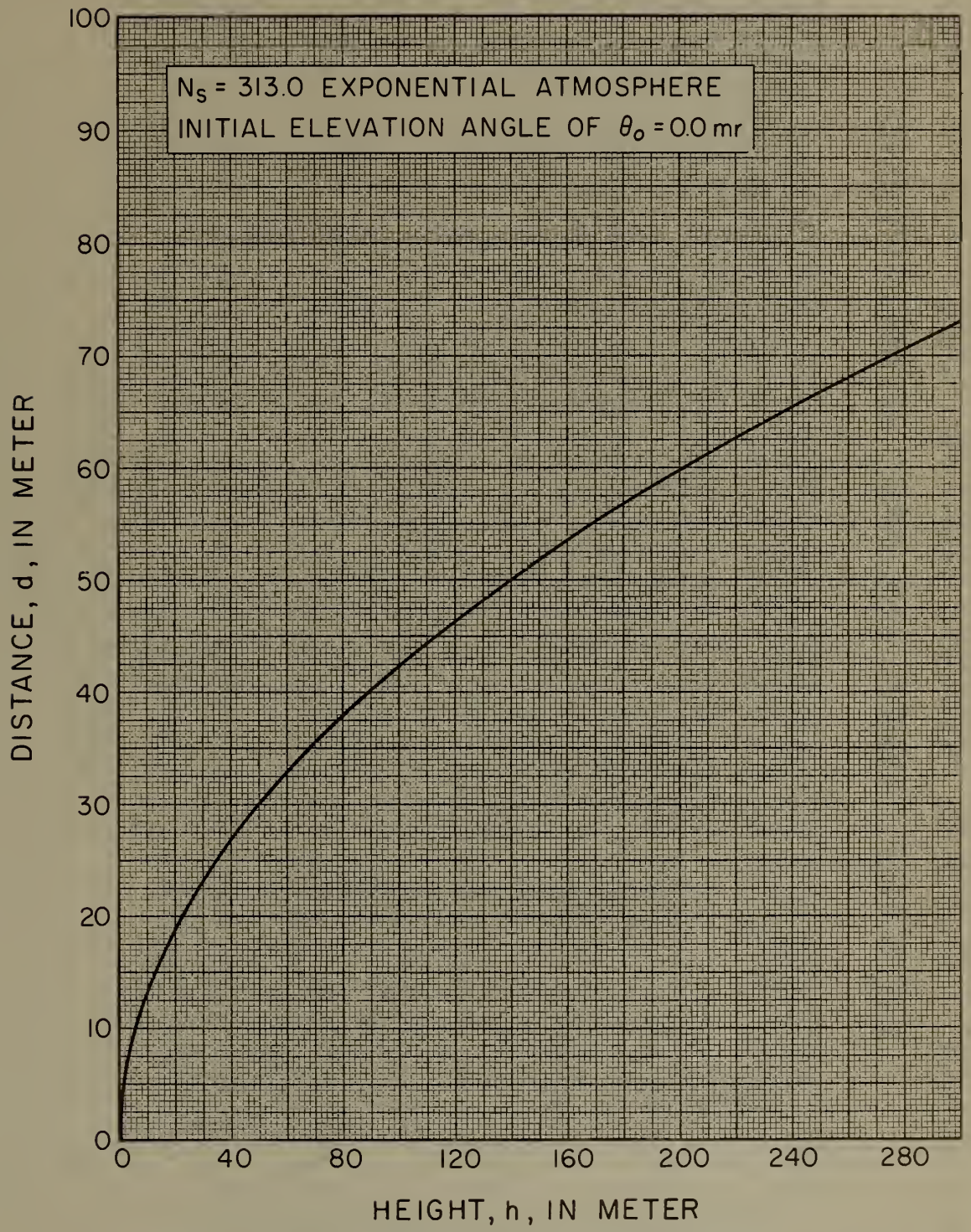

Figure 24

DISTANCE VERSUS HEIGHT ABOVE DUCT REPRESENTING AVERAGE SWAN ISLAND ATMOSPHERE

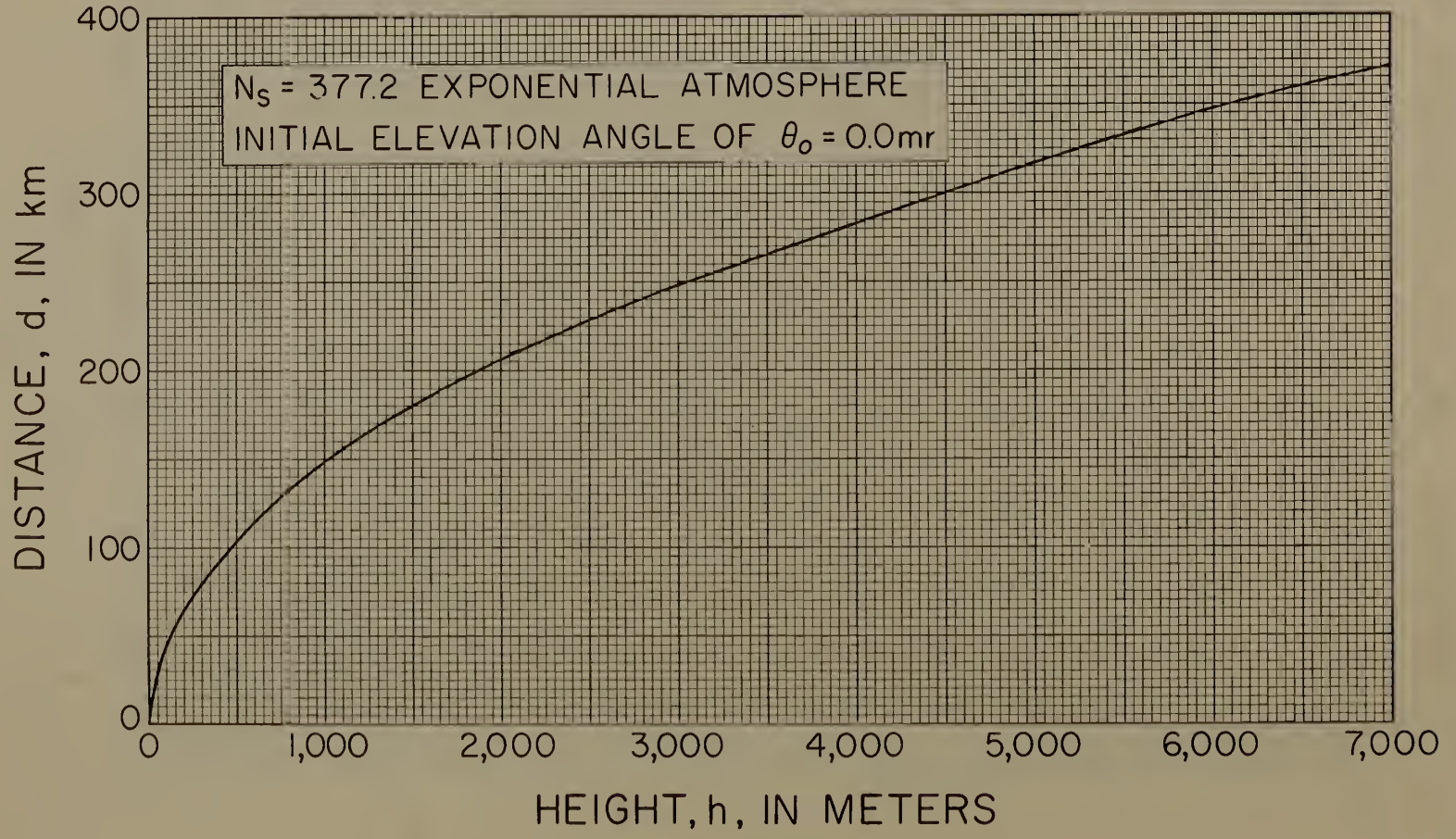

Figure 25

TABLE VII

For Swan Island, 108 m Duct

Hgt. of Trans. (Mtrs.)	February			May			August			November		
	Max. Duct Grad.	Mean	Min.	Max.	Mean	Min.	Max.	Mean	Min.	Max.	Mean	Min.
200	0.18	0.12	0.05	0.31	0.18	0.03	0.33	0.18	0.03	0.33	0.20	0.11
300	0.11	0.07	0.03	0.19	0.11	0.02	0.20	0.11	0.02	0.20	0.12	0.07
500	0.02	0.01	0.005	0.03	0.02	0.003	0.03	0.02	0.003	0.03	0.02	0.01
800	0.00	0.00	0.00	0.00	0.00	0.00	0.00	0.00	0.00	0.00	0.00	0.00
1000	0.00	0.00	0.00	0.00	0.00	0.00	0.00	0.00	0.00	0.00	0.00	0.00
1500	0.00	0.00	0.00	0.00	0.00	0.00	0.00	0.00	0.00	0.00	0.00	0.00
2000	0.00	0.00	0.00	0.00	0.00	0.00	0.00	0.00	0.00	0.00	0.00	0.00
3000	0.00	0.00	0.00	0.00	0.00	0.00	0.00	0.00	0.00	0.00	0.00	0.00
5000	0.00	0.00	0.00	0.00	0.00	0.00	0.00	0.00	0.00	0.00	0.00	0.00
7000	0.00	0.00	0.00	0.00	0.00	0.00	0.00	0.00	0.00	0.00	0.00	0.00

TABLE VII

For Fairbanks, Alaska, 185 m Duct

Hgt. of Trans. (Mtrs.)	February			May			August			November		
	Max. Duct Grad.	Mean	Min.	Max.	Mean	Min.	Max.	Mean	Min.	Max.	Mean	Min.
200	1.14	0.65	0.25	0.11	0.11	0.11	0.80	0.80	0.80	0.57	0.32	0.11
300	0.70	0.40	0.15	0.07	0.07	0.07	0.49	0.49	0.49	0.35	0.20	0.07
500	0.49	0.28	0.11	0.05	0.05	0.05	0.34	0.34	0.34	0.24	0.05	0.05
800	0.37	0.21	0.08	0.03	0.03	0.03	0.26	0.26	0.26	0.18	0.10	0.03
1000	0.28	0.16	0.06	0.03	0.03	0.03	0.20	0.20	0.20	0.14	0.08	0.03
1500	0.21	0.12	0.05	0.02	0.02	0.02	0.15	0.15	0.15	0.10	0.06	0.02
2000	0.20	0.11	0.04	0.02	0.02	0.02	0.14	0.14	0.14	0.10	0.056	0.02
3000	0.10	0.06	0.02	0.01	0.01	0.01	0.07	0.07	0.07	0.05	0.03	0.01
5000	0.12	0.07	0.03	0.01	0.01	0.01	0.08	0.08	0.08	0.06	0.03	0.01
7000	0.13	0.075	0.03	0.01	0.01	0.01	0.09	0.09	0.09	0.07	0.037	0.01

TABLE VII

For Fairbanks, Alaska, 65 m Duct

Hgt. of Trans. (Mtrs.)	February			May			August			November		
	Max. Duct Grad.	Mean	Min.	Max.	Mean	Min.	Max.	Mean	Min.	Max.	Mean	Min.
200	0.42	0.24	0.09	0.04	0.04	0.04	0.30	0.30	0.30	0.21	0.12	0.04
300	0.30	0.17	0.07	0.03	0.03	0.03	0.21	0.21	0.21	0.15	0.09	0.03
500	0.21	0.12	0.05	0.02	0.02	0.02	0.15	0.15	0.15	0.11	0.06	0.02
800	0.16	0.09	0.04	0.02	0.02	0.02	0.11	0.11	0.11	0.08	0.05	0.02
1000	0.11	0.06	0.02	0.01	0.01	0.01	0.08	0.08	0.08	0.05	0.03	0.01
1500	0.10	0.06	0.02	0.009	0.009	0.009	0.07	0.07	0.07	0.05	0.03	0.009
2000	0.06	0.04	0.01	0.006	0.006	0.006	0.04	0.04	0.04	0.03	0.17	0.006
3000	0.036	0.02	0.008	0.003	0.003	0.003	0.025	0.025	0.025	0.02	0.010	0.003
5000	0.068	0.039	0.015	0.006	0.006	0.006	0.048	0.048	0.048	0.034	0.019	0.006
7000	0.086	0.05	0.019	0.006	0.006	0.006	0.06	0.06	0.06	0.043	0.024	0.006

TABLE VII

For Swan Island, 135 m Duct

Hgt. Trans. (Mtrs)	February			May			August			November		
	Max. Duct Grad.	Mean	Min.	Max.	Mean	Min.	Max.	Mean	Min.	Max.	Mean	Min.
200	0.21	0.14	0.06	0.36	0.21	0.04	0.38	0.21	0.04	0.38	0.23	0.13
300	0.12	0.08	0.035	0.20	0.12	0.02	0.22	0.12	0.02	0.22	0.12	0.02
500	0.05	0.035	0.016	0.09	0.05	0.01	0.096	0.05	0.01	0.096	0.06	0.03
800	0.00	0.00	0.00	0.00	0.00	0.00	0.00	0.00	0.00	0.00	0.00	0.00
1000	0.00	0.00	0.00	0.00	0.00	0.00	0.00	0.00	0.00	0.00	0.00	0.00
1500	0.00	0.00	0.00	0.00	0.00	0.00	0.00	0.00	0.00	0.00	0.00	0.00
2000	0.00	0.00	0.00	0.00	0.00	0.00	0.00	0.00	0.00	0.00	0.00	0.00
3000	0.00	0.00	0.00	0.00	0.00	0.00	0.00	0.00	0.00	0.00	0.00	0.00
5000	0.00	0.00	0.00	0.00	0.00	0.00	0.00	0.00	0.00	0.00	0.00	0.00
7000	0.00	0.00	0.00	0.00	0.00	0.00	0.00	0.00	0.00	0.00	0.00	0.00

How high should the receiving antenna be to be free from fading loss caused by a ground-based superrefractive layer?

Since both of the distances required are within the standard horizon distance, d_{ho}, which, for a 500 meter transmitter is

$$d_{ho} = 92.181 \text{ km},$$

this is a case of within-the-horizon propagation.

Since the 40°N latitude position is within the temperate zone, use will be made of the Washington, D. C., model ducting atmosphere. As previously mentioned, 100 meters is the median mean duct thickness at Washington, D. C., and 200 meters is the median maximum duct thickness observed at Washington. These are the two duct thicknesses to use in this calculation. Also, since it is the spring of the year, figures 30 - 32 must be used to determine h_1.

For the 40 kilometer distance (case (a)), the subscript of equation (31) becomes

$$h_t - h_A = 500 - 100 = 400 \text{ meters},$$

which is then entered on the abscissa of figure 23, where,

$$d_o = d_{400} = 83 \text{ km}.$$

For a 200 meter thick duct,

$$h_t - h_A = 300 \text{ meters}.$$

Therefore, in this case,

$$d_o = d_{300} = 72 \text{ km}.$$

In either case, as can be seen from figure 8, d_o is greater than 40 kilometers. Therefore, any height of the receiving antenna will be

satisfactory at this point, since the first shadow zone has not yet been reached.

For the 90-kilometer distance (case (b)), it can be seen that this distance is beyond the onset point of the first shadow zone, and figures 30 - 32 must be used here.

All of figures 27 - 50 are used differently depending upon which side of the reflection point B of figure 51 one desires to locate an antenna. If on the left-hand side of point B, one must subtract the desired distance from the distance from B to the top of the duct traversed by the ray and use this new distance to determine height, h, in figures 27 - 50. This procedure must be followed every time the ray heads downward. If on the right-hand side of point B of figure 51 (or any other reflection point), one simply uses the distance from the reflection point directly. One must keep in mind that any previous half-lengths must be subtracted from the desired distance from the transmitter, as well as subtracting d_o, in order to obtain the distance used in figures 27 - 50.

Applied to the problem where figures 30 - 32 are used, for the maximum midspring ducting conditions (figure 30) and the 100-meter-thick duct, recalling d_o = 83 kilometers, the antenna is to be located

$$90 - 83 = 7 \text{ km}$$

beyond the onset point of the shadow zones. For the 200-meter duct the antenna is located

$$90 - 72 = 18 \text{ km}$$

beyond point A of figure 51. From figure 10, the half-length traveled by a ray in a 100-meter duct under maximum midspring ducting conditions is 30.5 kilometers. Thus, as described above, the distance used in figure 30 is

$$30.5 - 7.0 = 23.5 \text{ km}$$

to find h_1, because at 25 kilometers the ray is still sloping downward and hence is on the left-hand side of point B of figure 51. From figure 10, $d_{h\ell}$ = 43 kilometers for a 200 meter duct; therefore, the distance used in figure 30 is

$$43 - 18 = 25 \text{ km.}$$

Similarly, utilizing figures 11 and 12 for mean ducting and minimum ducting conditions for a 100-meter and 200-meter duct:

Figure 31 distance to be used for the 100-meter duct = 45 km.

Figure 31 distance to be used for the 200-meter duct = 56 km.

Figure 32 distance to be used for the 100-meter duct = 191 km.

Figure 32 distance to be used for the 200-meter duct = 262 km and hence

h_1 for a 100-meter duct under max. spring ducting conditions = 92.3 m.

h_1 for a 200-meter duct under max. spring ducting conditions = 166.0 m.

h_1 for a 100-meter duct under mean spring ducting conditions = 96.0 m.

h_1 for a 200-meter duct under mean spring ducting conditions = 187.0 m.

h_1 for a 100-meter duct under min. spring ducting conditions = 99.0 m.

h_1 for a 200-meter duct under min. spring ducting conditions = 199.0 m.

Figures 23 and 24 will be used to determine h_2 from the total distance, d. The distance to be used is obtained by subtracting the distance, d_o, from the desired distance. For the 100-meter duct, d_o = 83 kilometers and

$$d = 90 - 83 = 7 \text{ km.}$$

Likewise for the 200-meter duct, d_o = 72 km and

$$d = 90 - 72 = 18 \text{ km.}$$

Thus it is found that for the model assumed:

h_2 for the 100-meter duct height case will always be 3 meters,

h_2 for the 200-meter duct height case will always be 18 meters.

DISTANCE VERSUS HEIGHT ABOVE DUCT REPRESENTING AVERAGE SWAN ISLAND ATMOSPHERE

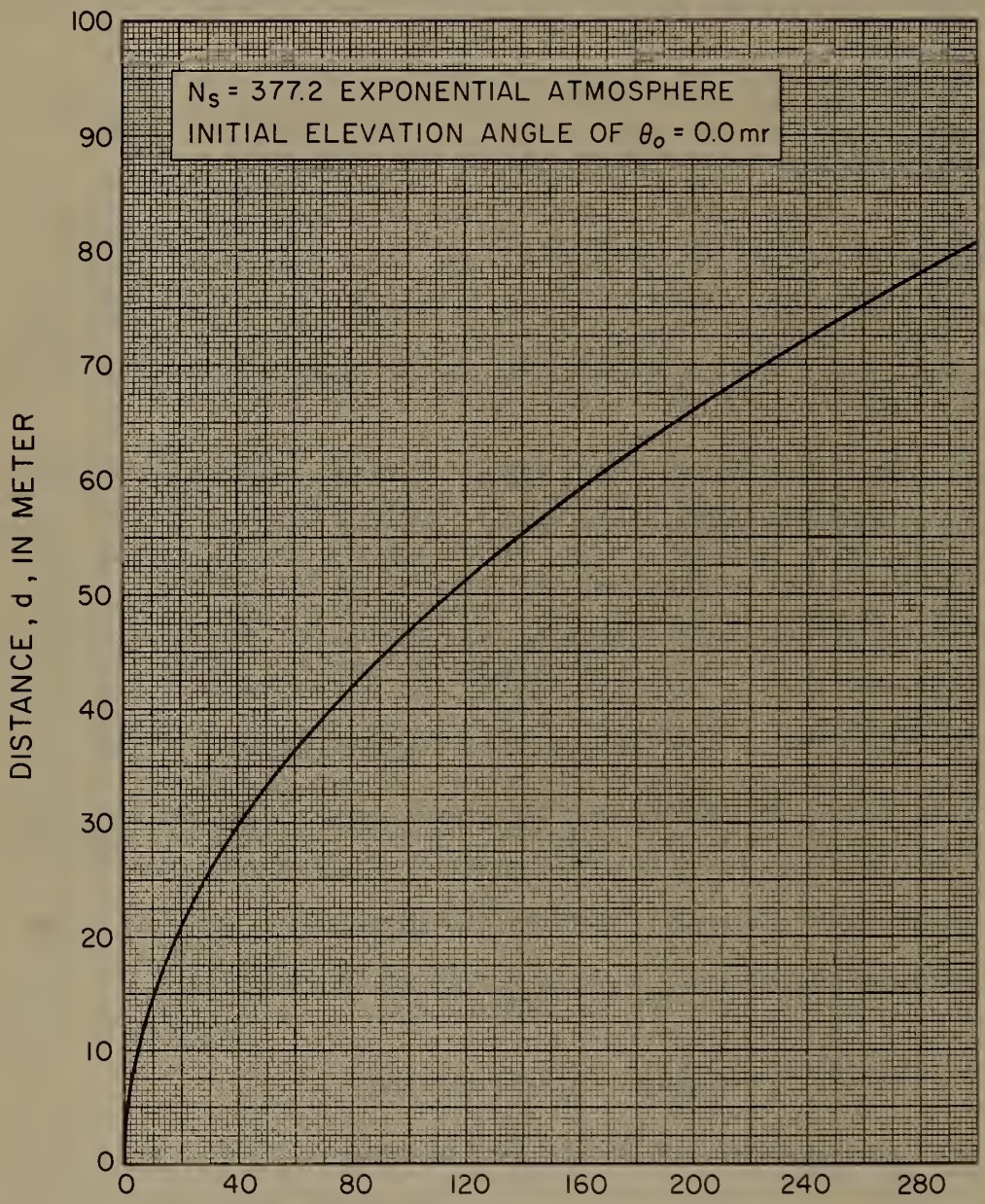

Figure 26

HEIGHT VERSUS DISTANCE IN THE FIRST HALF-LENGTH OF A RAY TRAPPED IN VARIOUS SURFACE DUCTS AT WASHINGTON D.C. MAXIMUM MIDWINTER (FEBRUARY) DUCTING CONDITIONS

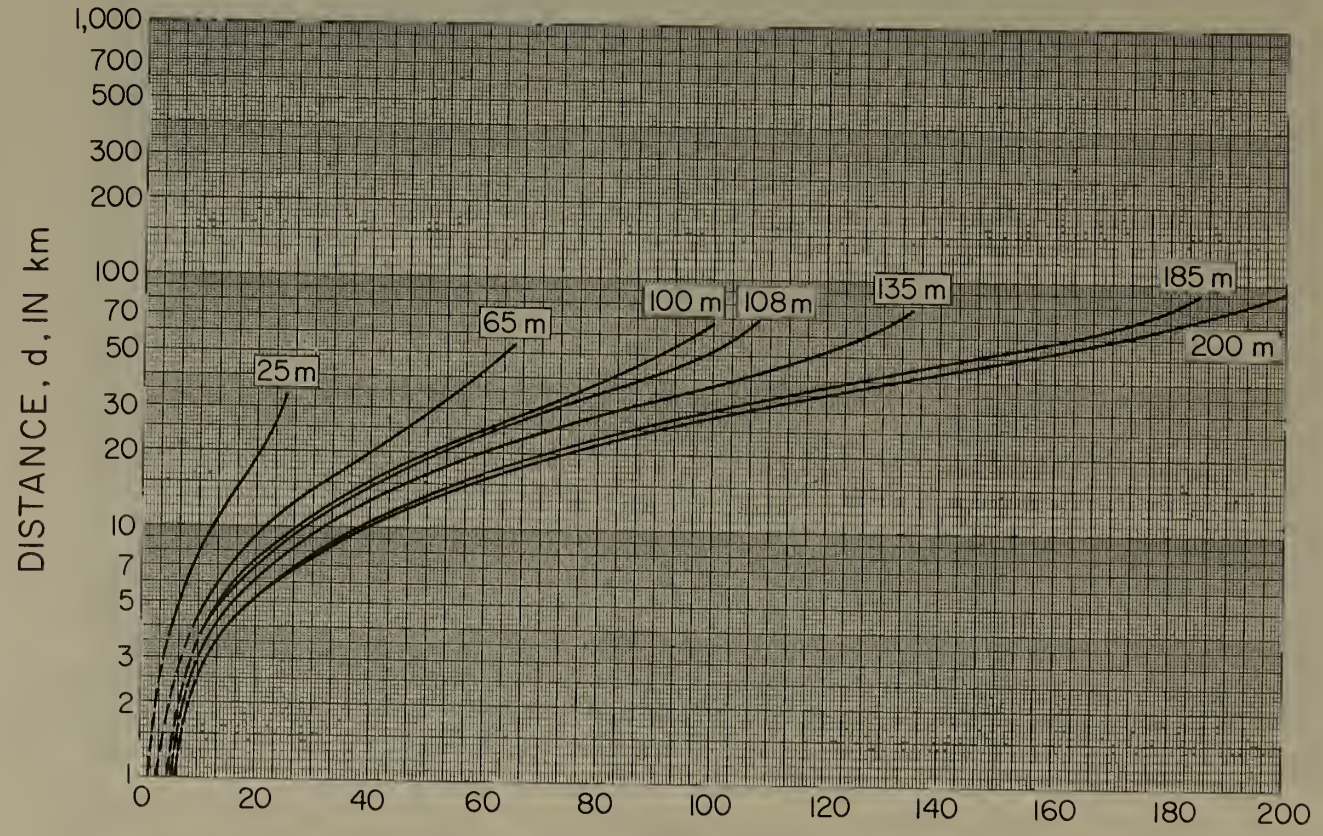

Figure 27

HEIGHT VERSUS DISTANCE AT WASHINGTON, D.C. FOR MEAN MIDWINTER (FEBRUARY) DUCTING CONDITIONS

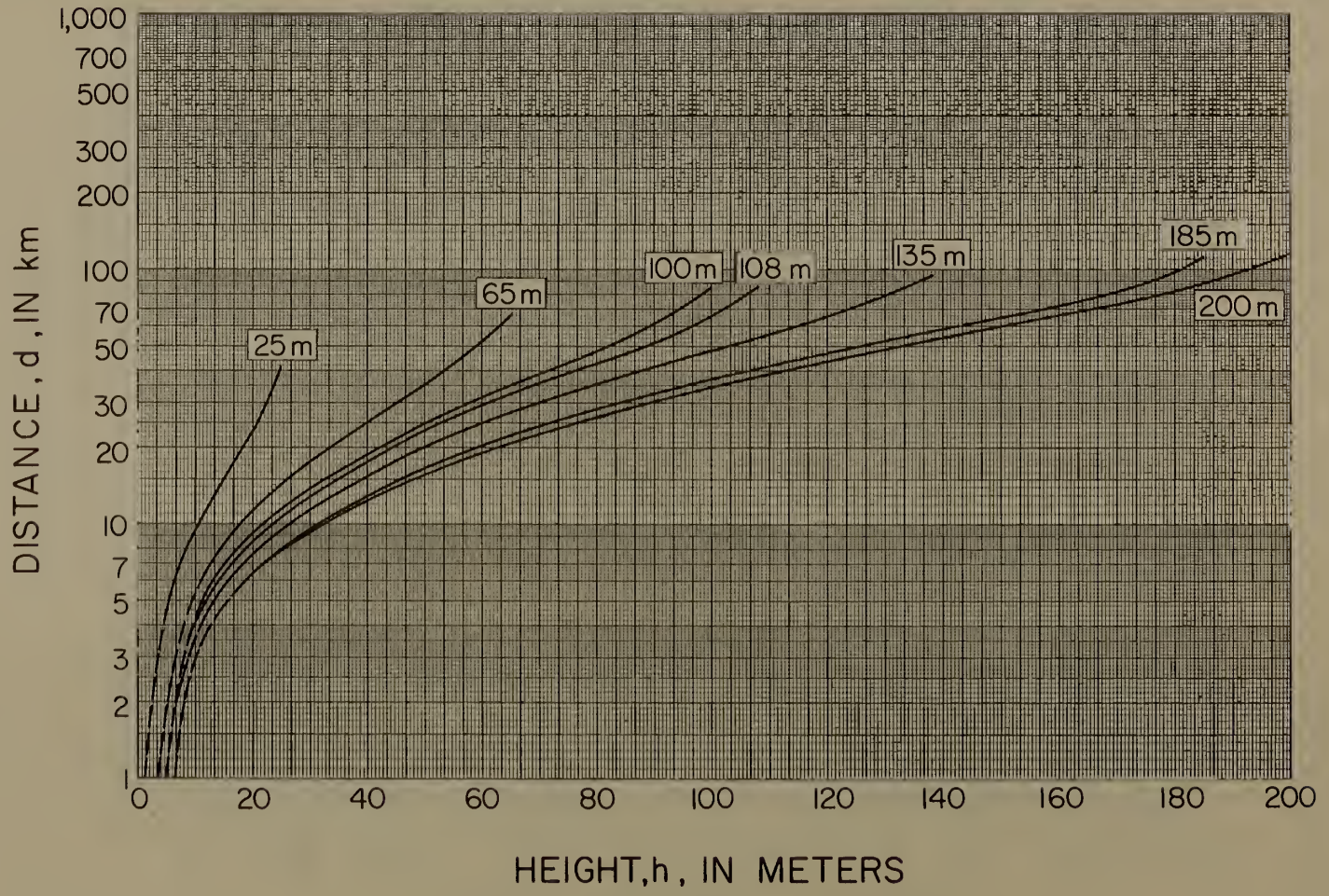

Figure 28

HEIGHT VERSUS DISTANCE AT WASHINGTON, D.C. FOR MINIMUM MIDWINTER (FEBRUARY) DUCTING CONDITIONS

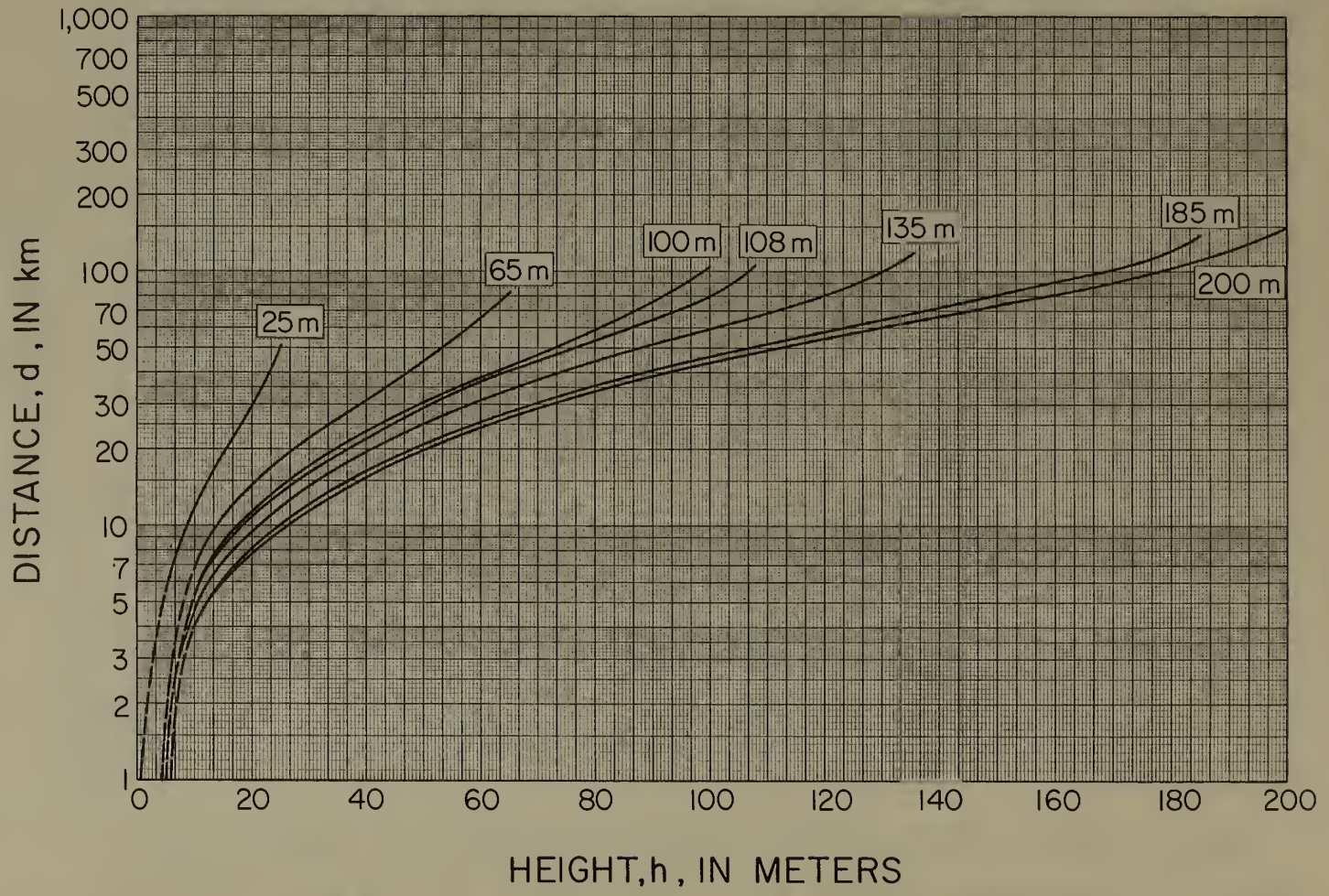

Figure 29

HEIGHT VERSUS DISTANCE AT WASHINGTON, D.C. FOR MAXIMUM MIDSPRING (MAY) DUCTING CONDITIONS

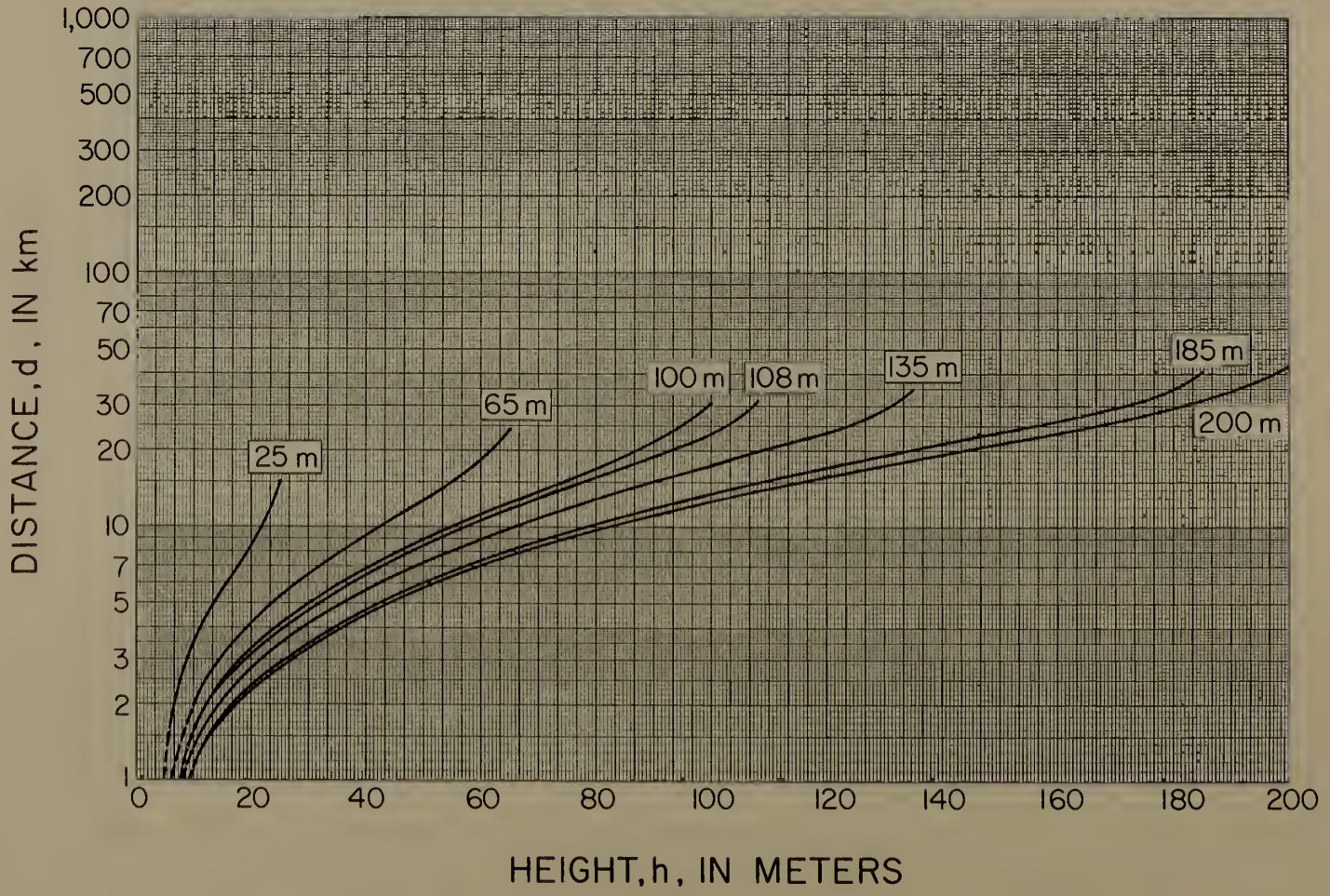

Figure 30

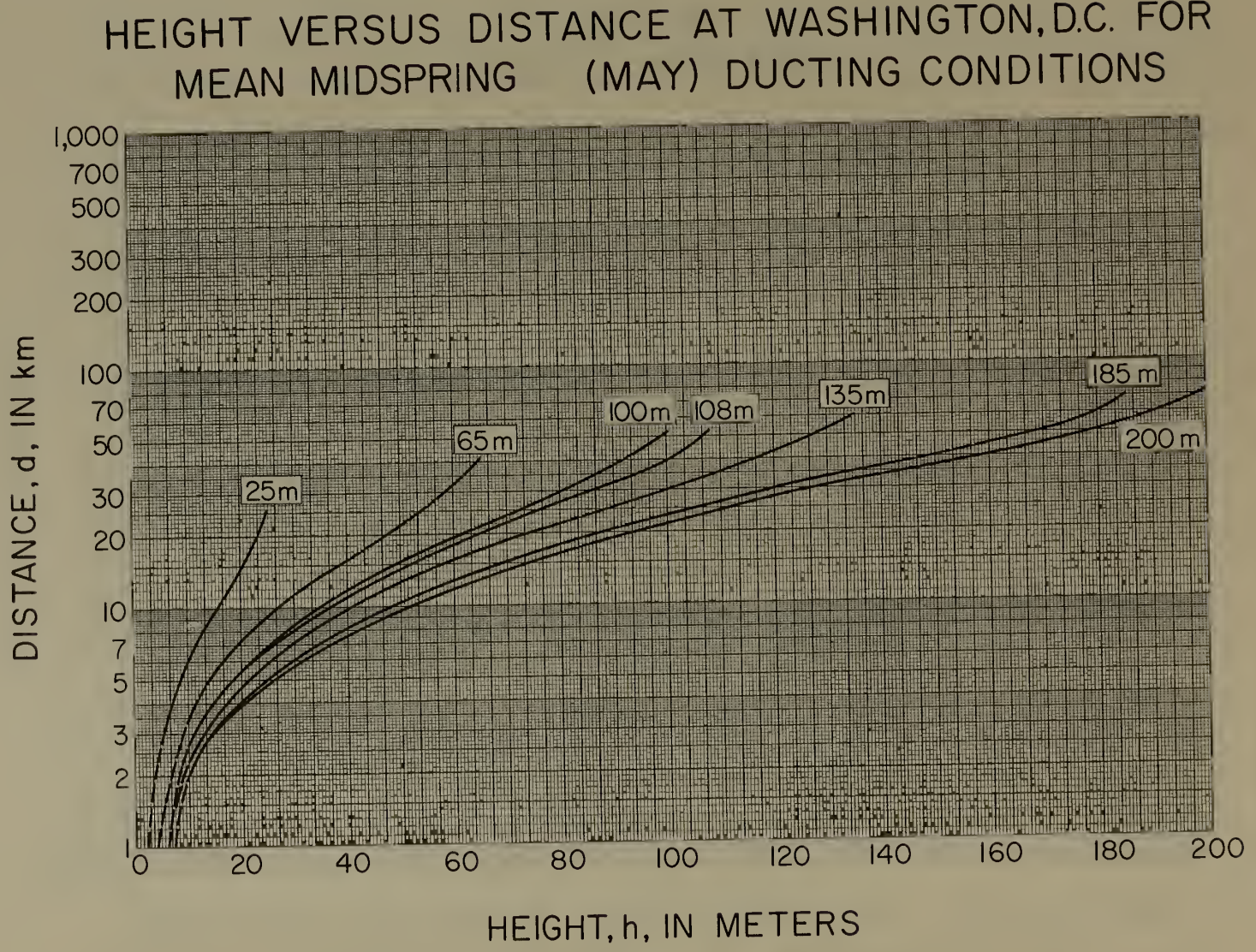
HEIGHT VERSUS DISTANCE AT WASHINGTON, D.C. FOR MEAN MIDSPRING (MAY) DUCTING CONDITIONS
DISTANCE, d, IN km
1,000
700
500
300
200
100
70
50
30
20
10
7
5
3
2
1
25m
65m
100m
108m
135m
185 m
200 m
0
20
40
60
80
100
120
140
160
180
200
HEIGHT, h, IN METERS

Figure 31

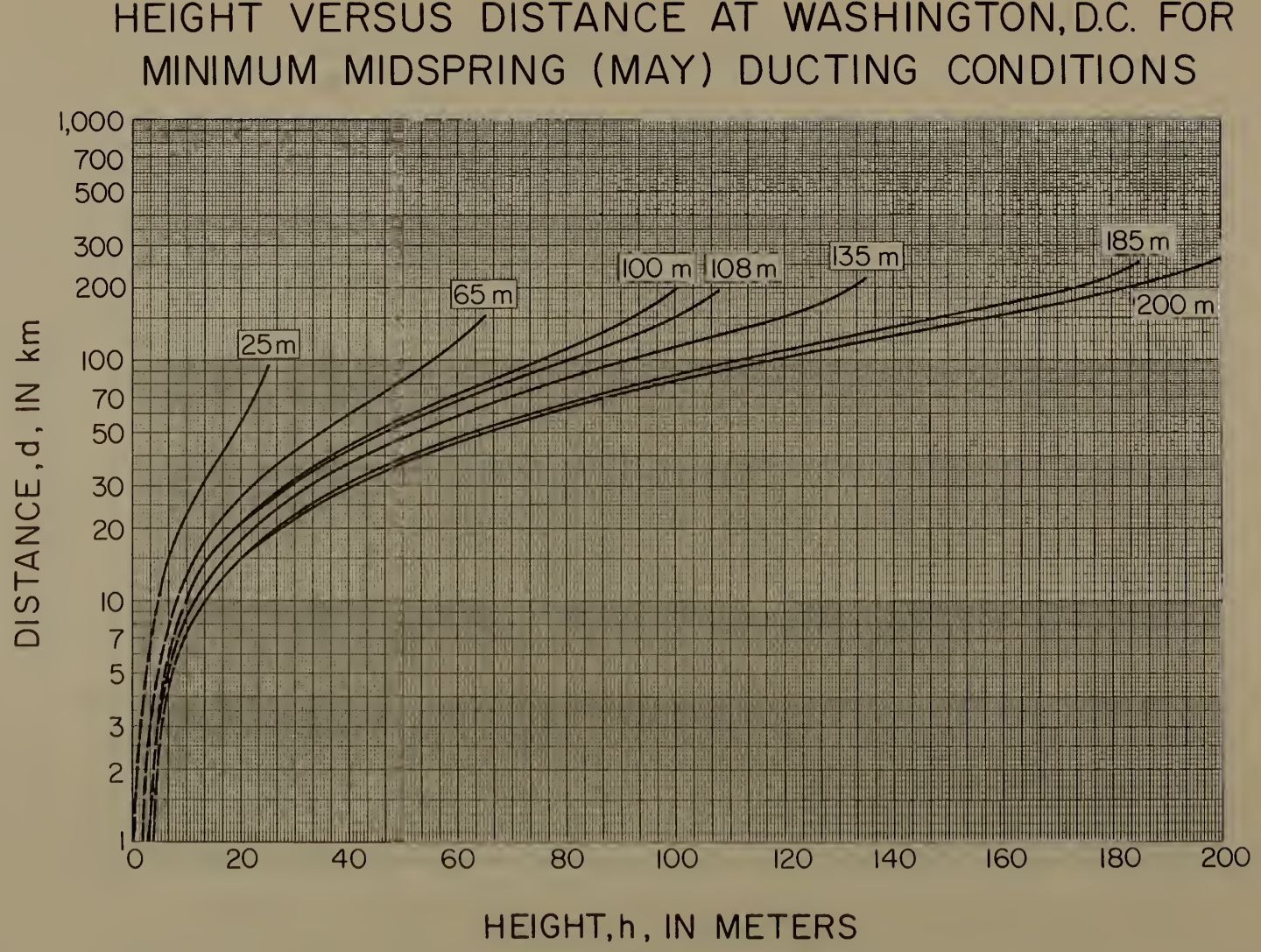
HEIGHT VERSUS DISTANCE AT WASHINGTON, D.C. FOR MINIMUM MIDSPRING (MAY) DUCTING CONDITIONS
DISTANCE, d, IN km
1,000
700
500
300
200
100
70
50
30
20
10
7
5
3
2
1
0
20
40
60
80
100
120
140
160
180
200
HEIGHT, h, IN METERS
25m
65 m
100 m
108m
135 m
185 m
200 m

Figure 32

HEIGHT VERSUS DISTANCE AT WASHINGTON, D.C. FOR MAXIMUM MIDSUMMER (AUGUST) DUCTING CONDITIONS

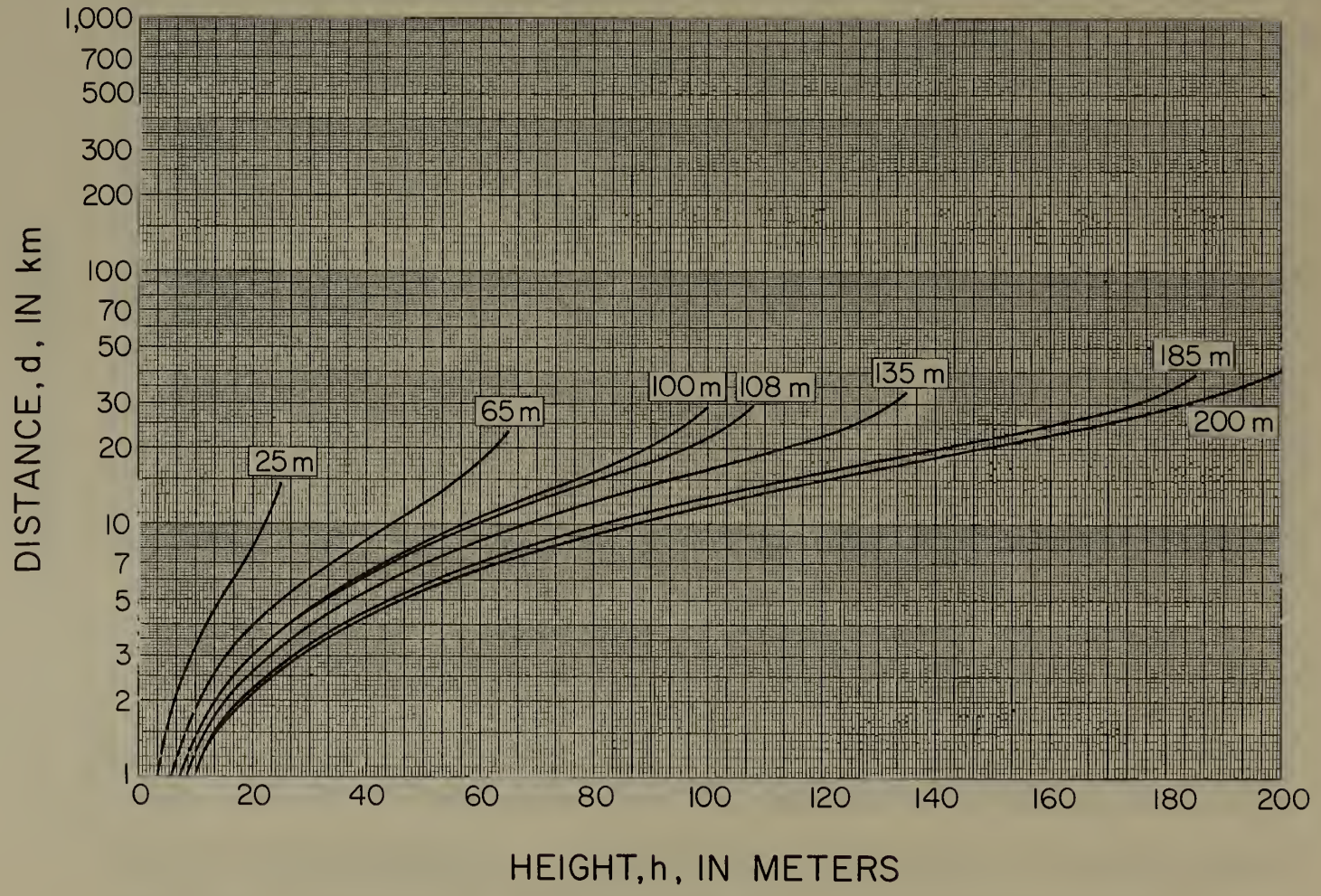

Figure 33

HEIGHT VERSUS DISTANCE AT WASHINGTON, D.C. FOR MEAN MIDSUMMER (AUGUST) DUCTING CONDITIONS

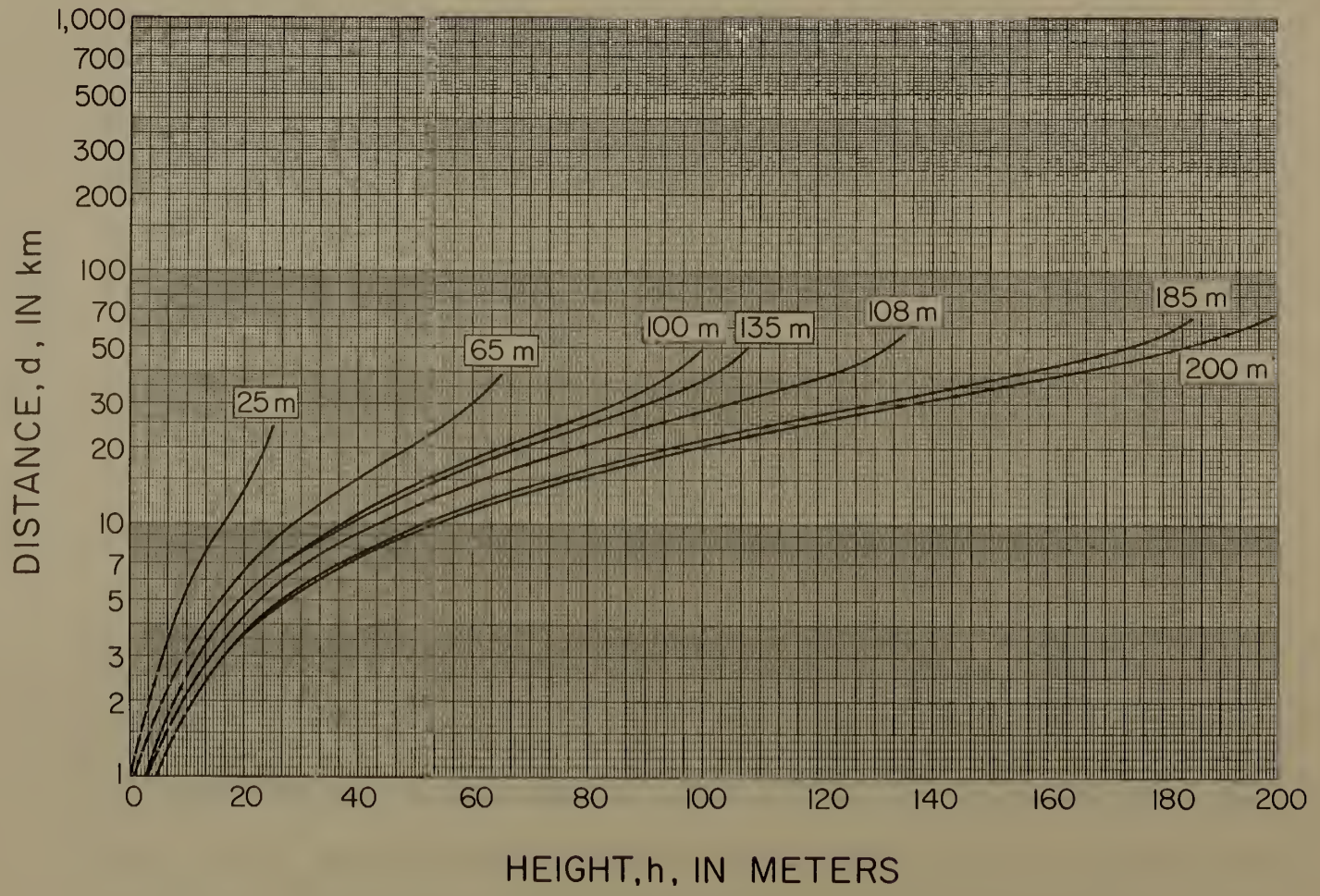

Figure 34

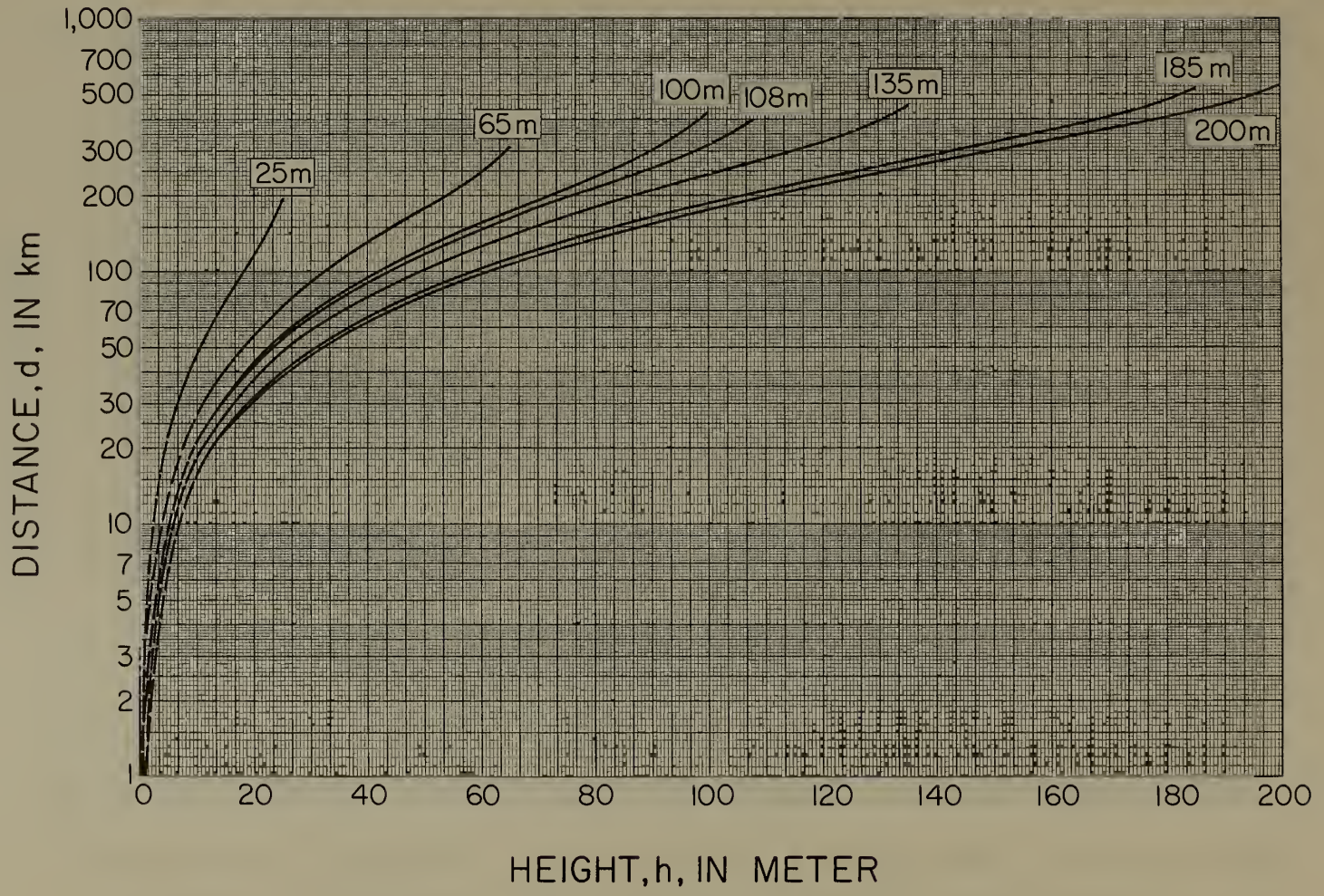
HEIGHT VERSUS DISTANCE AT WASHINGTON, D.C. FOR MINIMUM MIDSUMMER (AUGUST) DUCTING CONDITIONS
DISTANCE, d, IN km
1,000
700
500
300
200
100
70
50
30
20
10
7
5
3
2
1
0
20
40
60
80
100
120
140
160
180
200
HEIGHT, h, IN METER
25m
65m
100m
108m
135m
185m
200m

Figure 35

HEIGHT VERSUS DISTANCE AT WASHINGTON, D.C. FOR MAXIMUM MIDFALL (NOVEMBER) DUCTING CONDITIONS

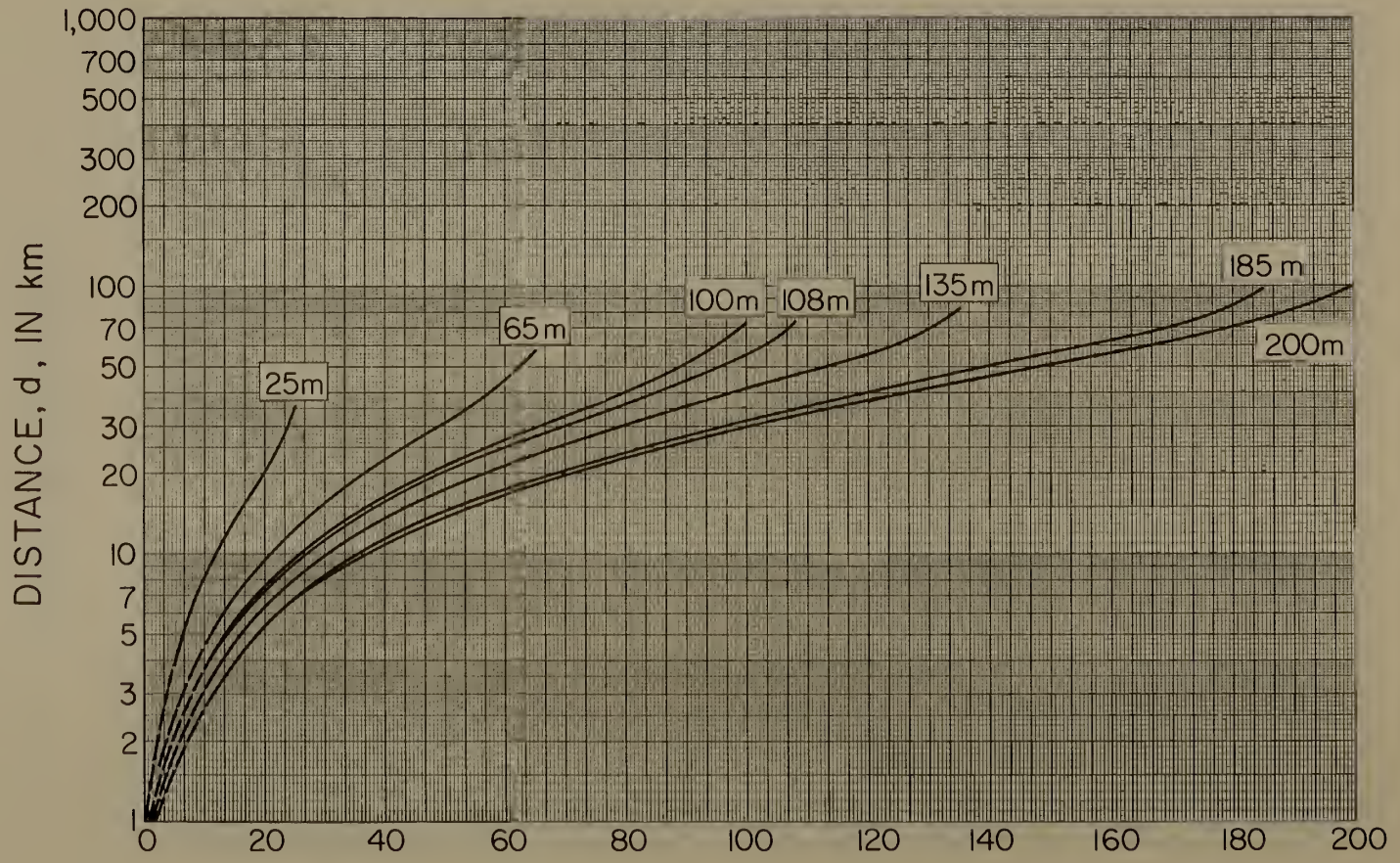

Figure 36

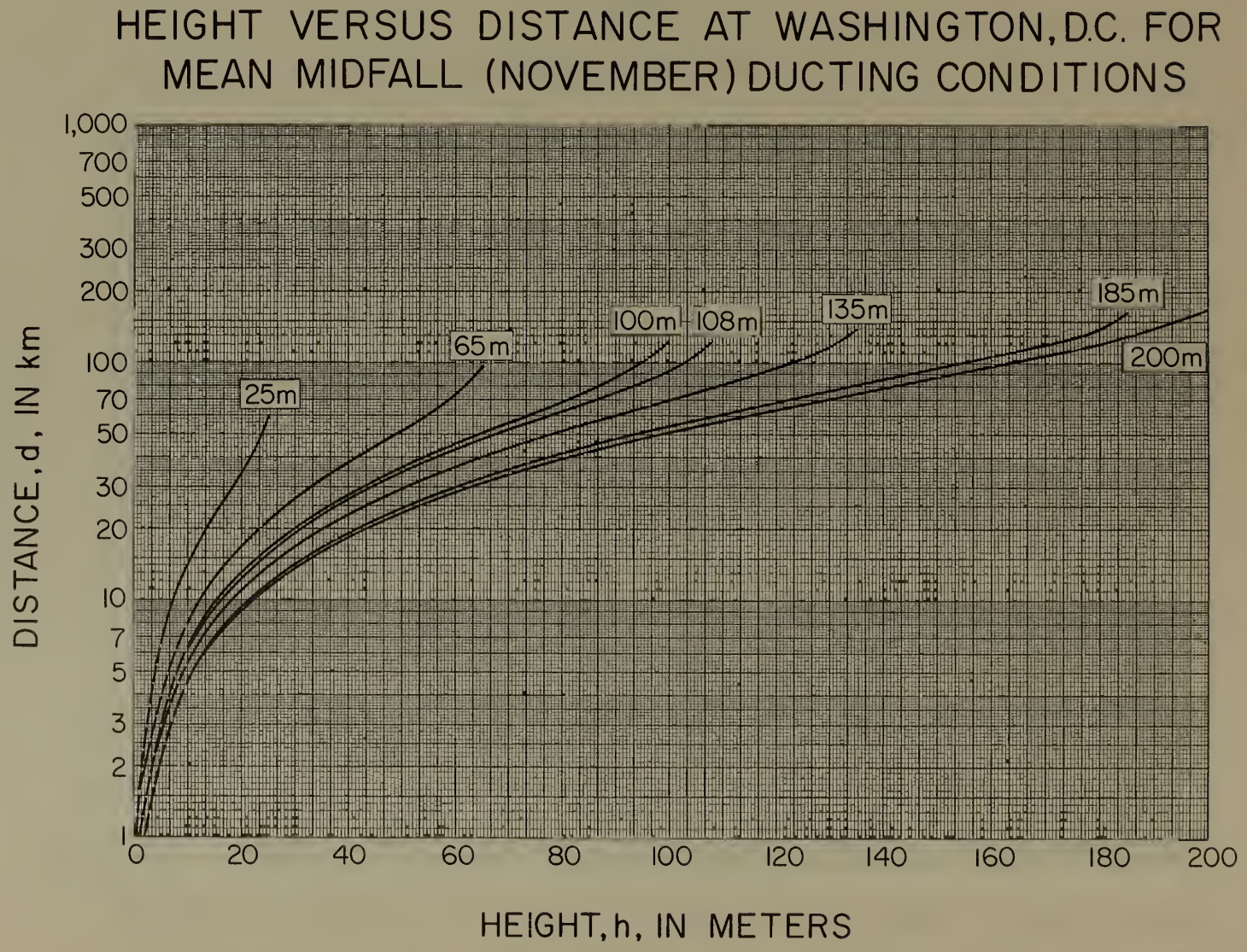
HEIGHT VERSUS DISTANCE AT WASHINGTON, D.C. FOR MEAN MIDFALL (NOVEMBER) DUCTING CONDITIONS
DISTANCE, d, IN km
1,000
700
500
300
200
100
70
50
30
20
10
7
5
3
2
1
0
20
40
60
80
100
120
140
160
180
200
HEIGHT, h, IN METERS
25m
65m
100m
108m
135m
185m
200m

Figure 37

HEIGHT VERSUS DISTANCE AT WASHINGTON, D.C. FOR MINIMUM MIDFALL (NOVEMBER) DUCTING CONDITIONS

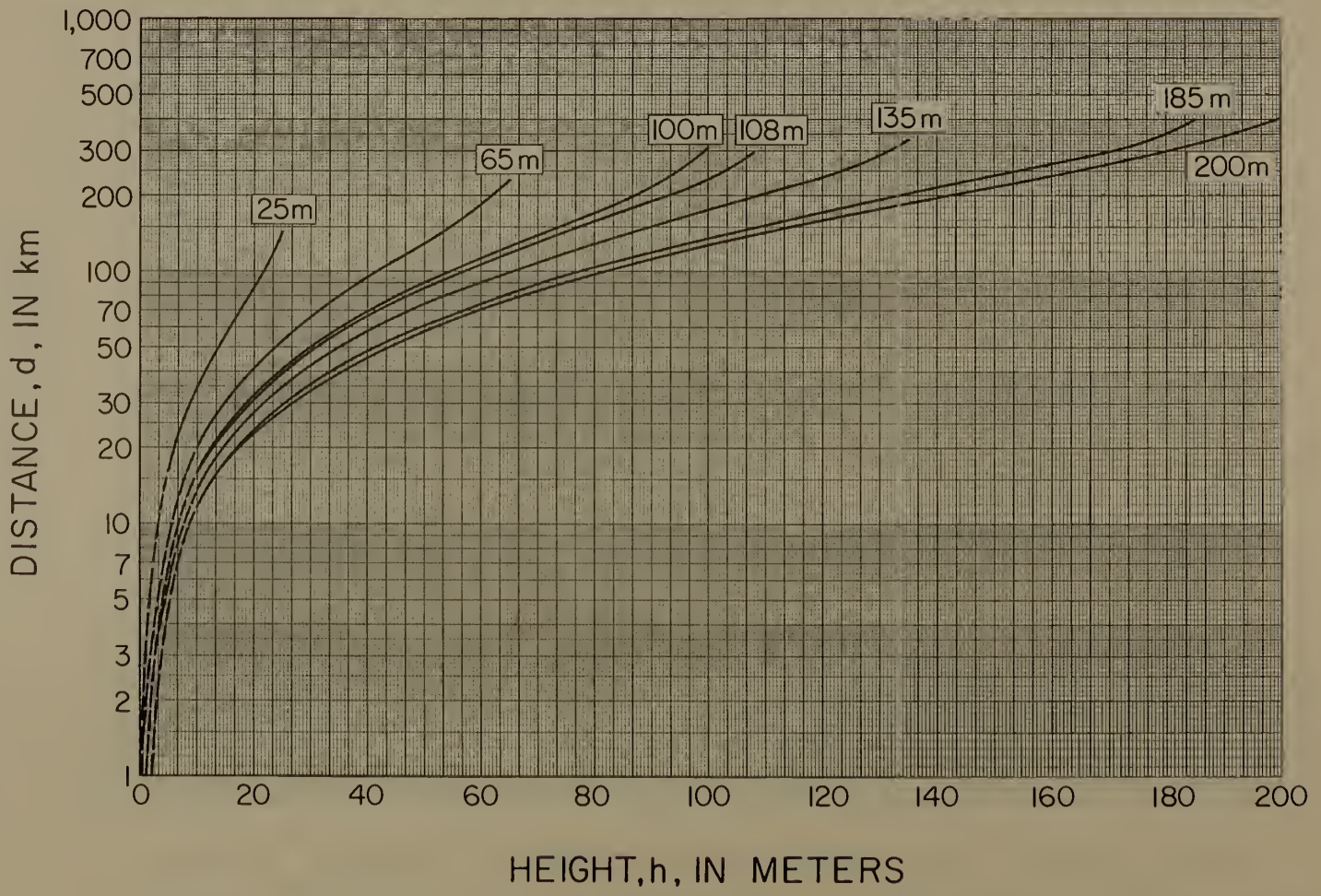

Figure 38

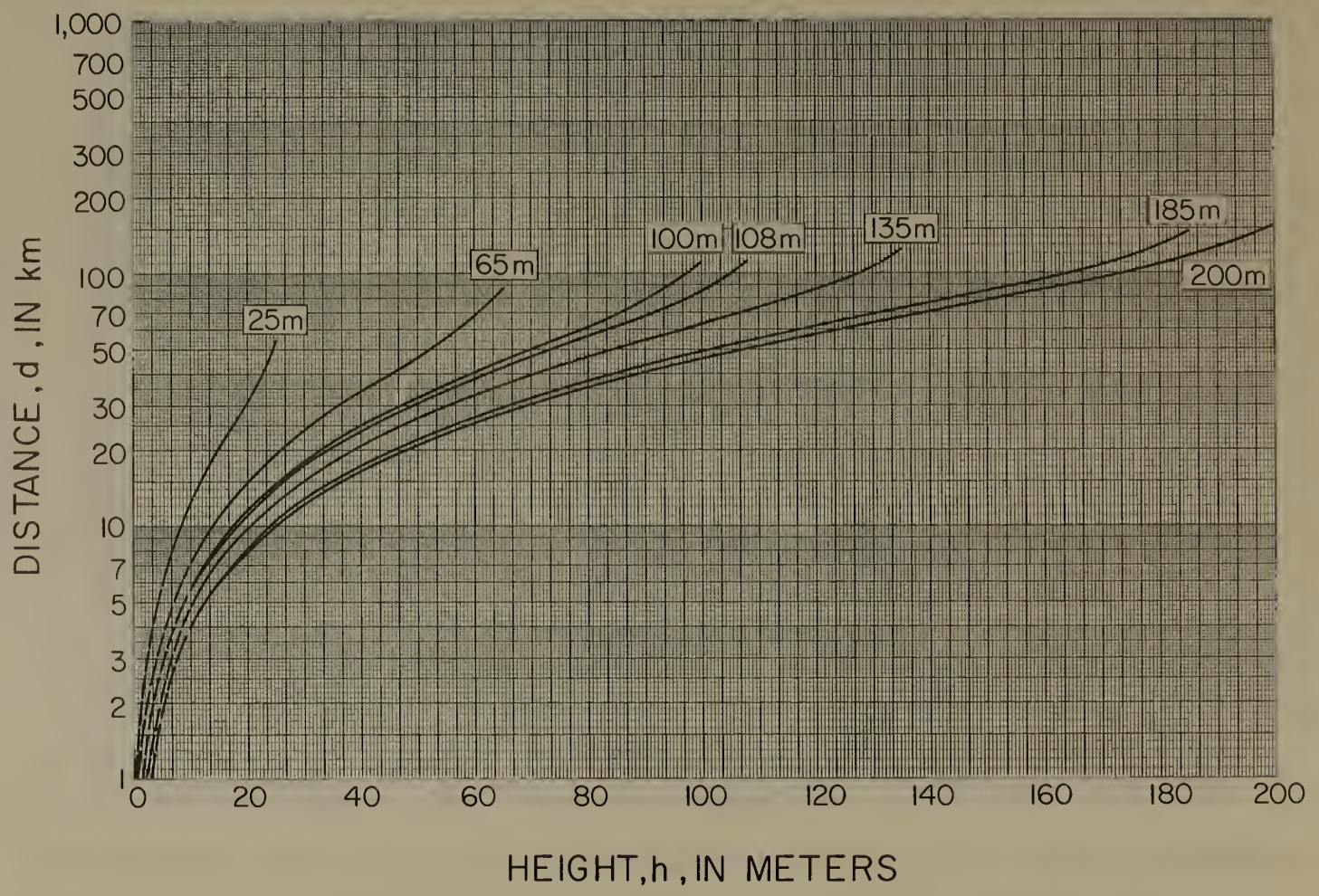
HEIGHT VERSUS DISTANCE AT SWAN ISLAND FOR
MEAN MIDWINTER (FEBRUARY) DUCTING CONDITIONS
DISTANCE, d, IN km
1,000
700
500
300
200
100
70
50
30
20
10
7
5
3
2
1
25m
65m
100m
108m
135m
185m
200m
0
20
40
60
80
100
120
140
160
180
200
HEIGHT, h, IN METERS

Figure 39

HEIGHT VERSUS DISTANCE AT SWAN ISLAND FOR MINIMUM MIDWINTER (FEBRUARY) DUCTING CONDITIONS

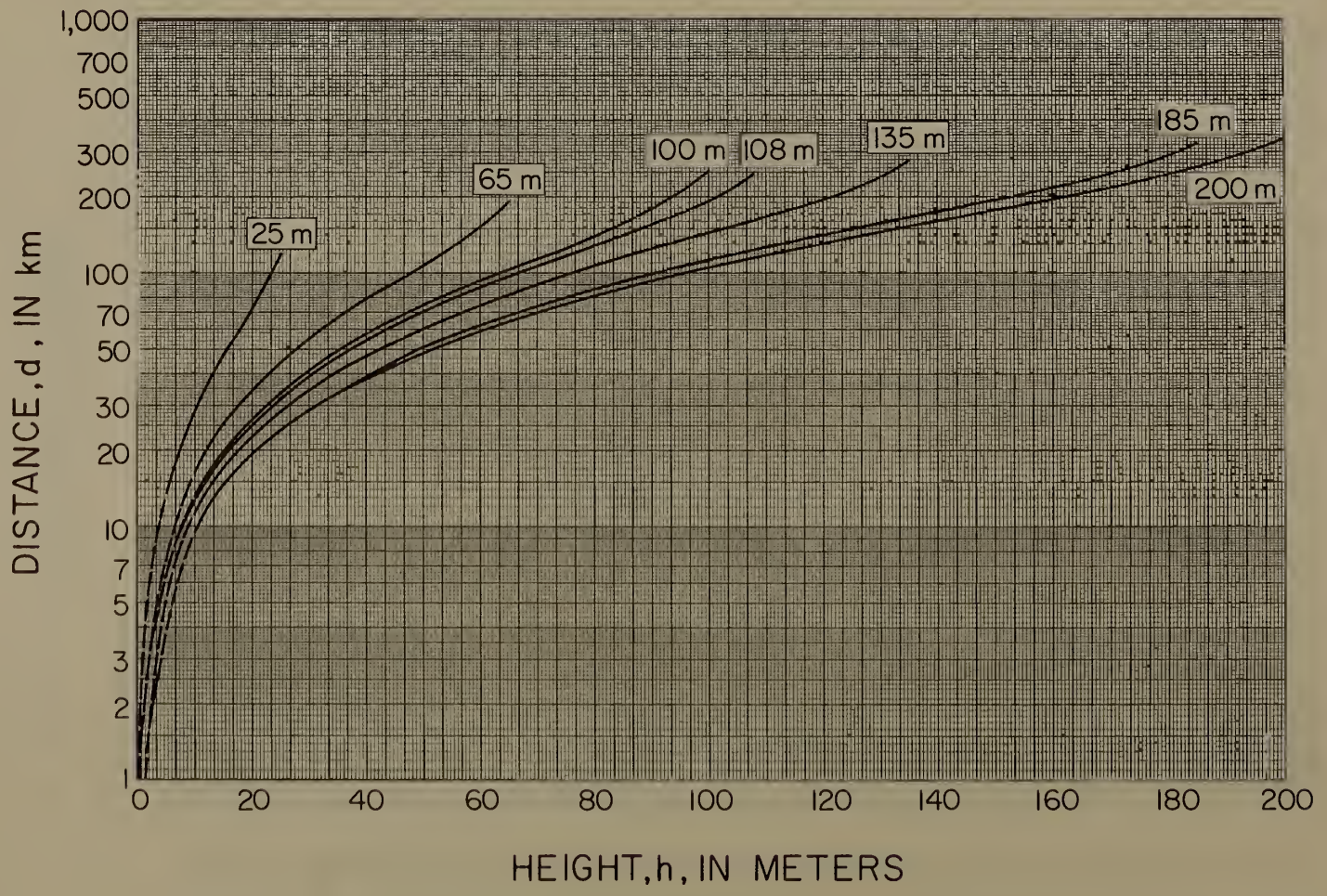

Figure 40

HEIGHT VERSUS DISTANCE AT SWAN ISLAND FOR MAXIMUM MIDSPRING (MAY) DUCTING CONDITIONS

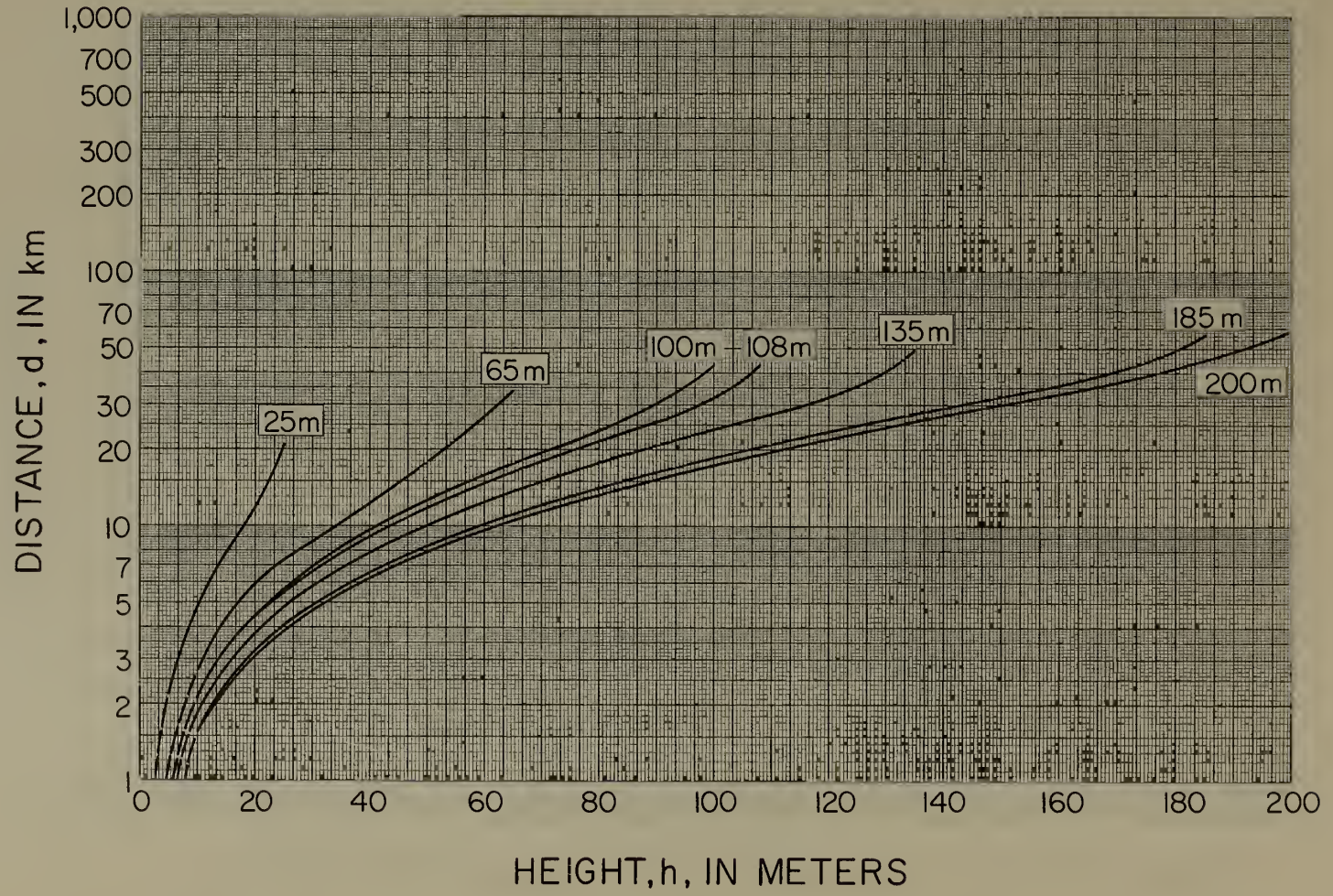

Figure 41

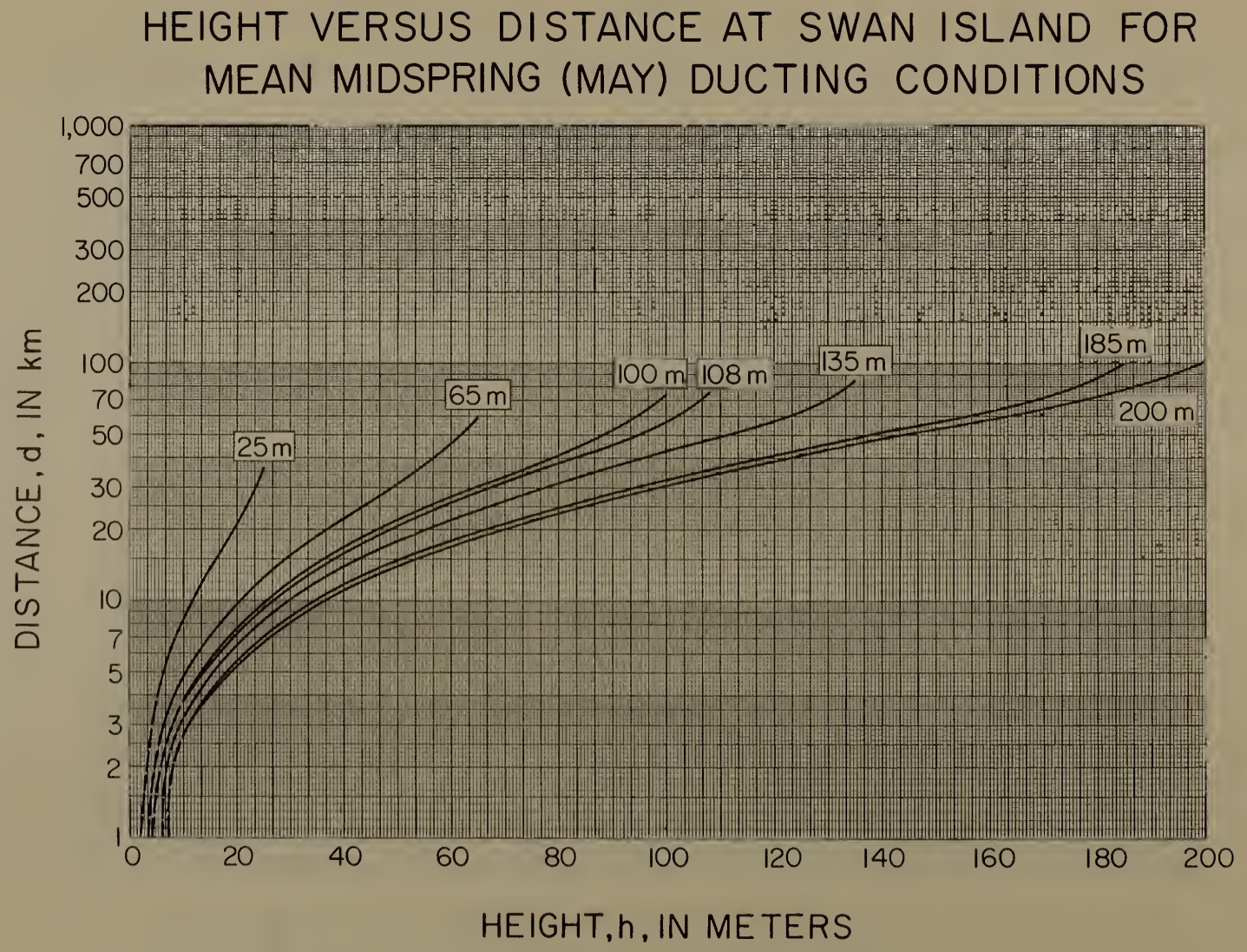
HEIGHT VERSUS DISTANCE AT SWAN ISLAND FOR
MEAN MIDSPRING (MAY) DUCTING CONDITIONS
DISTANCE, d, IN km
1,000
700
500
300
200
100
70
50
30
20
10
7
5
3
2
1
0
20
40
60
80
100
120
140
160
180
200
HEIGHT, h, IN METERS
25 m
65 m
100 m
108 m
135 m
185 m
200 m

Figure 42

HEIGHT VERSUS DISTANCE AT SWAN ISLAND FOR MAXIMUM MIDSUMMER (AUGUST) DUCTING CONDITIONS

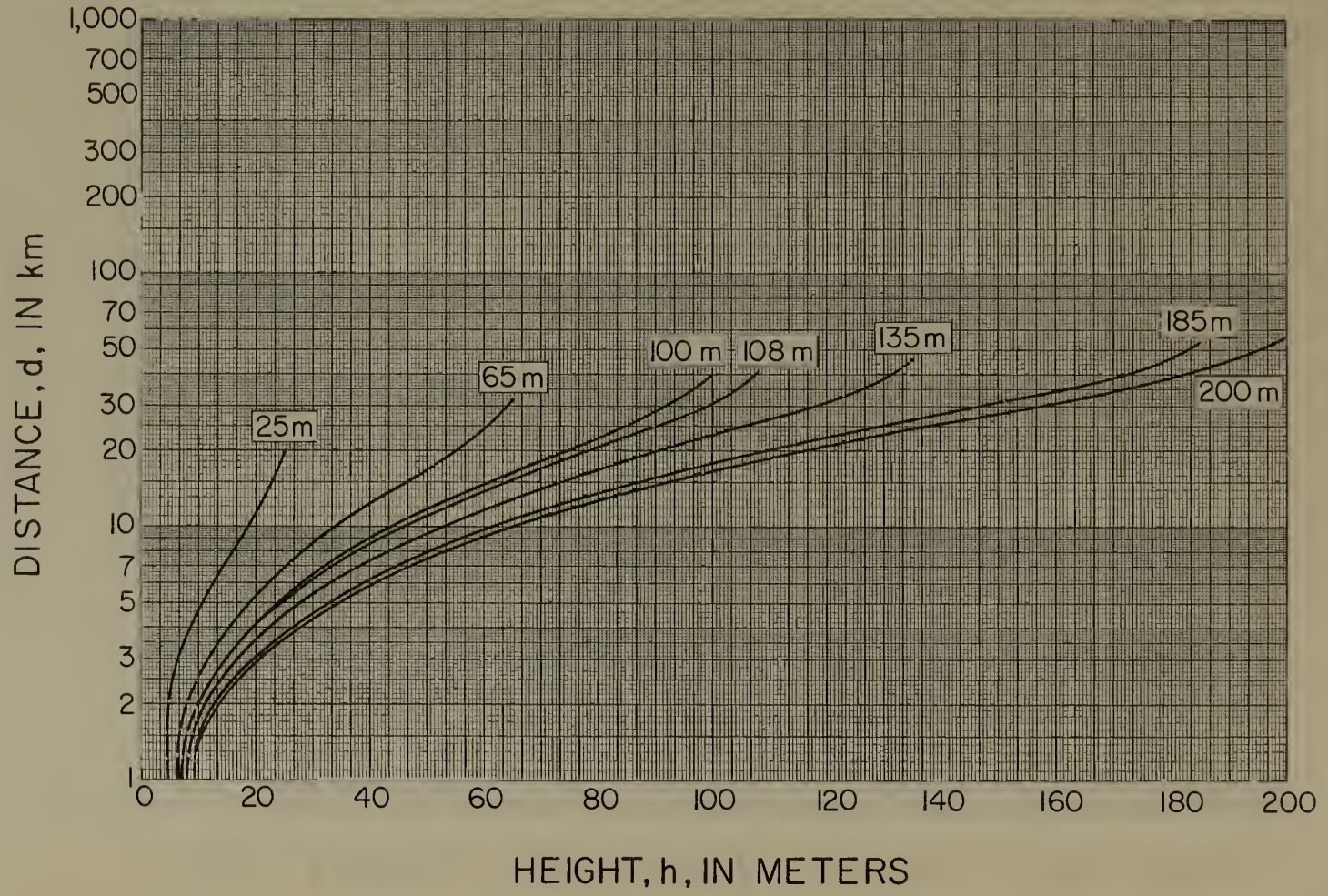

Figure 43

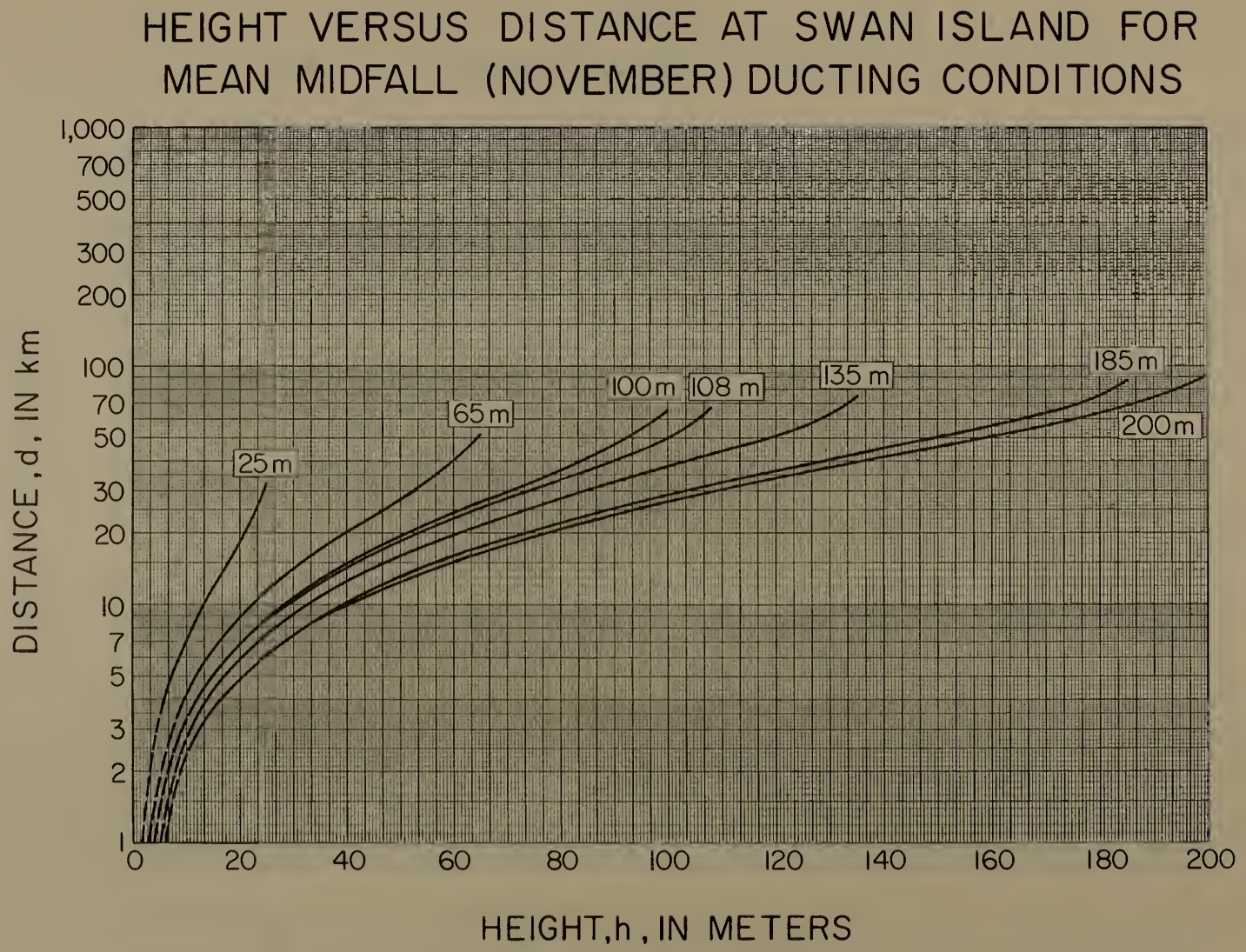
HEIGHT VERSUS DISTANCE AT SWAN ISLAND FOR
MEAN MIDFALL (NOVEMBER) DUCTING CONDITIONS
DISTANCE, d, IN km
1,000
700
500
300
200
100
70
50
30
20
10
7
5
3
2
1
0
20
40
60
80
100
120
140
160
180
200
HEIGHT, h, IN METERS
25 m
65 m
100 m
108 m
135 m
185 m
200 m

Figure 44

HEIGHT VERSUS DISTANCE AT FAIRBANKS FOR MAXIMUM MIDWINTER (FEBRUARY) DUCTING CONDITIONS

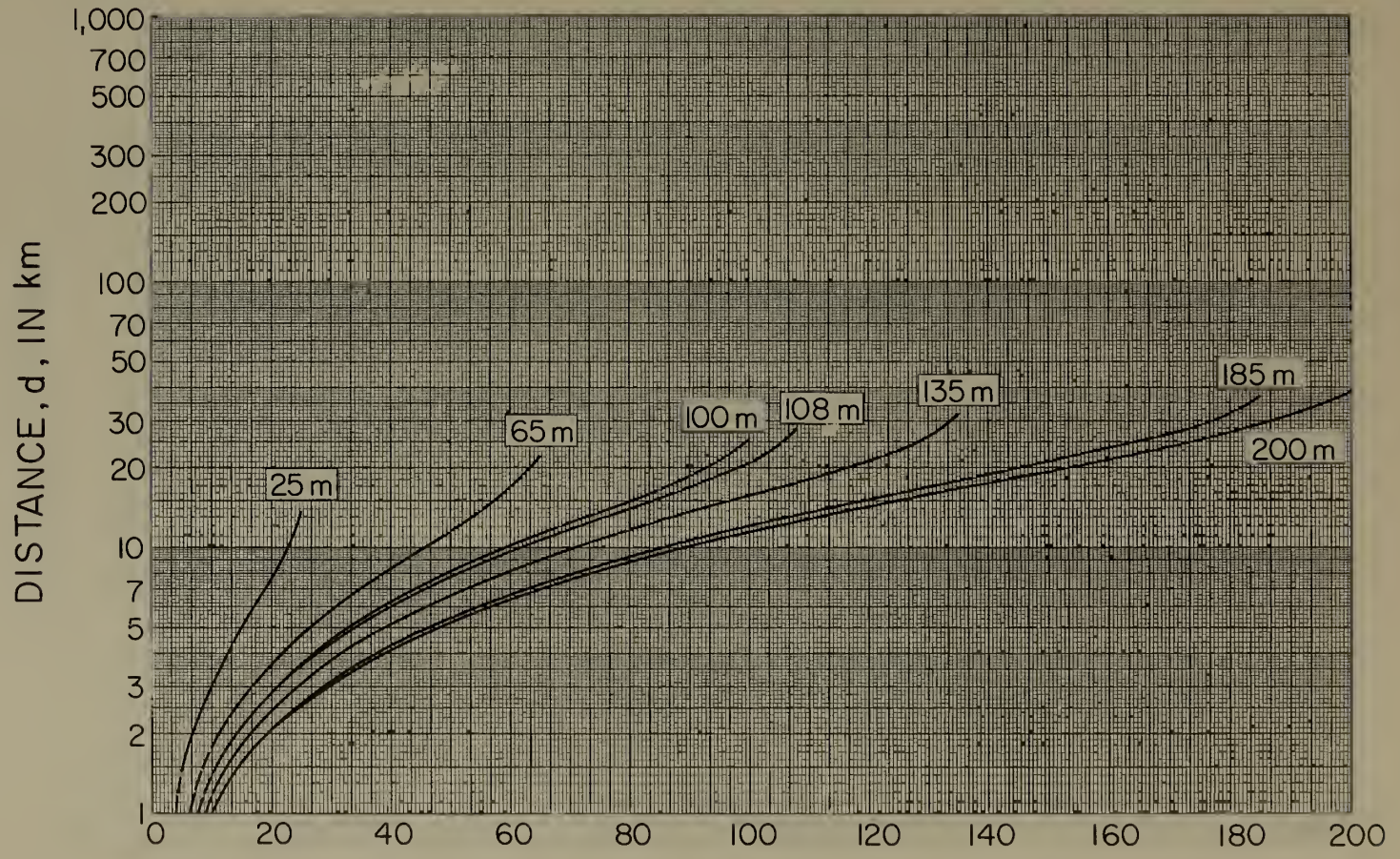

Figure 45

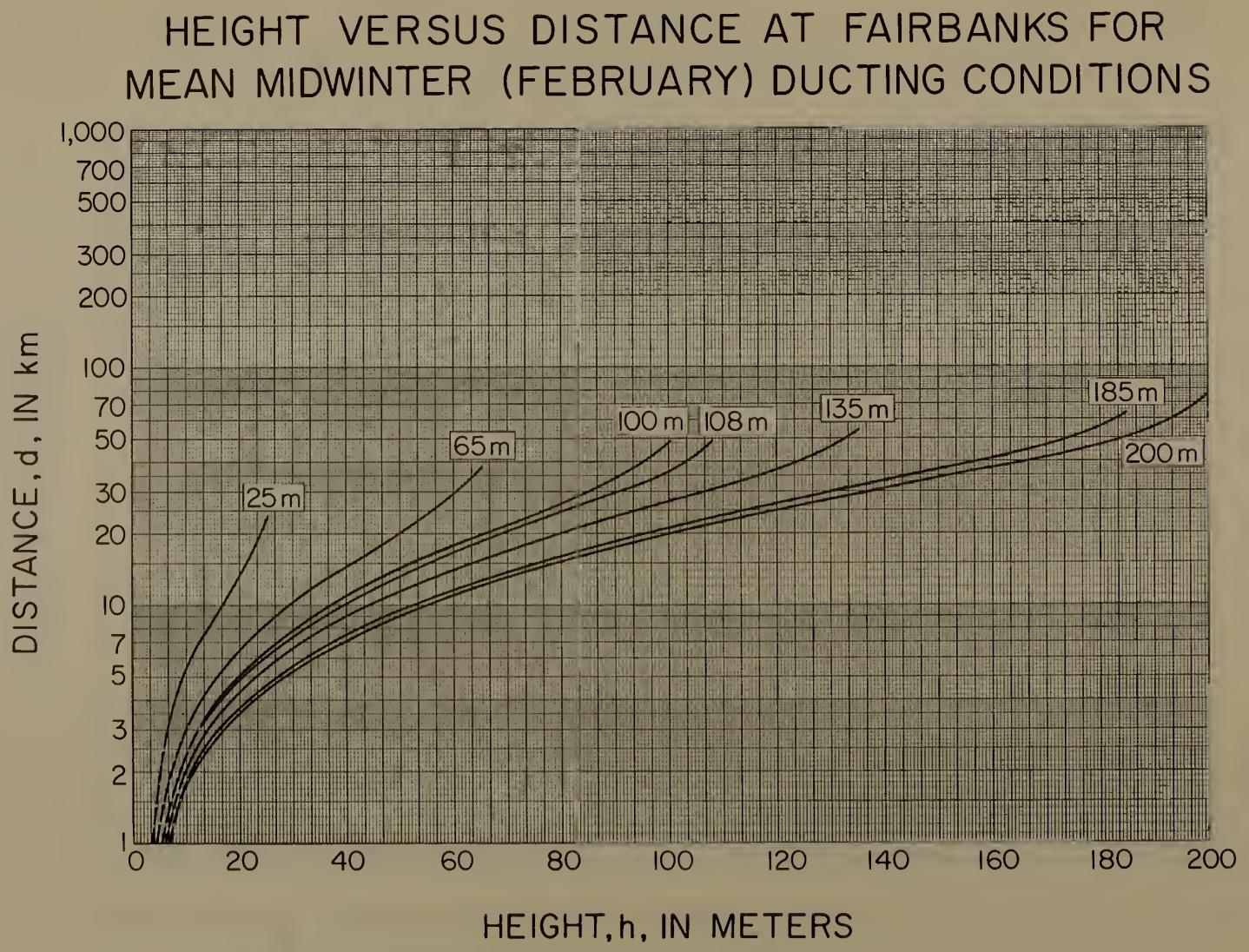
HEIGHT VERSUS DISTANCE AT FAIRBANKS FOR
MEAN MIDWINTER (FEBRUARY) DUCTING CONDITIONS
DISTANCE, d, IN km
1,000
700
500
300
200
100
70
50
30
20
10
7
5
3
2
1
0
20
40
60
80
100
120
140
160
180
200
HEIGHT, h, IN METERS
25 m
65 m
100 m
108 m
135 m
185 m
200 m

Figure 46

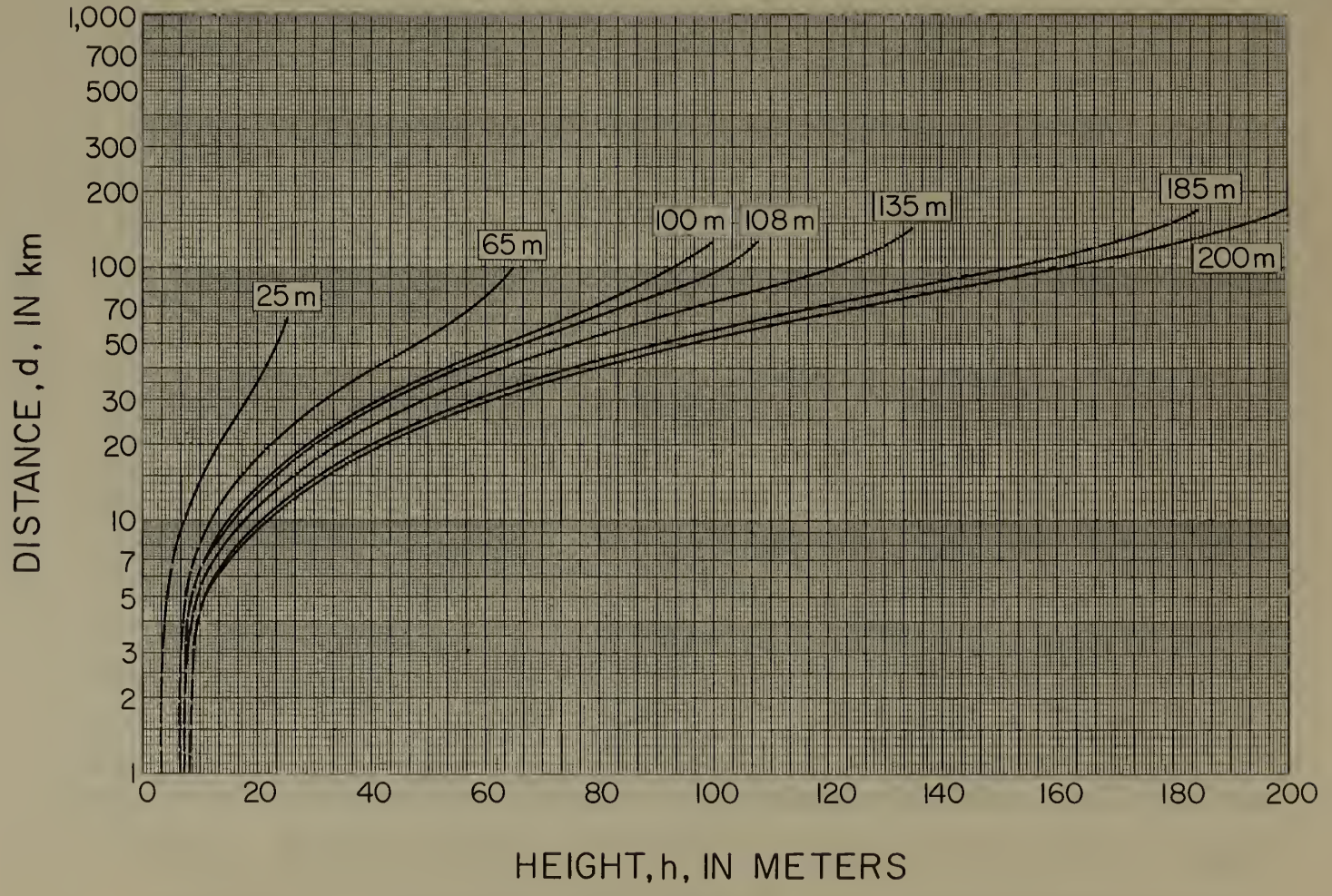
HEIGHT VERSUS DISTANCE AT FAIRBANKS FOR
MINIMUM MIDWINTER (FEBRUARY) DUCTING CONDITIONS
DISTANCE, d, IN km
1,000
700
500
300
200
100
70
50
30
20
10
7
5
3
2
1
0
20
40
60
80
100
120
140
160
180
200
HEIGHT, h, IN METERS
25 m
65 m
100 m
108 m
135 m
185 m
200 m

Figure 47

HEIGHT VERSUS DISTANCE AT FAIRBANKS FOR MEAN MIDSUMMER (AUGUST) DUCTING CONDITIONS

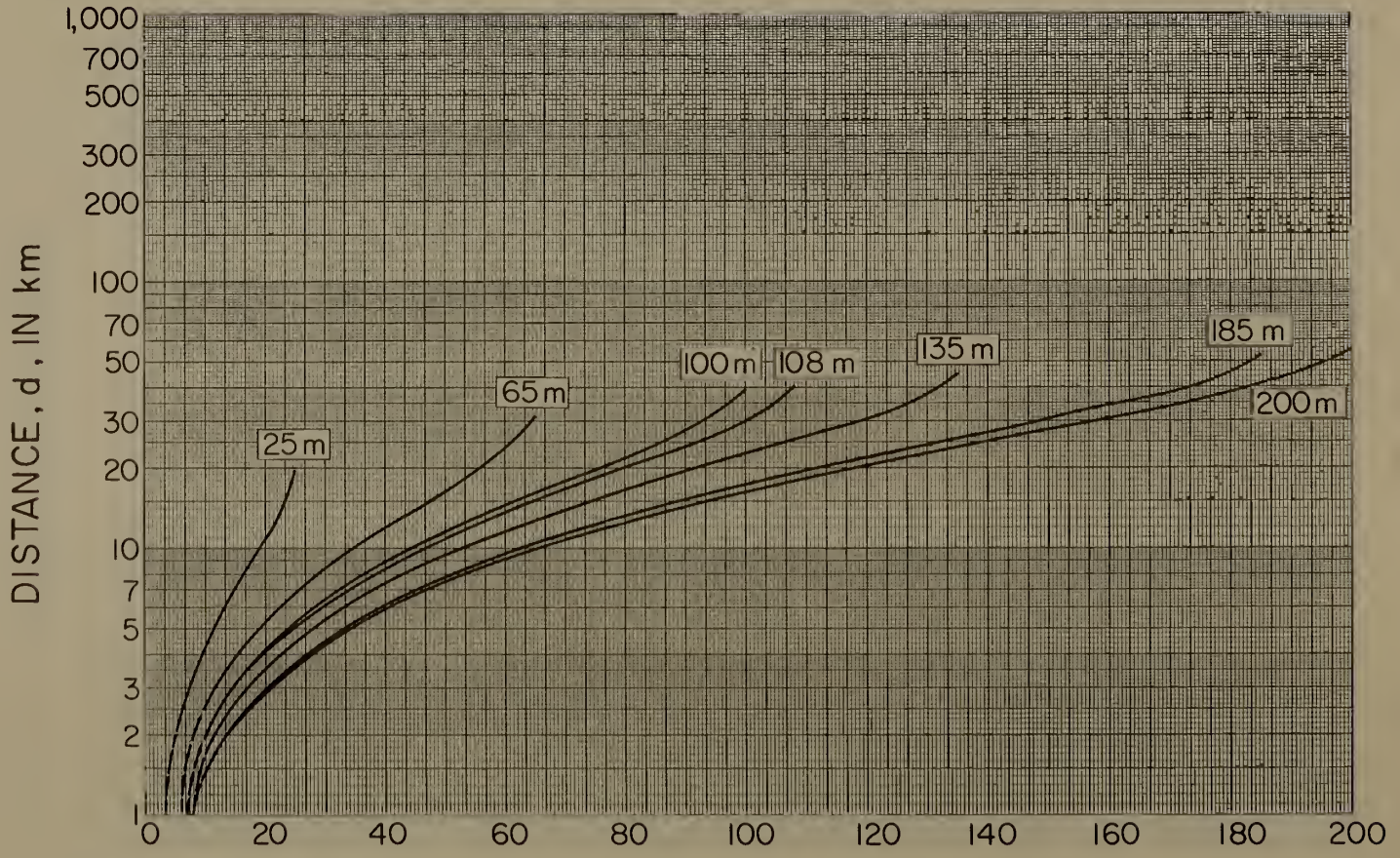

Figure 48

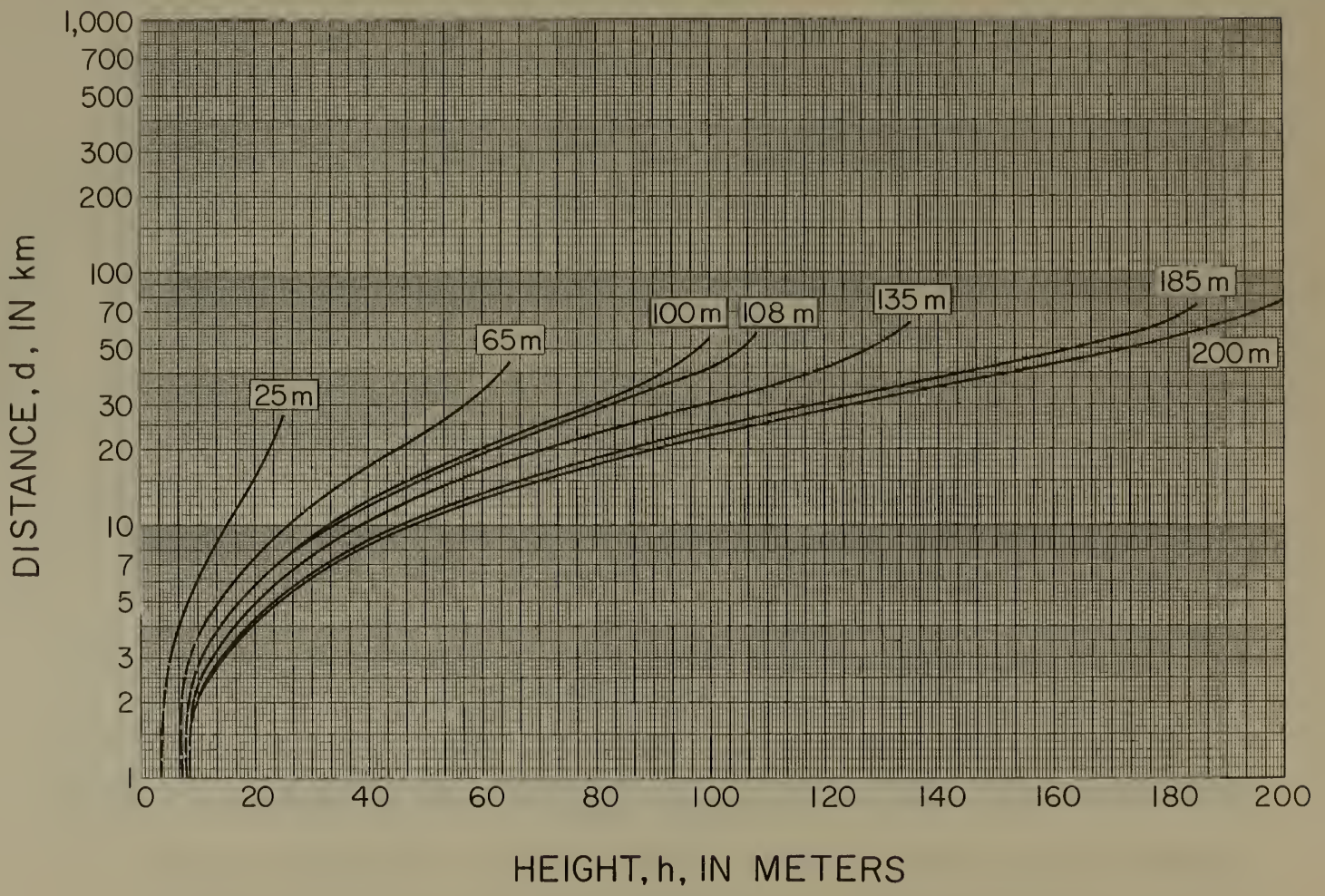
HEIGHT VERSUS DISTANCE AT FAIRBANKS FOR
MAXIMUM MIDFALL (NOVEMBER) DUCTING CONDITIONS
DISTANCE, d, IN km
1,000
700
500
300
200
100
70
50
30
20
10
7
5
3
2
1
25 m
65 m
100 m
108 m
135 m
185 m
200 m
0
20
40
60
80
100
120
140
160
180
200
HEIGHT, h, IN METERS

Figure 49

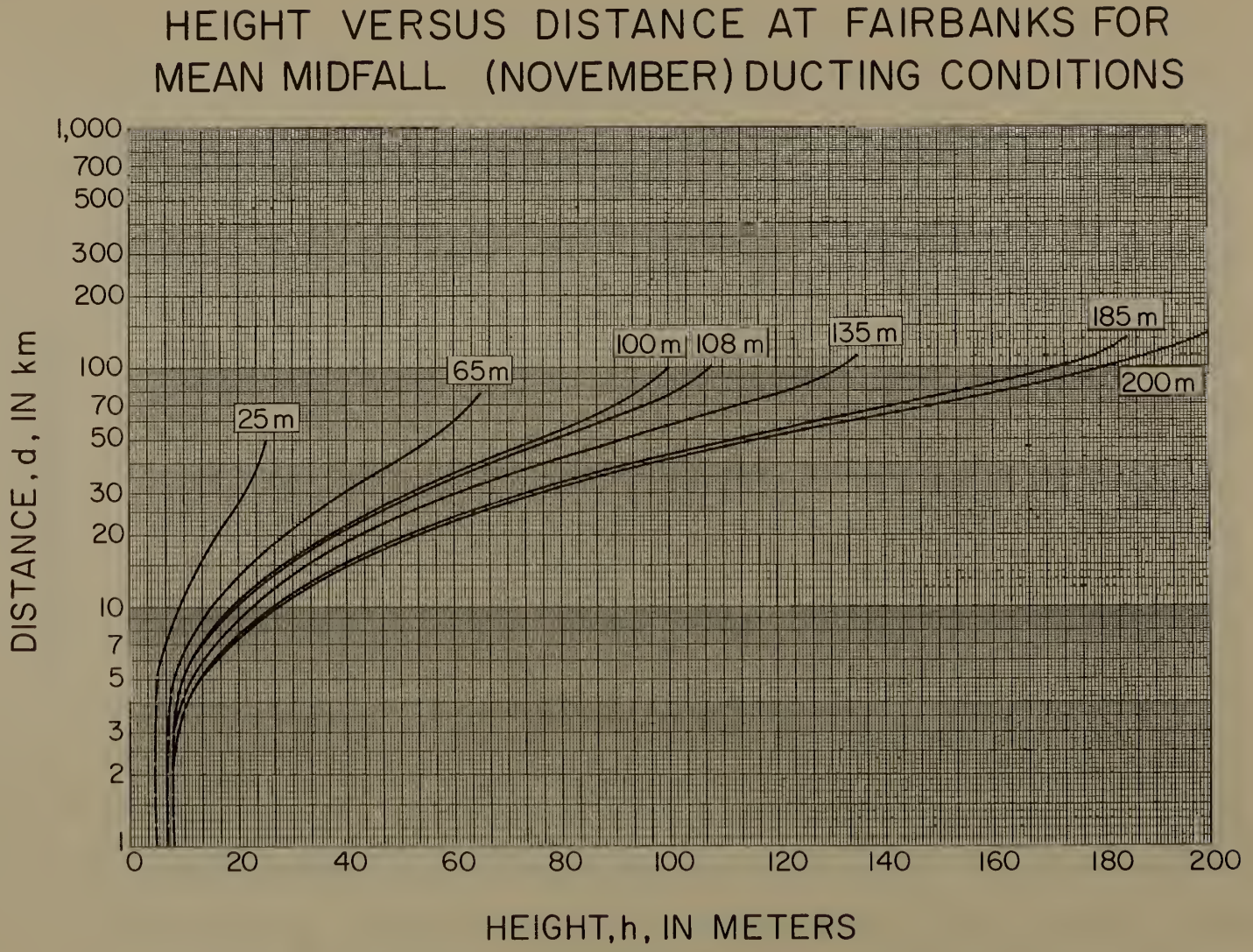
HEIGHT VERSUS DISTANCE AT FAIRBANKS FOR
MEAN MIDFALL (NOVEMBER) DUCTING CONDITIONS
DISTANCE, d, IN km
1,000
700
500
300
200
100
70
50
30
20
10
7
5
3
2
1
0
20
40
60
80
100
120
140
160
180
200
HEIGHT, h, IN METERS
25 m
65 m
100 m
108 m
135 m
185 m
200 m

Figure 50

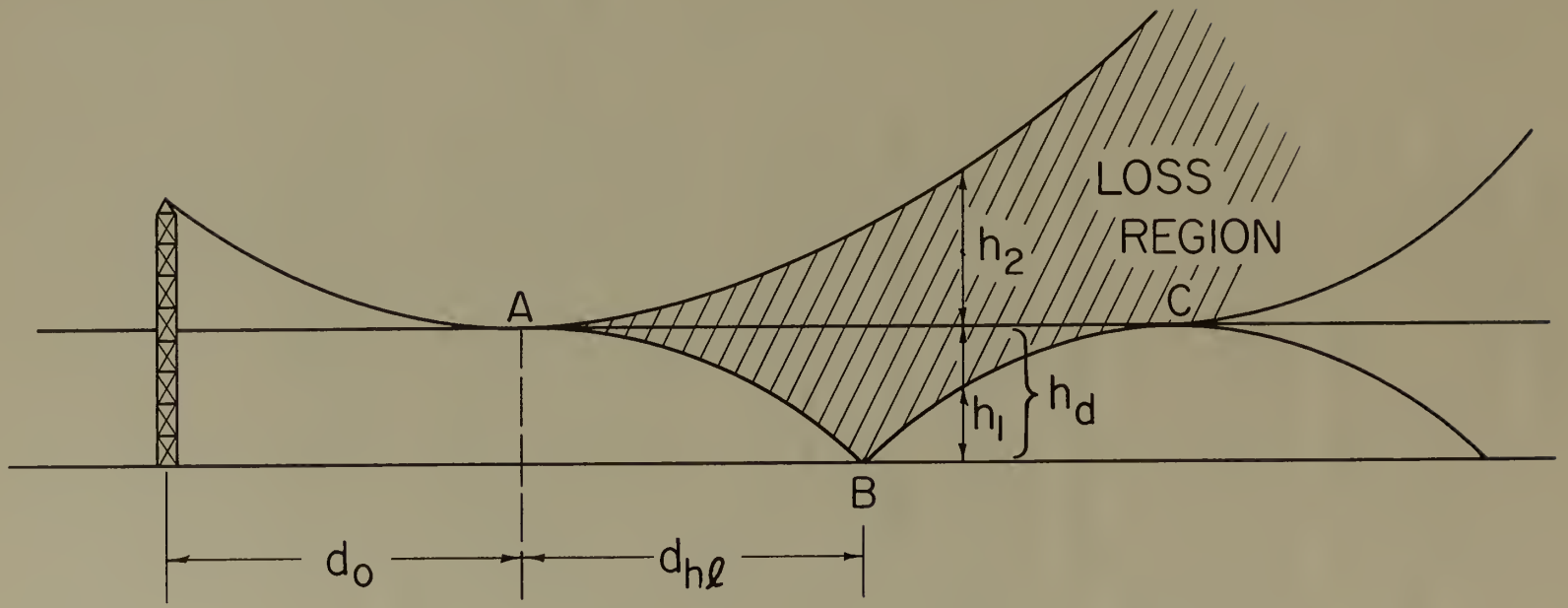

GEOMETRY OF THE SHADOW ZONE LOSS REGION

Figure 51

Since from equation (33)

$$h_1 \leq \text{loss region} \leq h_A + h_2.$$

Therefore, in answer to part (b) of the problem, for maximum ducting conditions with a 100-meter thick duct:

$$92.3 \text{ m.} \leq \text{loss region} \leq 3 + 100 \text{ m.}$$

$$\boxed{92.3 \text{ m.} \leq \text{loss region} \leq 103 \text{ m.}}$$

with a 200-meter thick duct:

$$166 \text{ m.} \leq \text{loss region} \leq 18 + 200 \text{ m.}$$

$$\boxed{166 \text{ m.} \leq \text{loss region} \leq 218 \text{ m.}}$$

For mean ducting conditions with a 100-meter thick duct:

$$\boxed{96 \text{ m.} \leq \text{loss region} \leq 103 \text{ m.}}$$

with a 200-meter thick duct:

$$\boxed{187 \text{ m.} \leq \text{loss region} \leq 218 \text{ m.}}$$

For minimum ducting conditions with a 100-meter thick duct:

$$\boxed{99 \text{ m.} \leq \text{loss region} \leq 103 \text{ m.}}$$

with a 200-meter thick duct:

$$\boxed{199.3 \text{ m.} \leq \text{loss region} \leq 218 \text{ m.}}$$

It should be pointed out that this method does not guarantee prevention of all fadeouts due to superrefraction, but merely affords an estimate. It is therefore recommended that if RAOB equipment is available, actual computations using equations (25) - (30) be made over a period of time to completely determine the ducting fadeout regions at a particular point.

11. VARIATIONS IN FADING

It should be remembered that the three-station model is representative of the arctic, temperate, and tropical zones only, and that great variations could be found within specific subdivisions of these areas. Furthermore, temporal variations are to be considered with respect to formation and decay of ducts. One must also consider the waveguide effect of ducts, in that they have a particular "cut-in" frequency, and will not respond to all frequencies as discussed in section 4. Thus, a fadeout may appear at one frequency and not at another. The fact that the atmosphere is never ideally homogeneous should also be considered. To obtain precise results, one should try to have RAOB or similar readings as close to the transmission path as possible when actually trying to run shadow zone calculations of his own. One should also avail himself of as many daily profiles for the purpose of determining N as possible, so as to get a closer picture of the hours during which superrefractive conditions can be anticipated, and also to obtain a picture of how the duct height varies between the times of its buildup and decay.

REFERENCES

Bean, B. R., and G. D. Thayer, C.R.P.L. exponential reference atmosphere, NBS Monograph 4 (October 29, 1959).

Booker, H. G., and W. Walkinshaw, The mode theory of tropospheric refraction and its relation to wave-guides and diffraction, pp. 80-126 of Meteorological Factors in Radio Wave Propagation. Report of a conference held on 8 April 1946 at The Royal Institution, London, by The Physical Society and The Royal Meteorological Society.

Bremmer, H., Terrestrial Radio Waves, pp. 131-138 (Elsevier Publishing Company, New York, 1949).

Cowan, L. W., A radio climatology survey of the U.S., Proceedings of the Conference on Radio Meteorology, November 9-12, 1953. The University of Texas, Austin, Texas.

Ikegami, F., Influence of an atmospheric duct on microwave fading, IRE Transactions on Antennas and Propagation, AP-7, 252-257 (July, 1959).

Kerr, D. E., Propagation of Short Radio Waves, pp. 9-22 (McGraw-Hill Book Company, Inc., New York, 1951).

Norton, K. A., The calculation of ground-wave field intensity over a finitely conducting spherical earth, Proc. IRE 29, 623-639 (December, 1941).

Price, W. L., Radio shadow effects produced in the atmosphere by inversions, Physical Society of London, Proceedings, 61(343), 59-78 (July, 1948).

Schulkin, M., Average radio-ray refraction in the lower atmosphere, Proc. IRE 40, 554-561 (May, 1952).

Smith, E. K., and S. Weintraub, The constants in the equation for atmospheric refractive index at radio frequencies, Proc. IRE 41, 1035-1037 (August, 1953).

U.S. DEPARTMENT OF COMMERCE
Luther H. Hodges, Secretary

NATIONAL BUREAU OF STANDARDS
A. V. Astin, Director

THE NATIONAL BUREAU OF STANDARDS

The scope of activities of the National Bureau of Standards at its major laboratories in Washington, D.C., and Boulder, Colorado, is suggested in the following listing of the divisions and sections engaged in technical work. In general, each section carries out specialized research, development, and engineering in the field indicated by its title. A brief description of the activities, and of the resultant publications, appears on the inside of the front cover.

WASHINGTON, D.C.

Electricity. Resistance and Reactance. Electrochemistry. Electrical Instruments. Magnetic Measurements. Dielectrics.

Metrology. Photometry and Colorimetry. Refractometry. Photographic Research. Length. Engineering Metrology. Mass and Scale. Volumetry and Densimetry.

Heat. Temperature Physics. Heat Measurements. Cryogenic Physics. Equation of State. Statistical Physics.

Radiation Physics. X-ray. Radioactivity. Radiation Theory. High Energy Radiation. Radiological Equipment. Nucleonic Instrumentation. Neutron Physics.

Analytical and Inorganic Chemistry. Pure Substances. Spectrochemistry. Solution Chemistry. Analytical Chemistry. Inorganic Chemistry.

Mechanics. Sound. Pressure and Vacuum. Fluid Mechanics. Engineering Mechanics. Rheology. Combustion Controls.

Organic and Fibrous Materials. Rubber. Textiles. Paper. Leather. Testing and Specifications. Polymer Structure. Plastics. Dental Research.

Metallurgy. Thermal Metallurgy. Chemical Metallurgy. Mechanical Metallurgy. Corrosion. Metal Physics.

Mineral Products. Engineering Ceramics. Glass. Refractories. Enameled Metals. Crystal Growth. Physical Properties. Constitution and Microstructure.

Building Research. Structural Engineering. Fire Research. Mechanical Systems. Organic Building Materials. Codes and Safety Standards. Heat Transfer. Inorganic Building Materials.

Applied Mathematics. Numerical Analysis. Computation. Statistical Engineering. Mathematical Physics.

Data Processing Systems. Components and Techniques. Digital Circuitry. Digital Systems. Analog Systems. Applications Engineering.

Atomic Physics. Spectroscopy. Radiometry. Solid State Physics. Electron Physics. Atomic Physics.

Instrumentation. Engineering Electronics. Electron Devices. Electronic Instrumentation. Mechanical Instruments. Basic Instrumentation.

Physical Chemistry. Thermochemistry. Surface Chemistry. Organic Chemistry. Molecular Spectroscopy. Molecular Kinetics. Mass Spectrometry. Molecular Structure and Radiation Chemistry.

• Office of Weights and Measures.

BOULDER, COLO.

Cryogenic Engineering. Cryogenic Equipment. Cryogenic Processes. Properties of Materials. Gas Liquefaction.

Ionosphere Research and Propagation. Low Frequency and Very Low Frequency Research. Ionosphere Research. Prediction Services. Sun-Earth Relationships. Field Engineering. Radio Warning Services.

Radio Propagation Engineering. Data Reduction Instrumentation. Radio Noise. Tropospheric Measurements. Tropospheric Analysis. Propagation Terrain Effects. Radio-Meteorology. Lower Atmosphere Physics.

Radio Standards. High Frequency Electrical Standards. Radio Broadcast Service. Radio and Microwave Materials. Atomic Frequency and Time Interval Standards. Electronic Calibration Center. Millimeter-Wave Research. Microwave Circuit Standards.

Radio Systems. High Frequency and Very High Frequency Research. Modulation Research. Antenna Research. Navigation Systems. Space Telecommunications.

Upper Atmosphere and Space Physics. Upper Atmosphere and Plasma Physics. Ionosphere and Exosphere Scatter. Airglow and Aurora. Ionospheric Radio Astronomy.


NBS